UNIVERSITÄT ZU LÜBECK

From Lübeck Institute of Experimental Dermatology

of the University of Lübeck

Director: Prof. Ralf J. Ludwig

“Search for B cell modulatory compounds”

-Old drugs for new implications-

Dissertation for Fulfillment of Requirements

for the Doctoral Degree

of the University of Lübeck

from the Department of Natural Sciences

Submitted by

Kazuko Matsumoto

from Fukushima, Japan

Lübeck 2018

First referee: Prof. Dr. Jennifer Hundt

Second referee: Prof. Dr. Rudolf Manz

Date of oral examination: May 16, 2019

Approved for printing. Lübeck, May 20, 2019

Declaration

I declare that I prepared this thesis by my own and that it has never been submitted for any other degree or qualification. The work described here is my own, completed personally unless otherwise stated. All sources of information are acknowledged by means of reference.

Acknowledgements

First and foremost, my acknowledgement goes to Professor Ralf Ludwig for giving me this lifetime opportunity to be a member of his group. Without his generosity, patience and continuous encouragement as well as optimistic feedbacks I received, I would have never completed my work at Lübeck. What he showed me was not limited to work but a precious lesson in life. Thank you very much.

I also say a big thank you to Dr. Katja Bieber, whom I describe as the “core” in AG Ludwig, for being my mentor and for her help and scientific advice. I am also grateful to my mentor professor Saleh Ibrahim for his support.

It was very fortunate that I could meet Dr. Hirose and Dr. Koga in Lübeck. Even the tiniest daily conversation with them was fun, comfort, and a big relief. Thank you.

I can never be grateful enough to my colleagues, especially to Claudia Kauderer for her technical help and her enormous contribution to the lab. Also, my gratitude for Lenche Chakievska and Saeedeh Ghorbanalipoor, thank you for being friends and sharing many interesting perspectives I never noticed.

I also need to mention that without the financial support from Deutsche Forschungsgemeinschaft, this work would have never been completed.

Last but not least, I would like to say thank you to my family for being supportive throughout my life.

Abstract (English)

Production of autoantibody targeted to self-component is one key feature in autoimmune diseases (AD). Since some of these autoantibodies are directly involved in the pathogenesis and they are produced by B-cell derived plasma cells, B cell modulation is one strategy in the management of AD. Drug repurposing aims to reevaluate existing drugs and utilize them for different indications. Compared to a conventional drug development, this method is beneficial in terms of time and cost efficiency.

In this project, we tested the hypothesis that some already in-use drugs might possess an unacknowledged B cell modulatory property - therefore could be utilized for the treatment of AD. To challenge this assumption, we first performed an in vitro screening of 1,200 commercially available and off-patent drugs approved for diverse therapeutic class, and were able to identify 48 compounds suppressed the proliferation of IL-21/CD40mAb simulated human B cells. Four out of 48 compounds (dipyridamole, docetaxel, colchicine and pyrvinium pamoate (PP)) which inhibited B cell proliferation with either strong or limited toxicity and did not affect T cell proliferation as well as ROS release from activated neutrophils were further scrutinized.

The potential of the these selected compounds as therapeutic agents in AD was evaluated in vivo using an immunization-induced animal model of epidermolysis bullosa acquisita (EBA), an autoimmune blistering disease in which a cascade of pathogenic events are triggered by the production of autoantibody against type VII collagen. Clinically, pretreatment the mice with three out of four candidate compounds (dipyridamole, docetaxel, and PP) before the disease induction resulted in a less severe disease phenotype. Furthermore, when mice were treated with PP, this clinical effect was accompanied by the reduction in the number of B cells as well as plasma cells (total and antigen-specific B cells and total plasma cells), and the amount of antigen-specific immunoglobulin G, all of which indicated the suppressive property of this drug in B cell biology.

When vWFA2-immunized mice were given PP after the disease establishment, the magnitude of the subsequent disease development was significantly less compared to that observed in vehicle-treated mice and the productions of total IgG and antigen-specific IgG were also suppressed, further supported the potential of this compound as a B-cell modulatory drug.

The molecular analysis employing RNA sequencing (confirmed by rt-PCR) revealed an increased CD37 expression on IL-21/mCD40Ab stimulated human B cells with PP treatment compared with those without the drug treatment. Considering the association between CD37 deficiency and B cell lymphoproliferative disease controlled by IL-6, a crucial B cell growth and differentiation factor, and a possible role of CD37 avoiding excess IL-6 signaling within B cells, the B cell modulatory effect of PP could partially be exerted by maintaining CD37 on cell surface, which to be elucidated in the future.

What highlights this work is that, by means of drug repurposing, we were able to demonstrate B cell modulatory property by PP, which has not been appreciated before. This work provided a possibility of utilizing this drug in the management of AD.

Abstract (German)

Das Hauptmerkmal von Autoimmunerkrankungen (AD) ist die Produktion von Antikörpern, die gegen Bestandteile des eigenen Organismus gerichtet sind und oft einen direkten pathogenen Einfluss auf die Erkrankung haben. Die Hemmung von Plasmazellen und B-Zellen, welche an der Entstehung dieser Autoantikörper maßgeblich beteiligt sind, stellt somit eine wichtige Therapieoption von AD dar. Da die konventionelle Medikamentenentwicklung oft sehr kostenintensiv und langwierig ist, stellt das „Repurposing“ von Arzneimitteln, also die Anwendung bekannter Substanzen bei neuen Indikationen eine vielversprechende Alternative hierfür dar.

Im Rahmen meiner Arbeit habe ich die Hypothese überprüft, ob bereits zugelassene Medikamente bisher nicht bekannte B-Zell-modulatorische Eigenschaften besitzen - und somit prinzipiell zur Therapie von AD in Frage kommen. Aus diesem Grund führte ich zunächst ein in-vitro-Screening von 1.200 kommerziell erhältlichen und patentfreien Medikamenten durch, die für verschiedene therapeutische Indikationen zugelassen sind (oder waren). Dabei konnte ich 48 Substanzen identifizieren, die die Proliferation von aCD40Ab/IL-21-stimulierten humanen B-Zellen inhibierten. Vier dieser Substanzen (Dipyridamol, Docetaxel, Colchicin und Pyrviniumpamoat), welche zusätzlich die T-Zellproliferation sowie die Freisetzung radikaler Sauerstoffspezies aus aktivierten neutrophilen Granulozyten nicht beeinflussten, wurden im Hinblick auf eine klinische Anwendung weiter untersucht.

Hierzu verwendete ich das immunisierungsinduzierte Tiermodell der Epidermolysis bullosa acquisita (EBA), einer immunkomplexabhängigen bullösen AD der Haut. Klinisch führte die Vorbehandlung der Mäuse mit drei von vier untersuchten Substanzen (Dipyridamol, Docetaxel und Pyrviniumpamoat) zu einer Verbesserung des Krankheitsbildes. Bei Mäusen, die mit Pyrviniumpamoat behandelt wurden, ging dieser klinische Effekt mit einer Verringerung der Anzahl von B-Zellen sowie Plasmazellen und der Menge des antigenspezifischen

Immunglobulins (Ig)G einher. Um die Mechanismen der Pyrviniumpamoat-vermittelten Effekte zu entschlüsseln, wurde eine RNA-Sequenzierung und anschließend eine RT-PCR der differentiell regulierten Gene durchgeführt. Hierbei zeigte sich nach Pyrviniumpamoatgabe auf stimulierten humanen B-Zellen eine erhöhte Expression von CD37, einem Schlüsselmolekül bei der Aufrechterhaltung von Keimzentren und der Produktion langlebiger Antikörper.

Zusammenfassend zeigt diese Arbeit, dass durch Screening bereits zugelassener Medikamente neue Eigenschaften aufgedeckt werden können, wie die Veränderung der B-Zell-Modulation durch Pyrviniumpamoat. Basierend auf den therapeutischen Effekten dieser Substanz im Tiermodell der EBA, ist Pyrviniumpamoat eine vielversprechende Substanz zur Therapie B-Zell-vermittelter AD.

Abbreviations

%BSA	percentage of affected body surface area
aCD40Ab	anti-human CD40 antibody
ACPA	anti-citrullinated protein antibody
ADs	autoimmune diseases
anti-dsDNA Ab	anti-dsDNA Ab
AP-1	activator protein-1
APC	Allophycocyanin
BCL-6	B-cell lymphoma 6
BCMA	B lymphocyte maturation antigen
BLIMP-1	B lymphocyte-induced maturation protein-1
BLyS	B lymphocyte stimulator
BR3	BAFF/BLyS receptor3
BrdU	5-bromo-2'-deoxyuridine
BSA	bovine serum albumin
CBC	complete blood count
CD	cluster of differentiation
cDNA	complementary DNA
COL7	type VII collagen
DEJ	dermal-epidermal junction
DMSO	dimethyl sulfoxide
DNA	deoxyribonucleic acid
dNTP	deoxynucleotide
DPBS	Dulbecco's Phosphate-Buffered Saline
dTTP	deoxythymidine triphosphate
dUTP	deoxyuridine triphosphate
EBA	epidermolysis bullosa acquisita
EBF1	Early B-cell factor 1
EGFR	Epidermal Growth Factor Receptor
ELISA	Enzyme-Linked ImmunoSorbent Assay
ERKs	extracellular signal-regulated kinases
EtOH	ethanol

FACS	fluorescence activated cell sorting
Fc/ Fc receptors	Fragment, crystallizable/ Receptors for the Fc portion of Ig
FCS	fetal calf serum
FITC	fluorescein isothiocyanate
GC	germinal center
GCs	glucocorticoids
GR	glucocorticoid receptors
hCol7	human type VII collagen
HLA	human leukocyte antigen
HRP	horseradish peroxidase
IC	immunocomplex
IFN	interferon
Ig	Immunoglobulin
IGF1	insulin-like growth factor-1
IL	Interleukin
i.p.	intraperitoneal
IRF-3	IFN regulatory factor 3
IRF-4	IFN regulatory factor 4
JNKs	c-Jun NH2-terminal kinases
MACS	Magnetic-activated cell sorting
MAPK	mitogen-activated protein kinase
mCOL7	murine type VII collagen
MHC	major histocompatibility complex
mRNA	messenger RNA
mTOR	mammalian target of rapamycin
NC1/ NC2 domain	noncollagenous domain 1/ domain 2
NFκB	nuclear factor-κB
NGS	Next generation sequencing
NME	new molecular entity
PAX5	paired box gene 5
PBMCs	peripheral blood mononuclear cells
PBS	Phosphate-Buffered Saline
PCs	plasma cells

PCR	polymerase chain reaction
PDD	phenotypic drug discovery
PDGF/PDGFR	platelet-derived growth factor/ PDGF-receptor
PE	phycoerythrin
PEG400	Polyethylene glycol 400
PI	propidium iodine
PI3K	phosphoinositide 3-kinase
PMNs	polymorphonuclear neutrophils
PP	Pyrvinium Pamoate
RA	Rheumatoid arthritis
RAS/RAF	rat sarcoma/rapidly accelerated fibrosarcoma
RNA/RNA-Seq	ribonucleic acid / RNA sequence
ROS	reactive oxygen species
SLE	Systemic lupus erythematosus
SOCS3	Suppressor of cytokine signaling 3
STAT3	signal transducer and activator of transcription 3
TACI	TNF transmembrane activator and calcium modulator and cyclophilin ligand interactor
T-bet	T-box expressed T cells
TDD	Targeted drug discovery
TMB	3,3',5,5'-tetramethylbenzidine
TNF-α	Tumor necrosis factor-α
VEGF/VEGFR	vascular endothelial growth factor/ VEGF receptor
vWFA2	von Willebrand factor A–like domain 2
XBP-1	X-box binding protein 1

Table of contents

1. Introduction

1.1 Drug discovery and development

1.1.1. Overview of drug discovery and development

Drug discovery and development is a challenging task requiring substantial amount of time and money. According to an economic model proposed by Paul *et al.* (1), the estimated total time and cost required for a typical large pharmaceutical company to launch a new molecular entity (NME), a medication containing an active ingredient that has not been previously approved for marketing in any form, would amount to 13.5 years and 1.78 billion US dollars (**Fig 1.1**). (N.B., the time and cost of target discovery research as well as post-launch investigation is excluded.)

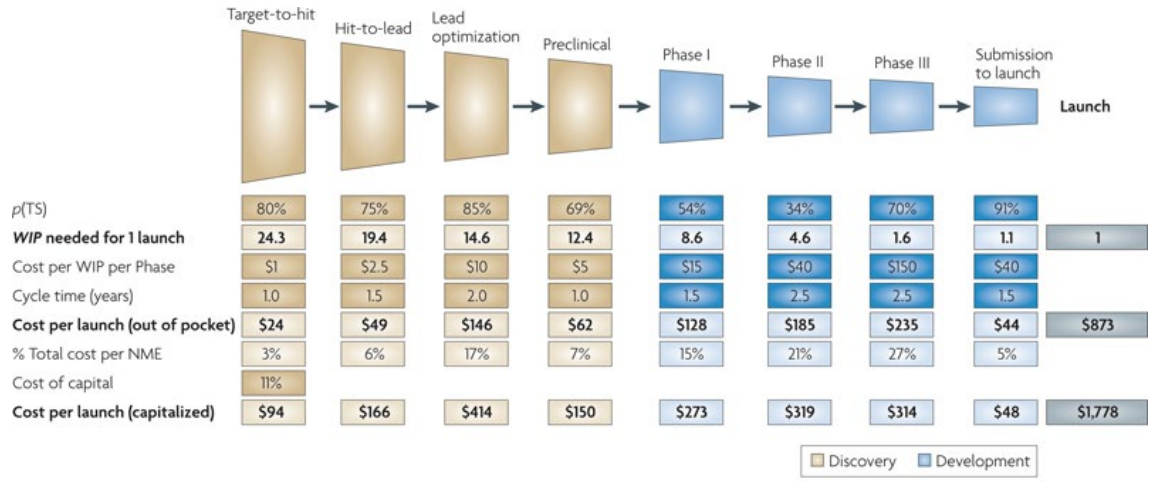

Fig1.1 Process of drug development and cost. Abbreviations: *p*(Ts): the probability of successful transition from one stage to the next, *WIP* (work in process): the number of candidates needed in each stage to achieve one new molecular entity (nME) launch. This model does not include investments for exploratory discovery research, post-launch expenses or overheads (that is, salaries for employees not engaged in R&D activities but necessary to support the organization). (from[1])

The process of drug development consists of two steps, preclinical and clinical steps. The former includes target identification and validation, where the biological effect and safety of the target will be investigated in vitro as well as in animals. Studies concerning pharmacodynamics, mutagenicity, teratogenicity, carcinogenicity, photocarcinogenicity, adsorption, distribution, metabolism, and excretion will be performed in this step (2).

In clinical step, candidate drugs which successfully pass the preclinical stage will be studied in humans. This step can be divided into four phases: 1) Phase I, test in 20-100 healthy volunteers or people with the disease to investigate the safety and dosage, 2) Phase II, test in up to several hundred people with the disease to investigate efficacy and side effects as well as optimal dose, 3) Phase III, test in 300 to 3,000 patients who have the disease to investigate efficacy and to monitor adverse reactions, and 4) Phase IV, a post drug approval test in several thousand patients who have the disease to keep monitoring safety and efficacy (3).

With regard to the rate for a new drug to be approved, only 35.2 % of the initial compounds of interest succeed to enter the clinical phase, and afterwards, only 8% of them proceed to the launch (**Fig 1.1**).

1.1.2 Factors hindering drug approval at preclinical steps

As shown in the low successful rate in phase II trial, 34% (**Fig 1.1**), “lack of efficacy” is the primary reason for failure of the projects (1). However, some problems can be detected at preclinical steps, namely, target identification.

First problem in the preclinical step of drug discovery is a low reproducibility of published findings. Prinz *et al.*, scientists from a pharmaceutical company Bayer, reported that, among 67 in-house validation projects of published findings, complete reproducibility was observed in only 14 projects (21%). Moreover, 43 projects (65%) had to be terminated because of the inconsistencies in results. In 11 projects (16%), the finding was not reproducible even when the validation was performed exactly the same manner as in the original publications (4). Similarly, in an attempt to test the reproducibility of 53 published papers including those presented in journals with >20 impact factor, Begley and Ellis reported that the compatible results could be obtained only in 6 cases (11%) (5).

Another factor contributing to a high failure in target identification is the method of approach. In target identification step, two major types of method are being employed, 1) phenotypic drug discovery (PDD), where, without knowing the molecular target, physiological responses induced by the substance of interest are evaluated by means of assays concerning cell cycle, differentiation, migration, cytokinesis, metastasis, tissue regeneration and stem cell induction, renewal, and differentiation (6, 7), and 2) targeted drug discovery (TDD), where a certain molecular target is selected beforehand and its effect on biological system is subsequently tested. In PDD, the detailed mechanism of action will be investigated afterward whereas the target in TDD approach is typically selected based on the results of previous in vivo human/animal and/or cellular studies investigating the relevance of those molecules to disease of interest (6, 7). Therefore, PDD is a function-based approach whereas TDD is a hypothesis-driven approach.

Since the advancement in molecular biology and clarification of human genome in 1990s, there has been an expectation that TDD approach would enhance the drug discovery process. However, despite the increased number of candidate molecules in drug discovery

step, the actual number of the US Food and Drug Administration (FDA) approved NMEs has been relatively stable for the last 20 years (7). Among 50 first-in-class small-molecule drugs approved between 1999 and 2008, PDD approach led to the approval of 28 drugs whereas the number was 17 in TDD approach (8).

Even though the precise reason for this less efficiency in TDD approach is unknown, one factor could be the redundancy in the drug discovery (9). One report revealed that a significant numbers of drug-development projects were targeting the same molecules, mTOR, cMet, VEGF/VEGFR, c-Kit. PDGF/PDGFR, PI3K, HER2, and EGFR, and there were >24 ongoing projects per each molecule. Moreover, in the case of drug development projects targeting VEGF/VEGFR, high unsuccessful rate of 30-40% has been reported (10). In other words, substantial amount of resources and commitment from pharmaceutical companies is inefficiently directed at the same molecules but the effort often does not reach a successful launch.

In conclusion, launching a new drug requires enormous amount of time and money and the advance in molecular biology and a better understanding of diseases pathogenesis have not yet brought satisfactory improvement in the drug development process.

1.1.3 Drug repurposing

Drug repurposing is an approach to find new indications of existing drugs and widen their clinical applications. By utilizing previously studied bioavailability, efficacy and safety of the drugs of interest together with more detailed clarification of the pathogenesis of target diseases, a more time-saving and cost-efficient drug development is feasible (11, 12).

Among a number of successful cases, metformin, an oral anti-type2 diabetic medication, is now being investigated its property as an anti-cancer drug. In diabetes, therapeutic action of metformin includes suppression of hepatic glucose output and increase in glucose uptake in the muscle by regulating genes involved in gluconeogenesis in the liver and genes encoding glucose transporters in the muscle. As a result, metformin decreases plasma levels of glucose and insulin (13).

Along with its efficacy in diabetes, there had been accumulating observational findings that diabetic patients treated with metformin showed a lower risk of cancer development as well as lower cancer-related mortality compared to those receiving other forms of treatment such as exogenous insulin, sulfonylurea (14-16). A meta-analysis of 66 studies of diabetics receiving metformin concluded that the drug treatment was associated with 14% and 30% reduction in cancer incidence and mortality, respectively (16). Another study reported a similar result, 31% reduction in cancer incidence/mortality risk, and this was especially correlated with pancreatic and hepatocellular cancer (17). This led to a re-evaluation of metformin as an anti-cancer drug.

Studies have demonstrated anti-cancer property of metformin including 1) direct inhibitory effect of the drug on mitochondria complex I formation, which is required for ATP production and the subsequent ATP triggered signaling events to modulate mTOR activity, 2) indirect effect to generate starvation in cells which subsequently inhibits energy-dependent insulin/insulin-like growth factor-1 (IGF1) signaling pathway. This leads to the decrease in downstream events involving PI3K/Akt/mTOR and/or RAS/RAF/mitogen-activated protein kinase (MAPK) pathways (18, 19). Furthermore, other off-target effects of metformin on cell apoptosis (20), cell migration (21), gene expression in cancer cells (22), modulation of memory T cell function (23) has been reported.

The positive effect of metformin on cancer prognosis has been tested in human clinical trials. In prostate cancer, patients were pre-treated with metformin while waiting for the radical prostatectomy and the tissue proliferation was assessed by Ki67 staining. Among the available samples of 22 cases, 28.6% reduction in proliferation was observed (24). A similar effect was observed in endometrial cancer patients (n=31). Before and after 4-week metformin treatment, 90% of patients showed a reduction in cell proliferation assessed by Ki-67 staining ranging from 30.3%-51.0%. Moreover, level of phosphorylated AMPK (5'-adenosine monophosphate-activated protein kinase, an enzyme indirectly activated by metformin) was significantly elevated in post-treatment cancer tissue (25). At the year of 2016, more than 50 phase I-III clinical trials concerning efficacy of metformin in cancer prevention, presurgical treatment, and adjuvant treatment were ongoing (19).

As has been stated above, drug repurposing is a highly useful and promising approach in exploring new treatment strategy and could offer a solution to unmet medical needs.

1.2 Immune system and Autoimmune diseases

1.2.1 Immune system

The development of immunology could trace back to the Edwards Jenner's discovery that small pox, a lethal infectious disease mediated by variola virus, could be prevented by inoculate people with pus from cowpox blister (26). This finding, now acknowledged as the foundation of vaccination, is based on the protective mechanism against pathogens, namely, immune system.

Two types of immune system have been recognized, innate immunity and adaptive immunity. Innate immunity is known as the first lines of defense. The mode of action for the

protection includes epithelial and/or mucosal barriers, destruction of the pathogens via compliment system, and phagocytic activity by cells expressing receptors (pattern recognition receptors) recognizing non-self, common structures of pathogens such as polysaccharide, lipoprotein, nucleic acids (Pathogen-associated molecular patterns). Even though its action is rapid, within minutes, and can react to wide range of pathogens, innate immune response does not last long, lacks in pathogen-specificity, and does not induce immune memory (27).

On the other hand, adaptive immunity is known for its target-specific immunological response and immune memory. Whereas innate immunity uses universally conferred, or genetically encoded, pattern recognition receptors, adaptive immunity acquires antigen-specificity through its development via a mechanism called clonal selection and expansion (27)(**Fig 1.2**).

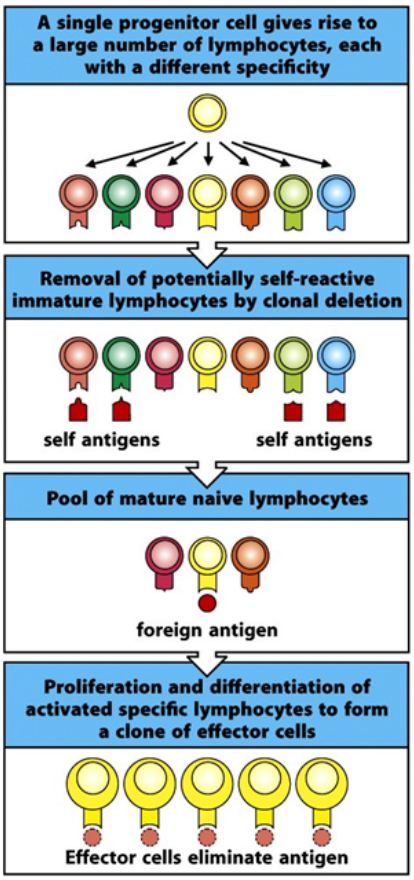

Fig1.2 Clonal selection in adaptive immunity. A large number of lymphocytes bearing a receptor recognizing single antigen arise from lymphoid progenitor cells. Through developmental stages, lymphocytes inducing strong self-reactive response will be eliminated. When mature naïve lymphocyte encounter a pathogenic antigen, only cells bearing specific receptor against the corresponding antigen will be activated and proliferate for a clone formation. (from[(27))

T cells and B cells are the key players in adaptive immunity, and each cell expresses unique cell surface receptor recognizing a specific antigen. In case of the invasion by pathogens, only lymphocytes carrying specific receptors responding to the corresponding pathogens are selected and proliferate for the following antigen clearance process. With regard to the effector functions of lymphocytes, T cells exert their properties via their own cytotoxicity ($CD8^+$ T cells) or by providing other immune cells, such as B cells, neutrophils, macrophages, with “help” so that those cells can function effectively (helper T cells). On the other hand, the most crucial role of B cells in adaptive immunity is to differentiate into plasma

cells and produce antibodies, or immunoglobulin, which can eliminate pathogens through neutralization, opsonization, and complement activation (**Fig 1.3**).

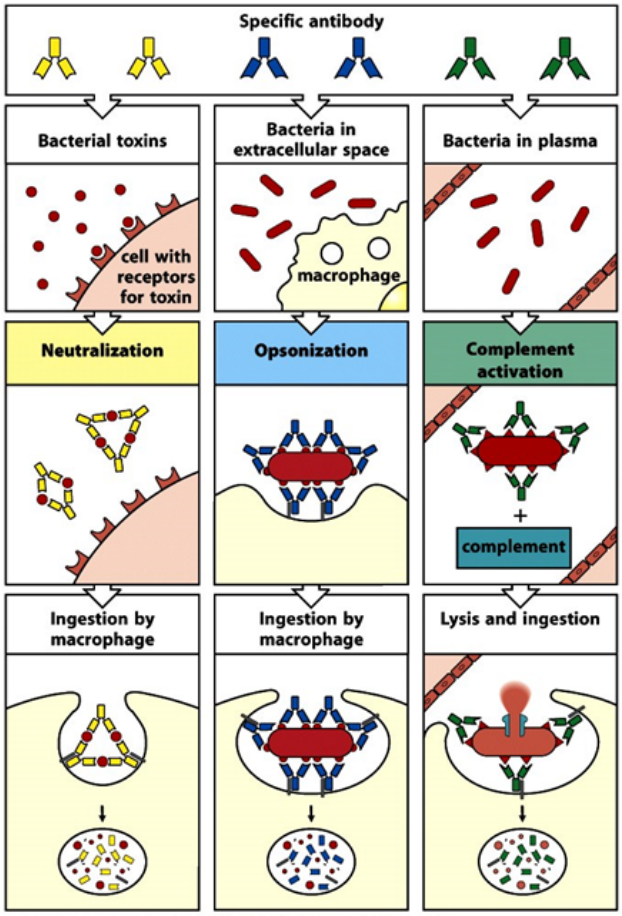

Fig1.3 Pathogen clearance by immunoglobulin. Antibody can eliminate pathogens by neutralization (left panel), opsonization (middle panel), and complement activation (right panel). (from(27))

A fraction of T and B cells remain as memory cells to confer long-lasting immunity and, upon re-challenge by the same pathogen, they can act rapidly to differentiate effector cells (27). **Table 1.1** illustrates the summary of the response by innate and adaptive immunity.

Table1.1 Comparison of the phases of immune responses by innate immunity and adaptive immunity. (revised from(27))

Phases of the immune response			
Responses		**Typical time after infectino to start of response**	**Duration of response**
Innate immune response	Inflammation, complement activation, phagocytois, and destruction of pathogen	Minutes	Days
Adaptive immune response	Interaction between antigen-presenting cells and antigen-specific T cells: recognition of antigen, adhesion, co-stimulation, T cell proliferation and differentiation	Hours	Days
	Activation of antigen-specific B cells	Hours	Days
	Formation of effector and memory T cells	Days	Weeks
	Interaction of T cells with B cells, formation of germinal centers, Formation of effector B cells (plasma cells) and memory B cells. Production of antibody	Days	Weeks
	Emigration of effector lymphocytes from peripheral lmphoid organs	A few days	Weeks
	Effector cells and antibodies eliminate the pathogen	A few days	Weeks
Immunological memory	Maintenance of memory B cells and T cells and high serum or musosal antibody levels. Protection against reinfection	Days to weeks	Can be lifelong

1.2.2 Autoimmune diseases

The primary purpose of immunity is to protect a host from harmful pathogens. In order to avoid attacking host's own components, a mechanism for the immune system to discriminate self from non-self is required. When this checking scheme, or self-tolerance, is impaired, the damage resulting from host's own immune response could be presented as autoimmune diseases (ADs) even though the presence of autoimmunity itself is not necessarily linked to the development of ADs.

According to an epidemiological study from USA, 3.2% (one in 31 American people) were estimated to be affected by ADs, and the risk of developing ADs was 2.7 times higher in women than men. The most prevalent diseases were hyperthyroidism, insulin dependent diabetes mellitus (IDDM), pernicious anemia, rheumatoid arthritis (RA), thyroiditis, and vitiligo, which accounted for 93% of all the diseases surveyed (28).

With regard to the system enables immune system to discriminate self from non-self, lymphocytes are to be "educated" during the developmental stages and harmful self-damaging lymphocytes will be eliminated in the primary lymphoid tissues (central tolerance) and in the periphery (peripheral tolerance). In the case of T cells, this process takes place in thymus; Immature T cells which can recognize major histocompatibility complex (MHC) class molecules expressed by thymic stromal cells can proceed to further development (positive selection), and T cells bearing TCRs which strongly recognize self-antigens provided by MHC-expressing thymic macrophages and dendritic cells will be subsequently deleted (negative selection). Thus, T cells capable of recognizing "self" but do not exhibit excessive reaction to self-antigens leave thymus and enter the periphery. Similarly, immature B cells bearing surface IgM are to be tested self-reactivity in bone marrow before entering the periphery. B cells expressing autoantigen-reactive receptors are yield for receptor editing and if this step is unsuccessful, these self-reactive cells will be eliminated by apoptosis (29). In the periphery, control of self-reactive lymphocytes is exerted by anergy (30-32), deletion (33, 34), suppressive functions by regulatory T cells (35, 36).

In addition to the system eliminating autoreactive lymphocytes discussed above, another crucial factor in the development of ADs is genetics. The susceptibility of some mice strain to certain autoimmune diseases (i.e. NOD mice as an animal model for type 1 diabetes or NZB/W F1 mice for SLE), a high concordance of 25% for monozygotic twins to develop SLE

(37) as well as higher SLE incidence in African-American women compared to Caucasian women (38), and different disease incidence in men and women, are all suggestive of genetic association in ADs. **Table 1.2** and **Table 1.3** illustrate examples of gene associations with autoimmune symptoms and association of human leukocyte antigen (HLA) serotype with ADs.

Table1.2 Genetic association in autoimmune syndromes. (revised from (27))

Proposed mechanism	Murine models	Disease phenotype	Human gene affected	Disease phenotype
Antigen clearance and presentation	C1q knockout	Lupus-like	*C1QA*	Lupus-like
	C4 knockout		*C2, C4*	
			Mannose-binding lectin	
	AIRE knockout	Multi-organ autoimmunity resembling APECED	*AIRE*	APECED
	Mer knockout	Lupus-like		
Signaling	SHP-1 knockout	Lupus-like		
	Lyn knockout			
	CD22 knockout			
	CD45 E613R point mutation			
	B cells deficient in all Src-family kinases (triple knockout)			
	Fc-γRIIB knockout (inhibitory signaling molecule)		*FCGR2A*	Lupus
Co-stimulatory molecules	CTLA-4 knockout (blocks inhibitory signal)	Lymphocyte infiltration into organs		
	PD-1 knockout (blocks inhibitory signal)	Lupus-like		
	BAFF overexpression (transgenic mouse)			
Apoptosis	Fas knockout (lpr)	Lupus-like with lymphocyte infiltration	*FAS* and *FASL* mutations (ALPS)	Lupus-like with lymphocyte infiltration
	FasL knockout (gld)			
	Bcl-2 overexpression	Lupus-like		
	Pten heterozygous deficiency			
T_{reg} development/function	*scurfy* mouse	Multi-organ autoimmunity	*FOXP3*	IPEX
	foxp3 knockout			

Table1.3 Association of HLA serotype and susceptibility to autoimmune diseases. (revised from (27))

Associations of HLA serotype susceptibility to autoimmune disease			
Disease	**HLA allele**	**Relative risk**	**Sex ratio (♀:♂)**
Ankylosing spondylitis	B27	87.4	0.3
Acute anterior uveitis	B27	10	<0.5
Goodpasture's syndrome	DR2	15.9	~1
Multiple sclerosis	DR2	4.8	10
Graves' disease	DR3	3.7	4-5
Myasthenia gravis	DR3	2.5	~1
Systemic lupus erythematosus	DR3	5.8	10-20
Type 1 diabetes mellitus	DR3/DR4 (heterozygote)	~25	~1
Rheumatoid arthritis	DR4	4.2	3
Pemphigus vulgaris	DR4	14.4	~1
Hashimoto's thyroiditis	DR5	3.2	4-5

On the other hand, environmental factors are not negligible considering majority of people possessing susceptible genes do not develop the disease, 75% discordance in induction of SLE among monozygotic twins. For example, RA is a joint-destructive disease characterized by the presence of antibody against citrullinated protein (anti-citrullinated protein antibody, ACPA) (39). Even though smoking and periodontitis had been identified as environmental risk factors (40, 41), the significance of these habit/event on the disease was not understood. However, subsequent studies demonstrated that epithelial damage by smoking and the infection with *Porphyromonas gingivalis*,bacteria, a bacteria responsible for most cases of periodontitis, can induce peptidylarginine deiminases (PAD), an enzyme facilitates citrullination of various physiological peptides (39, 42). Therefore, originally harmless peptides can be transformed into neo-antigen by smoking or bacterial infection via citrullination mediated by PAD and presented to immune cells as foreign antigen. This leads to the formation immunocomplex consisting of citrullinated protein and APCA, which subsequently stimulate monocyte/macrophage to release pathogenic cytokine such as IL-6 and TNF-α (39). This is one example linking environmental factor with loss of self-tolerance.

Thus, excess self-reactive immune response leading to tissue/organ damages is the concept of ADs and their cause is multifactorial. Even though all immunological reactions could be responsible for the pathogenesis, when adaptive immunity, especially B cell immunity, is employed in the process of the development of ADs, its involvement can be seen as a presence of antibodies against self-components. **Table 1.4** illustrates examples of disease specific autoantibodies.

Table1.4 Examples of autoantibodies. (revised from[(43))

Disease	Autoantibody	Clinical associations
SLE	dsDNA	Highly specific for SLE with renal disease and increased IFN
	Sm	Highly specific for SLE with renal disease and increased IFN
	Ribosimal P0, P1, P2	Highly specific for SLE, increased risk of neuropsychiatric disease
	RNA helicase A	Highly specific for SLE; marker for early lupus
Mixed connective tissue disease (MCTD)	RNP	Highly sensitive for MCTD but not specific
Systemic sclerosis	Scl-70 (topoisomerase I)	Highly specific for SSc with poor prognosis
	Fibrillarin	Highly specific for SSc
	RNA polymerase I/III	Highly specific for SSc with poor prognosis
CREST syndrome	Centromere	
Polymyositis	tRNA synthetases	Highly specific for myosits with "anti-synthetase syndrome" (myositis, interstitial lung disease, inflammatory arthritis, Raynaud's phenomenon, mechanic's hands)
	Signal recognition particle (SRP)	Highly specific for myositis with poor prognosis
Sjögren's syndrome (SS)	Ro60 (SS-A)	Sicca syndrome in primary or secondary SS, neonatal lupus/heart block
	Ro52	Sicca syndrome in primary or secondary SS, neonatal lupus/heart block
	La (SS-B)	Sicca syndrome in primary or secondary SS, neonatal lupus/heart block
Rheumatoid arthritis (RA)	Cyclic citrullinated peptide	Highly specific for RA

1.2.3 Epidermolysis bullosa acquisita (EBA)

Epidermolysis bullosa acquisita (EBA) is a rare autoimmune skin blistering disease characterized by the autoantibody production against type VII collagen (COL7), a structural protein consisting of anchoring fibril which is located at the dermal-epidermal junction (DEJ) of skin (44). (**Fig 1.4**). Its annual incidence is 0.2-0.5 case per million people, and patients with EBA may show either classical mechanobullous phenotype associated with tense blisters and skin fragility on trauma-prone, extensor side of skin (33%), or inflammatory phenotype resembling bullous pemphigoid or mucous membrane pemphigoid (66%) (45).

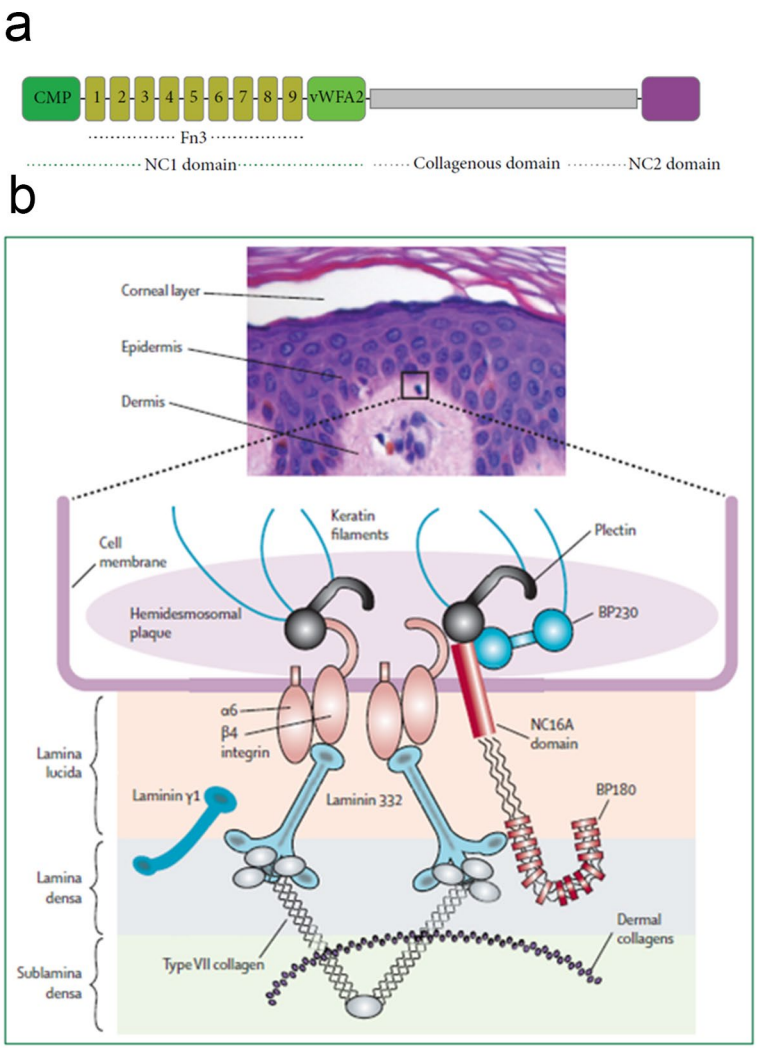

Fig1.4 Schematic diagram of dermal-epidermal junction and type VII collagen. (a) Type VII collagen (COL7) consists of noncollagenous domain 1 (NC1 domain), collagenous domain, and noncollagenous domain 2 (NC2 domain). The C-terminal of NC1 shows immunogenicity and has high homology with von Willebrand factor A, therefore this part is termed von Willebrand factor A–like domain 2 (vWFA2). **(b)** Location of Type VII collagen in the skin. (from(44, 45))

With regard to the disease development, previous studies have suggested that a cascade of events triggered by autoantibody production leads to the clinical skin manifestations (**Fig 1.5**).

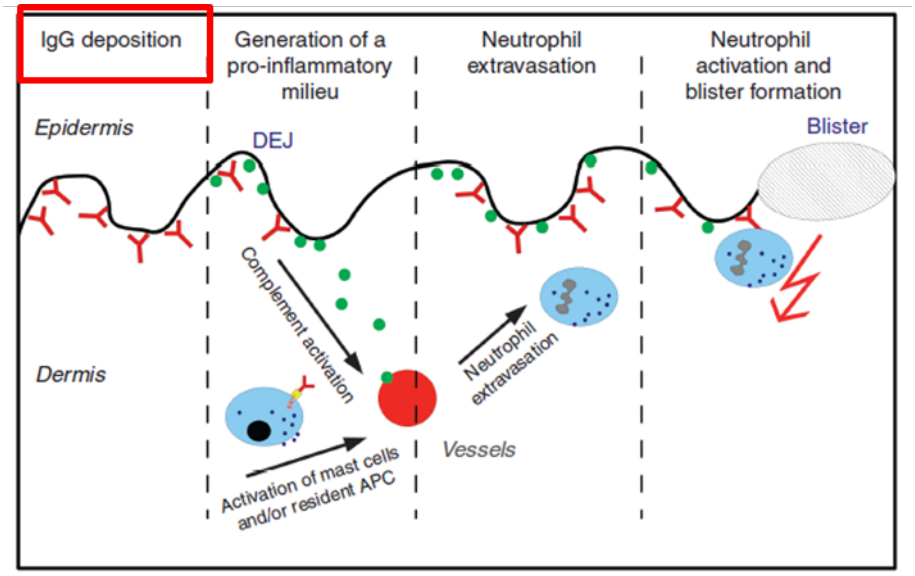

Fig1.5 Suggested mechanism of EBA disease induction. Autoantibody directed at type VII collagen forms immunocomplexes at dermal-epidermal junction, which activates complement system via interaction with Fc receptors. Recruited neutrophil will be activated and release tissue-injuring substances such as reactive oxygen species, leading to the blister formation. (from[(46)])

In 2005, Sitaru *et al.* confirmed the pathogenicity of antibody against COL7 in disease induction. In this study, affinity purified IgG obtained from rabbits immunized with recombinant noncollagenous 1(NC1) domain of murine COL7, which has been identified to be immunodominant (47), was repetitively injected in three different strains of mice: nude mice, BALB/c, and C57BL/6. All passive transfer of antigen-specific IgG, dose ranging from 3.75mg to 15mg, induced skin lesions such as blisters, erosions, and crusts accompanied by the deposition of rabbit IgG as well as murine C3 at DEJ (48). In the same year, Woodley *et al*. also demonstrated the pathogenicity of the anti-collagen VII antibody by inducing subepidermal skin blisters and erosions in the hairless immune competent mice injected with IgG fraction from rabbits immunized with human type VII collagen (49). In the following year, Woodley *et al*. confirmed the pathogenicity of EBA patients' IgG against NC1 domain of COL7. When passively transferred with affinity purified human EBA IgG, SKH1 mice

developed blisters, erosion, and blisters. Moreover, more intense disease severity was observed when mice received higher dose of antibody (50). In human, there was a case report of a baby who presented multiple erosions, blisters at birth and was born to a 32 year-old mother with EBA (51). Serum sample from the infant demonstrated IgG deposition at DEJ on salt-split primate skin, and was also positive for ELISA detecting IgG directed at NC1 domain of COL. With only supportive care, all of the skin lesions spontaneously subsided at two month of age. Based on the serological assessment and clinical course, a diagnosis of congenital epidermolysis bullosa acquisita was made and vertical transfer of EBA antibody from mother was speculated to have induced the neonatal skin lesions. Thus, autoantibody production is strongly connected with disease induction of EBA *in vivo* and in humans.

Treatment of EBA is challenging and is being performed empirically in most cases. Systemic used of corticosteroids is the mainstream, followed by other immunosuppressive agents including methotrexate, azathioprine, cyclosporine, cyclophosphamide (45). Other than that, treatments with dapsone, colchicine, intravenous immunoglobulin have been reported to offer favorable outcomes. A retrospective clinical follow-up of 30 EBA cases reported that, at one year after initiation of the treatment, complete or partial remission was observed only in 33.3% or 20.8%, respectively, and median time to remission was nine months (52). Even though the rarity of this disease is an obstacle to conduct more convincing controlled studies at larger scales, high dependence on unspecific immunosuppressive treatments with relatively low efficacy urges to explore better treatment options in EBA.

1.3 Treatment of autoimmune diseases

1.3.1 Immunosuppression and Adverse effects

Given that many manifestations in ADs stem from dysregulated immune response, it is plausible that the immunosuppression is the commonly practiced treatment method. Currently used immunosuppressive drugs include corticosteroids, cytotoxic agents (i.e. cyclophosphamide, an alkylating agent), antimetabolites (i.e. methotrexate, azathioprine, mycophenolate), pooled polyclonal antibodies, and newly developed drugs affecting cell surface molecules, soluble mediators such as cytokines, and intracellular proteins (53, 54).

Since the discovery of their anti-inflammatory effect in 1940's, Glucocorticoids (GCs), steroid hormones secreted from adrenal glands, have been widely used as therapeutics in autoimmune disorders (55, 56). Their functions can be exhibited in a variety way, including regulation in cytokine production, phagocytosis, antigen-presentation, migration, and survival in immune cells (57, 58).

GCs induce cell death to lymphocytes and their progenitors (59, 60), which is the rationale of the use of glucocorticoids in chemotherapies of hematologic malignancies (61, 62). With regard to the steroid sensitivity of different cell types, Liddicoat *et al* demonstrated that, using PBMC from healthy human donors, peripheral B cells were the most sensitive population to dexamethasone-induced apoptosis (survival index (S.I.) of 0.41) followed by natural killer (NK) cells (S.I. 0,60), and peripheral T cells (S.I. 0.98) (60). This high glucocorticoid induced cell death (GICD) in normal B cells was correlated with the expression of glucocorticoid receptors (GR) 1A3, one of untranslated exons expressed exclusively in hematopoietic cells as well as brain (63-65). GR 1A3 could regulate GICD by 1) promoting transcription of

pro-apoptotic genes (65, 66), and by 2) increasing the transcription of membrane located GR which induces cell lysis (67-69).

At molecular level, GCs can modulate transcription of steroid-target genes and/or other genes regulated by transcription factors such as activator protein-1 (AP-1) and nuclear factor-κB (NFκB). Upon pro-inflammatory stimuli, AP-1 and NFκB are activated to facilitate the downstream transcription of pro-inflammatory molecules (70, 71). GCs- GR complex can counteract with AP-1 and NFκB and suppress their transcription activities, which ultimately results in a reduced inflammatory response. In addition to AP-1 and NFκB, glucocorticoids can also interact with other transcription factors such as the interferon (IFN) regulatory factor 3 (IRF3), T-box expressed T cells (T-bet), and GATA3 (72). In addition, GCs-GR complex can modulate intracellular signaling pathways by interacting with molecules such as the extracellular signal-regulated kinases (ERKs), the c-Jun NH2-terminal kinases (JNKs), the p38 isoforms (p38s), and ERK5 (73). Also, the existence of GR isoforms and modifications of the structure of GR by phosphorylation, ubiquitination, acethylation also contribute to the functional diversity of steroids (74).

Despite the clinical benefit, however, immunosuppression is also directed at protective immunity. Therefore there will be always a trade-off between treatment benefits and adverse effects including opportunistic infections. In fact, infectious disease is the major cause of death in patients with ADs.

In a review about infection-related morbidity and mortality in patients with ADs (SLE, RA, myositis, Granulomatosis with polyangiitis, and systemic sclerosis), Falagas *et al.* reported that 51% of the studied population had episode(s) of infection and 29% had serious cases. Overall mortality due to infection was 5.2% (range 1.2–36%) whereas the mortality of serious cases was 24% (75). With regard to the contribution of immunosuppressive

treatment to infection, a comparative study between RA patients receiving steroid treatment (n=112) and those who did not (n=112) demonstrated that steroid use, especially 10-15mg/day prednisolone, was associated with the incident of hospitalization-requiring infectious diseases (odds ratio 8.0) (76).

Not only infections, osteoporosis, diabetes, cardiovascular complications (hypertension, dyslipidemia), peptic ulcers, mood disorders, glaucoma, growth retardation in children, hormonal disturbance are all associated with treatment with GC (56, 77, 78). With regard to steroid induced osteoporosis, as low as oral prednisone 5mg/day intake can reduce bone mineral density (79), and a regular assessment of bone metabolism and prophylactic treatment with bisphosphonate, vitamin D, or calcium is recommended (77). Similarly, for the management of steroid-induced hyperglycemia, which is attributable for GCs function to create insulin resistance and to increase glycogenesis in liver (80), oral glucose lowering agents are inadequate in many cases and exogenous insulin is often required (81). Also, long-term (in years), high-dose (>8 mg prednisolone a day) use of GCs is considered to an independent risk factor for the development of cardiovascular complications in patients with ADs (82).

Thus, along with an ongoing immunosuppressive treatment, appropriate monitoring for its side effects is indispensable and additional medical interventions are often required, and that could be another burden to patients, to care-provider, and to the society.

1.3.2 B cell-targeted treatment in autoimmune diseases

As discussed earlier (**1.2.2** and **1.2.3**), not all but some autoreactive antibodies play crucial roles in the pathogenesis of ADs. Considering that the source of these pathogenic antibodies

is B cell-derived plasma cells, regulating B cells immunity is an effective strategy for the treatment of ADs.

One example of B cell modulation in ADs is a use of rituximab, a monoclonal antibody against CD20 expressing cells. In RA, rituximab use is approved only in patients who failed to respond to anti-TNF treatment. However, in an open-label, randomized controlled, head-to-head study with 295 active seropositive RA patients, Porter *et al.* reported the equal efficacy of rituximab treatment (n=144) to TNF inhibitors treatment (adalimumab or etanercept, n=151) (83). When compared the change in disease severity assessed by DAS28 ESR (28 joint count disease activity score, an evaluation marker taking into account both clinical and serological findings) after 12 months of treatment, reduction in DAS28 ESR in rituximab group and TNF inhibitor were -2.6 [SD 1.4] and -2.4 [SD 1.5], respectively. In addition, the percentage of patients who switched the treatment form TNF inhibitor to rituximab was larger than that of patients switched from rituximab to TNF inhibitor (32% vs 19%, p=0.008), and the inefficacy was the primary reason. The cost-effectiveness analysis demonstrated that, during the 12-month study period, the total health-care costs in rituximab treatment were significantly lower than anti-TNF treatment (£9405 vs £11 523, p<0·0001).

Another B cell modulation can be exemplified with the development of belimumab in SLE. B lymphocyte stimulator (BLyS) is a member of TNF superfamily: soluble and membrane-bound proteins regulating immune responses and is a crucial growth factor for B cells (84). Its gene is expressed by cells of myeloid origin, and its receptors, TACI (TNF transmembrane activator and calcium modulator and cyclophilin ligand interactor), BCMA (B lymphocyte maturation antigen), and BR3 (BAFF/BLyS receptor3), are primarily expressed on B cells (84, 85). Upon BLyS-BLyS receptor ligation, B cell proliferation as well as

differentiation is promoted, results in increased immunoglobulin production both *in vitro* and *in vivo* (84).

It has been demonstrated that excess BLyS is associated with the development of autoimmune-like symptoms. Transgenic mice overexpressing BLyS spontaneously had higher numbers of mature activated B cells and plasma cells in the periphery (e.g. in spleen), showed an enhanced germinal center reaction and elevated circulating IgM/IgG, produced autoantibodies such as anti-double-stranded DNA antibody (anti-dsDNA Ab) and rheumatoid factor, and showed abnormal kidney function represented by proteinuria (86). Similarly, in human, Petri *et al*. showed that, in a two-year observational study with 245 SLE patients, clinical lupus disease activity was positively correlated both with presence of anti-dsDNA Ab and with plasma BLyS level. At the same time, anti-ds-DNA Ab level was associated with plasma BLyS level (85).

In 2000, Gross *et al*. engineered a soluble TACI-Ig fusion protein binding to active form of BLyS and tested its effect on B cell immunity (87). They demonstrated that binding of BLyS to B cells was prevented in the presence of TACI-Ig and the proliferation of active B cells was suppressed *in vitro*. Moreover, female NZBWF1 mice treated with TACI-Ig showed delayed onset of proteinuria and their overall survival was prolonged, which was accompanied by a significant reduction in the peripheral B cells. These findings highlighted a possibility of TACI-Ig, or neutralizing BLyS, as a potential treatment of autoimmune diseases and led to the production of belimumab; a human IgG1λ monoclonal antibody binding to soluble human BLyS.

In the phase II randomized, double-blind, placebo-controlled study of belimumab (n=449), active SLE patients treated with belimumab had a significant reduction in the peripheral blood B cell fractions; after one year treatment, the percentage reduction of $CD19^+$, $CD20^+$,

naïve B cells ($CD20^+/CD27^-$), activated B cells ($CD20^+/CD69^+$), and plasmacytoid B cells ($CD20^+/CD138^+$) were 49.3%, 54.1%, 70.8%, 70.4%, and 62.5%, respectively (88).

The clinical efficacy and safety was confirmed at a larger trial. In the 52-week phase III, randomized, placebo-controlled study of belimumab targeting 867 active SLE patients, the frequency of improvement in SLE Responder Index, a collective evaluation method consisting of physicians' assessment, disease exacerbation, change in disease activity index, was significantly higher in belimumab treated patients than that of placebo group. Serologically, belimumab treated patients had reduction in anti-dsDNA Ab and/or IgG, IgM, IgA level, recovered from low complimentemia. There was no difference in the incidence of adverse effects including infections, abnormal laboratory findings, or discontinuation of the treatment among the treatment groups. Additionally, steroid-sparing effect of belimumab treatment was also confirmed: the number of patients whose steroid dose was successfully decreased more than 50% was significantly higher in belimumab treated group (89).

Not only in SLE or RA, the efficacy of B cell modulation has been reported in other autoimmune diseases such as multiple sclerosis (90, 91), myasthenia gravis (92, 93), vasculitis (94). Thus, B cell-targeting treatment is an established strategy in the management of ADs.

1.3.3 Problems of newer therapeutics

Despite the remarkable clinical effects, one significant burden of newly developed therapeutics in ADs is cost.

An epidemiological study using data from The National Database of the Collaborative Arthritis Centres (NDBA) in Germany reported that, during the 10-year study period from 2002 to 2011, the cost for biologic anti-rheumatic diseases increased €3,598 for a younger patient (18-64 years old) and €2,265 for an older patient (>64 years old). Even though there was a reduction in the cost for inpatient treatment (hospital admission, length of hospital stay) and rehabilitation as well as a reduction in indirect medical cost (financial burden for sick leave or work disability), the overall increase of annual medical cost for a patient at working age and for a retired patient was €2,981 to €2,437 and €2,981, respectively (95).

Not only affecting medical economy, use of high-priced medications could also negatively influence on patients' disease outcome. In addition to the disease severity, age, or accessibility to rheumatologists, Desai *et al*. identified that the type of patients' insurance was also one distinct factor preventing RA patients form receiving a treatment with biologic agents (96), i.e. if a treatment with costly medications is not covered by insurance, patients are less likely to be treated with biologics. This indicates a possible delay of the optimal treatment, ill-health of patients, and subsequent increase of the indirect medical costs.

Another emerging issue of newer treatments is safety including the reactivation of hepatitis B virus (HBVR) among patients with hematological malignancy or autoimmune diseases receiving chemotherapy or treatment with biologics. Rituximab is the most reported drug among them. According to a case series analysis of five studies, incidence of HBVR was significantly higher in patients treated with rituximab (20 of 244, 8.2%) than those treated other treatment regimen without rituximab (3 of 453, 0.6%) (97). Analysis of 31 HBVR case reports of rituximab-treated patients with lymphoproliferative disorders revealed that in 29%, HBVR occurred more than 6 months after the last rituximab treatment, 17 out of 31 patients (55%) had liver failure and 15 (48%) died (97).

Upon HBV infection, in addition to the cytotoxic property of CD8+ cells, cytokines such as TNF-α, IFN-γ released by $CD8^+$ cells and/or NK cells play crucial roles in the eradication of the virus: viral load is decreased via mechanisms such as viral capsid destabilization, viral protein degradation, HBV RNA degradation (98). Even though the pathogenesis of HBVR and the its connection with B cell depletion therapy are yet to be clarified, previous studies suggest that lowering B cell number leads to the decreased T cell immune response against HBV, which allows the virus to replicate intensively (98, 99). Subsequently, liver dysfunction occurs as a result of strongly activated anti-viral immunological response, mainly due to the cytotoxic effect of $CD8^+$ T cells, when the immune reconstitution takes place after rituximab treatment (98, 100).

Under the current situation, high medical cost and unclear long-term safety could prevent patients' access to newer treatment options and its therapeutic efficacy cannot be evenly distributed.

1.4 Aim of the study

Most patients with ADs require life-long treatment. Therefore, an ideal treatment would be the one providing maximum benefit with minimum adverse effects. In this sense, the conventional steroid-based treatment is unsatisfactory.

Thanks to the advancement in the clarification of the pathogenesis at molecular level together with the development of target-specific medications, treatment options in ADs have been expanded. However, newer treatments are not universally available for all patients due to the cost and the uncertainty of long-term safety. Also, drug development is a daunting task requiring substantial amount of time and money with relatively low success-rate.

On the other hand, there is a possibility that already in-use drugs might possess unacknowledged, off-targeted properties as immunomodulators. Successful examples of drug repurposing led us to test this method in the discovery of alternative treatment options in ADs. Provided the crucial roles of B cells in the pathogenesis together with the availability of an animal model reproducing human disease, EBA was an ideal autoimmune disease to investigate.

Using a drug library containing licensed but off-patent chemical compounds and an EBA mouse model, the presented study aimed to discover unknown abilities of existing drugs to affect B cell immunity and to test their potentials as B cell modulating therapeutics in ADs.

2. Material and Method

2.1 Studies with human blood samples

Blood samples were obtained from healthy volunteers. Prior to the study participation, all donors provided written informed consent. The study was approved by the ethical committee of University of Lübeck (AZ: 09-140) and conducted according to the Declaration of Helsinki.

2.1.1 Isolation of peripheral blood mononuclear cells

Peripheral blood mononuclear cells (PBMCs) were isolated from EDTA anticoagulated whole blood by density gradient centrifugation over Ficoll-Paque PLUS (GE Healthcare, Uppsala. Sweden). The whole blood was diluted with Dulbecco's Phosphate-Buffered Saline (DPBS, gibco/Thermo Fisher Scientific, Waltham, MA, USA) at 1:1 (v/v). Diluted blood, 19 mL, was carefully layered onto 15 mL Ficoll-Paque in a 50 mL tube. The tubes were centrifuged at 400 g for 25 minutes (min), at room temperature (RT), without brake. After removing upper layer containing plasma, the ring-form layer of mononuclear cells (PMBCs) was taken to a new 50 mL tube. After washing the cell pellet twice with MACS buffer (PBS with 0.5% BSA (Carl Roth, Karlsruhe) and 2mM EDTA (Carl Roth, Karlsruhe) at 170 g for 10 min at RT, cells were resuspended in 2 mL MACS buffer in a 15mL tube, then the number of obtained cells was determined with manual counting with Neubauer chamber (Marienfeld Superior, Lauda-Königshofen, Germany) at dilution factor of 1:50. The cell suspension was washed again with MACS buffer at 330 g for 7 min at 4˚C, followed by B or T cell separation.

2.1.2 Magnetic-activated cell sorting of B and T cells

Human B cells or T cells were isolated by magnetic separation using B Cell Isolation Kit II or Pan T Cell Isolation Kit (Miltenyi Biotec, Bergisch Gladbach) based on the manufacturer's instruction. After the final washing step of PBMC isolation, cell pellet was resuspended with MACS buffer at 40 µL buffer/1x10^7 cells and labelled with a cocktail of biotin-conjugated antibodies against non-B cell surface molecules (CD2, CD14, CD16, CD36, CD43, and CD235a, for B cell isolation) or non-T cell surface molecules (CD14, CD15, CD16, CD19, CD34, CD36, CD56, CD123, and CD235a, for T-cell isolation) at 10 µL antibody/1x10^7 cells, then incubated for 10 min at 4˚C in the dark. Subsequently, 30 µL buffer/1x10^7 cells and anti-biotin monoclonal antibodies conjugated to MicroBeads was added at 20 µL antibody/1x10^7 cells, then incubated for 15 min at 4˚C in the dark. Magnetically labelled cells were washed, resuspended with MACS buffer at 500 µL buffer/1x10^8 cells, and then, passed through a column (LD columns for B cells and LS columns for T cells, Miltenyi Biotec, Bergisch Gladbach) placed on a magnetic separator (MACS Separators, Miltenyi Biotec, Bergisch Gladbach). Non-labelled cells are B cells or T cells, respectively, therefore the flowthrough was collected and the number of obtained cells was determined, kept on ice until use. The purity of isolated B cells or T cells was >95% or >90%, respectively.

2.1.3 Isolation of polymorphonuclear neutrophils

For assay of reactive oxygen species (ROS) production by immunocomplex (IC) stimulated polymorphonuclear neutrophils (PMNs), human PMNs were purified from EDTA-anticoagulated whole blood of healthy donors. PMN fraction was isolated by density gradient centrifugation using Polymorohprep™ (Axis-Shield/ Alere Technologies AS, Oslo, Norway). Whole blood, 18 mL, was layered onto the same volume of Polymorohprep™ in a

50 mL tube. The tubes were centrifuged at 430 g for 50min at RT, without brake. Among the two rings of cell layer, the bottom layer was collected to a new 50mL tube then washed with RPMI 1640 with phenol red (RPMI 1640 with HEPES and L-Glutamine, Lonza, Basel, Switzerland) at 240 g for 10 min at 4˚C. To remove red blood cells, the pellet was resuspended in 4 mL lysis buffer consisting of distilled water (Fresenius KABI, Bad Homburg v. d. Höhe) and 0.9% NaCl (Fresenius KABI, Bad Homburg v. d. Höhe) at 4:1 (v/v) and incubated for 30 seconds, then washed with RPMI with phenol. The lysis step was repeated until the red color of cell pellet faded. After the final lysis step, cell pellet was washed with Chemiluminescence (CL) medium consisting of RPMI without phenol red (RPMI 1640 with stab. glutamine, w/o Phenol red, w/o glucose, with 2.0 g/L NaHCO3 (GENAXXON bioscience, Ulm) supplemented with 1% heat-inactivated fetal calf serum (FCS, Biochron, Berlin), 2 g/mL glucose (Sigma-Aldrich, Hamburg), and 5.95 g/L HEPES (PAN Biotech, Aidenbach)).

2.2 Mice

B6.SJL-H2s (B6.s) mice were held at the animal facility at University of Lübeck and kept under pathogen-free condition. Mice aged 8-10-week were used for each experiment. Experimental procedures were performed under anesthesia with intraperitoneal (i.p.) injection of ketamine (70-80 mg/kg, Sigma-Aldrich, Hamburg) and xylazine (7-10 mg/kg, Sigma-Aldrich, Hamburg) so that the pain would be as minimal as possible. All studies were approved by the local authorities of the Animal Care and Use Committee (Kiel, Germany) and only certified individuals performed the animal experiments.

2.3 Compounds

Prestwick chemical Library® (Prestwick Chemical, Illkirch-Graffenstaden, France), a collection of 1,200 licensed but off-patent drugs, was used for *in vitro* screening. Compounds were provided on 96-well plates and dissolved at 10 mM in dimethyl sulfoxide (DMSO). Compounds were further diluted at desired concentration for each *in vitro* assay.

For *in vivo* studies, dipyridamole, colchicine, pyrvinium pamoate were purchased from Sigma-Aldrich (Hamburg). Docetaxel was purchased from Selleck Chemicals (Houston, TX, USA). As stock solutions, dipyridamole, pyrvinium pamoate, and docetaxel were dissolved in DMSO (Sigma-Aldrich, Hamburg) for the final DMSO concentration in intraperitoneal (i.p.) injection solution to be 10%. Colchicine was dissolved in DPBS. Dipyridamole and pyrvinium pamoate injection solution consisted of 10% DMSO, 40% Polyethylene glycol 400 (PEG400), 15% propylene glycol (all purchased from Sigma-Aldrich, Hamburg) and 35% DPBS. Docetaxel injection solution consisted of 10% DMSO, 30% PEG400, 0.5% Tween80® (Sigma-Aldrich, Hamburg), 5% propylene glycol, and 54.5% distilled H2O (Ampuwa®, Fresenias KABI, Bad Homburg v. d. Höhe). Mice in control group were administered solvent.

2.4 Cell culture and proliferation assay

For proliferation assay, isolated B or T cells were cultured on a 96-well flat-bottom culture plate for suspension cells (Sarstedt, Nürmbrecht) at 20,000 cells/ well (B cells) or 50,000 cells/well (T cells) density in 200 µL/well RPMI 1640 medium supplemented with 0.3 g/L L-glutamine (Lonza, Basel, Switzerland), 10% heat-inactivated FCS, 1% non-essential amino acids solution (NEAA, gibco/Thermo Fisher Scientific, Waltham, MA, USA), 100 U/mL penicillin and 100 µg/mL streptomycin (PAN Biotech, Aidenbach). Recombinant human IL-21 (IL-21, 100 ng/mL, Cell Sciences, Newburyport, MA, USA) as well as anti-human CD40

antibody (aCD40Ab, 1 μg/mL, clone # 82111, R&D systems, Minneapolis, MN, USA) were used for B cell stimulation. T cells were stimulated with anti-human CD3 antibody (0.5 μg/mL, clone UCHT1, BioLegend, Fell) and anti-human CD28 antibody (1.0 μg/mL, clone CD28.2, BioLegend, Fell). Cells were cultured for five days (B cells) or three days (T cells) in the presence or in the absence of indicated concentrations of compounds and kept in a humidified incubator at 37˚C with 5% CO_2. Compounds in the chemical library used in this project were dissolved in DMSO at the concentration of 10 mM. For in vitro assays, the final DMSO concentration was adjusted to be lower than 0.01%. Cell proliferation was quantified by 5-bromo-2'-deoxyuridine (BrdU) incorporation assay (Roche applied science, Penzberg) according to manufacturer's protocol. Briefly, cells were pulsed with BrdU (BrdU final concentration, 10 μM) for the last 16 hours of incubation. On the day of analysis, culture plates were centrifuged at 300 g for 10 min then the supernatant was removed by flicking off the plates. When the plates were dried completely, 200 μL/well fixation and DNA denaturation solution (ready-to use) was added to each well and incubated for 60 min at RT in the dark. After removing the solution by flicking off the plates, 100 μL/well peroxidase-conjugated anti-BrdU antibody (diluted provided stock antibody at 1:100) was added to each well and the plates were incubated for 120 min at RT in the dark. After 3 times wash the plates with PBS, enzymatic color reaction was developed by TMB and BrdU incorporated cells were detected by measuring the absorbance at 450 nm with a spectrophotometer (Wallac 1420 multilabel counter, PerkinElmer, Rodgau). All data were recorded in duplicate and results were normalized to the value obtained from stimulated B or T cells without drug treatment.

2.5 Cell viability assay

Cell viability was determined based on the cell membrane integrity (permeability) assessed by propidium iodine (PI, BioLegend, Fell) staining method. Isolated human B cells were cultured as described above. On day five, cells were harvested in 5 mL FACS tubes (Sarstedt, Nürmbrecht) and washed with DPBS and incubated with PI for 15 min at 4˚C at a final concentration of 5 µg/mL in 500 µL FACS buffer (PBS with 0.5% BSA). Percentage of PI positive cells was analyzed by flowcytometer (FACSCalibur, Becton Dickinson, Heidelberg) and cell viability was presented as PI negative cells. All data were normalized to the viability of stimulated B cells without drug treatment.

2.6 Cell preparation and quantification of ROS generation from IC-stimulated PMNs

ROS production by IC-stimulated PMNs was assessed by luminol-dependent chemiluminescense assay as previously described (101). Briefly, after the purification, obtained PMNs were resuspended in CL medium (see **Studies with human blood samples** section) so that the cell density would be $2x10^6$ cells/mL. Cell suspension was labeled with luminol solution (prepared by dissolving 2.2 mg luminol (Sigma-Aldrich, Hamburg) in 8.8 µL 2N NaOH solution (Carl Roth, Karlsruhe)) at a dilution of 1:20 ((v/v) luminol:PMNs) just before seeding on a plate. For IC formation, a white 96-well plate (Greiner Bio-One, Frickenhausen) was coated with 50 ng/well recombinant human collagen VII (hCol7, in house production) dissolved in 0.05 M carbonate-bicarbonate buffer (pH9.6) overnight at 4˚C. After washing with PBS-T (=PBS with 0.05% Tween 20®), plate was blocked with blocking buffer (1% BSA in PBS-T) for one hour. After washing, plate-fixed hCol7 was incubated with 0.224 µg/well recombinant anti-human Col7 IgG1 antibody (in

house production) dissolved in blocking buffer for one hour at RT for immunocomplex (IC) formation. After washing, 200,000 cells/well luminol-labeled PMNs were seeded on the IC-pre-coated plate in the presence or in the absence of indicated concentrations of drugs of interest. Released ROS was indirectly measured as luminescence from oxidized-luminol and presented as counted photon per min (Wallac 1420 multilabel counter, PerkinElmer, Rodgau). The reaction was recorded at 37˚C for 2 hours and 20 min (60 repeats). Overall ROS production was presented as area under the curve calculated from 60 repeats measurements.

2.7 Flowcytometry

For the study of *in vitro* plasmablast generation from human B cell, cell surface marker expression was analyzed. Human B cells were isolated from PBMCs and cultured as described above. On day five, all cells under each culture conditions were individually collected in 5 mL FACS tubes, washed with PBS and surface staining with the following antibodies was performed, FITC-conjugated mouse anti-human CD19 (clone HIB19), PE-conjugated mouse anti-human CD27 (clone M-T271), APC-conjugated mouse anti-human CD38 (clone HIT2), all purchased from BD Biosciences (Heidelberg). After washing, the pellet was resuspended in 100 µL FACS buffer then stained with the anti-CD19, anti-CD-27, and anti-CD-38 (all used at 1:20 dilution), then incubated for 15 min at 4˚C in the dark. Cell were washed and resuspended in 500 µL FACS buffer. The percentage of plasmablasts, determined as $CD19^{+}CD27^{++}CD38^{++}$ fraction (102-104), was obtained on a FACS Calibur flow cytometer (FACSCalibur, Becton Dickinson, Heidelberg). A total of 50,000 events per sample were recorded.

In *in vivo* experiments, numbers of total/antigen-specific B cells or plasma cells in the draining lymph nodes (LNs) were studied as previously described (105). Briefly, cell suspensions were prepared from popliteal and inguinal LNs harvested from recombinant murine vWFA2-immunized mice by breaking the capsule of lymph nodes and passing the samples through 70 µm cell strainers (BD Falcon, Heidelberg). After manually counting the total cells in each pool of LNs, $10x10^6$ cells were used for staining using 1.5 mL tubes (Sarstedt, Nürmbrecht). In order to prevent unspecific antibody binding, FcγRs were blocked with rat anti-mouse CD16/CD32 at 0.5 µg/million cells (Clone 2.4G2, BD Biosciences, Heidelberg) for 5 min at 4˚C in the dark, followed by surface staining with PE-conjugated rat anti-mouse CD138 (Clone 281-2, BioLegend, Fell, used at 1:400 dilution) and Alexa-405 (Life Technologies, Darmstadt)-coupled anti-mouse B220 (clone GK1.5, eBioscience, in-house production, used at 1:100 dilution) for 10 min at 4˚C in the dark. Cells were washed with PBS at 300 g for 10 min at 4˚C then resuspend in 100 µL/tube Cytofix/Cytoperm (BD Biosciences, Heidelberg) for cell fixation and permeabilization and incubated for 40 min at RT in the dark. After washing with 1xBD Perm/Wash™ Buffer (BD Biosciences, Heidelberg) at 450 g for 10 min at 4˚C, intracellular staining was performed with recombinant murine vWFA2 coupled with Alexa Flour 488 (Life Technologies, Darmstadt) at 1:100 dilution for 20 min at 4˚C in the dark for the detection of antigen-specific cells. Cells were washed again with 1xBD Perm/Wash™ Buffer at 450 g for 10 min at 4˚C, then resuspended in 500 µL/tube FACS buffer. Total numbers of each cell fraction were calculated by multiplying the manually counted total cell number in LNs by the frequency of each cell fraction obtained by LSRII flow cytometer (BD Biosciences, Heidelberg). One million events per sample were recorded and all data were analyzed using FlowJo software (TreeStar Inc., Ashland, USA).

2.8 Enzyme-Linked ImmunoSorbent Assay (ELISA)

In vitro immunoglobulin M and G production by human B cells was measured by Enzyme-Linked ImmunoSorbent Assay (ELISA). Briefly, isolated B cells were cultured as described above. On day five, culture supernatant was collected and stored at -20°C until analysis. A 96-well plate (NUNC immunolplate, Thermo Scientific, Waltham, MA, USA) was coated with 1:100 diluted goat anti-human IgM coating antibody or goat anti-Human IgG-Fc coating antibody (Bethyl Laboratories, Montgomery, TX, USA) in 0.05 M carbonate-bicarbonate buffer (pH 9.6) for one hour at RT. Followed by 30-minute blocking with blocking buffer (see **2.6 Cell preparation and quantification of ROS generation from IC-stimulated PMNs**), 1:2 diluted culture supernatant (blocking buffer was used for the diluent) was added and incubated for one hour at RT. After washing, 1:10,000 diluted detection antibody, HRP-conjugated goat anti-Human IgM or anti-Human IgG (Bethyl Laboratories), was added and incubated for 1 hour at RT. After washing, the enzymatic color reaction was developed with 1 step Turbo TMB-ELISA (Thermo Scientific) and stopped with 1 M H_2SO_4. Absorbance at 450 nm was read on a spectrophotometer (Wallac 1420 multilabel counter, PerkinElmer, Rodgau). All data were normalized to the value obtained from stimulated B cells without drug treatment.

The same method was employed for the detection of circulating total IgG or IgM in vWFA2-immunized mice using commercially available quantification set (Bethyl Laboratories). Briefly, after being coated with 1:100 diluted goat anti-mouse IgM coating antibody or goat anti-mouse IgG-Fc coating antibody (Bethyl Laboratories) in 0.05 M carbonate-bicarbonate buffer (pH 9.6) for one hour at RT, plates were blocked for 30 min at RT with blocking buffer. 1:10,000 (IgM ELISA) or 1:50,000 (IgG ELISA) diluted murine sera (blocking buffer was used for the diluent) obtained at different time points were added and

the plates were incubated for one hour at RT. HRP conjugated detection antibodies for human IgM or human IgG-Fc were diluted at 1:50,000 for both IgM and IgG ELISA. Color reaction was developed with 1 step Turbo TMB-ELISA and stopped with 1 M H_2SO_4. Absorbance at 450 nm was read on a spectrophotometer (Wallac 1420 multilabel counter, PerkinElmer). All data were quantified using a standard curve generated from the readouts of serially diluted reference serum provided in the measurement kit (Bethyl Laboratories).

Detection of circulating antigen-specific antibody in vWFA2-immunized mice was measured as previously described with minor modifications (45). Briefly, a 96-well plate was coated with 50 ng/well recombinant murine vWFA2 in 0.05 M carbonate-bicarbonate buffer (pH 9.6) overnight at 4°C in the dark. After washing and blocking with blocking buffer for 30 min, 1:20,000 diluted murine sera obtained at different time points were added and the plates were incubated for one hour at RT (blocking buffer was used for the diluent). After washing, 1:20,000 diluted detection antibody (peroxidase-conjugated donkey anti-mouse IgG (H+L) antibody, Jackson Immuno Research, West Grove, PA, USA) was added and incubated for one hour at RT. The reaction was developed with TMB and stopped with 1 M H_2SO_4. Absorbance at 450 nm was read on Wallac 1420 multilabel counter (PerkinElmer, Rodgau). All data were semiquantified using a standard curve generated from the readouts of serially diluted reference sera (a pool of sera from vWFA2-immunized mice). All samples were measured in duplicate. All steps in vWFA2-specific IgG subclass ELISA assays were performed in the same manner as vWFA2-specific IgG ELISA. Dilutions of serum samples and corresponding detection antibodies are the following; Serum 1:20,000, HRP conjugated goat anti-mouse IgG1 detection antibody 1:50,000 (A90-105P-34, Bethyl Laboratories), HRP conjugated goat anti-mouse IgG2a detection antibody 1:50,000 (A90-107P, Bethyl

Laboratories), HRP conjugated goat anti-mouse IgG2b detection antibody 1:100,000 (A90-109P-29, Bethyl Laboratories).

2.9 Induction of experimental EBA and treatment protocol

Experimental EBA was induced as described previously (45, 106). Briefly, recombinant von Willebrand factor A–like domain 2 (vWFA2) protein of murine type VII collagen (mCOL7) was produced using prokaryotic expression system (107). Mice were immunized with 120 μg/head vWFA2 protein in both hind footpads in conjunction with Titermax® (CytRx Corporation, Los Angeles, CA, USA) as adjuvant. 2 mg/mL vWFA2 protein solution in PBS was emulsified with the same volume of Titermax® and 60 μL (vWFA2 protein solution and Titermax was mixed at 1:1 (v/v) ratio) emulsion was injected in each footpad.

In the prophylactic approach, treatment with each drug was started one day before the immunization and continued throughout the experimental period. Treatment regimen was determined based on previous studies with some modifications. Dipyridample was given at 60 mg/kg, 5 days a week (108), docetaxel was given at 10 mg/kg, once a week (109), colchicine was given at 0.4 mg/kg, 5 days a week (110), pyrvinium pamoate was given with a dose-escalating scheme (111); 0.1 mg/kg for the first week, 0.3 mg/kg for the second week, 0.6 mg/kg until the end of the experiment, 5 days a week. All compounds were given by i.p. injection route.

Serum samples were obtained weekly and disease severity presented as percentage of body surface area affected by skin lesions (%BSA) was recoded every week from week 4. Mice were killed at week 8 by cervical dislocation. On the last day of the experiment, a pool of draining lymph nodes (bilateral inguinal and one popliteal lymph nodes) was harvested

and used for flowcytometric analysis. Collected serum samples were kept at -20˚C until immunoglobulin ELISA.

In the therapeutic approach, EBA was induced described above. Disease severity was recorded weekly from week 4. When %BSA reached >2%, mice were randomly allocated to treatment either with PP or solvent. Inclusion was continued until week 8, and when mice did not develop >2% BSA lesion, they were excluded from further analysis. After the allocation, mice received corresponding treatment for six weeks. Blood sampling was performed every week and the same sample set as described above was collected on the final day and analyzed accordingly.

2.10 RNA extraction, RNA sequence, real-time quantitative PCR

2.10.1 RNA extraction

In order to identify potential target genes affected by PP treatment within B cells, RNA sequencing (RNA-Seq) was performed. Human B cells were isolated from healthy donors as previously described. Isolated B cells were unstimulated (n=3) or stimulated with IL-21 (100 ng/mL) and aCD40Ab (1 µg/mL), and stimulated cells were further untreated (n=3) or treated with 0.1 µM PP (n=3). Cells were seeded at 1×10^6 cells/well density on a flat bottom 24-well culture plate (greiner bio-one, Frickenhausen) in 1 mL RPMI1640 supplemented with 0.3 g/L L-glutamine, 10% FCS, 1% NEAA, 100 U/mL penicillin, and 100 µg/mL streptomycin. After 24-hour incubation at 37˚C with 5% CO_2, cells were collected in a 15 mL tube, washed with DPBS, then transferred to a 1.5 mL Eppendorf tube. After another washing step, the supernatant was removed and the whole RNA was extracted using RNeasy® Mini Kit (QIAGEN, Hilden) following manufacturer's instruction. Briefly, the pellet was lysed and

homogenized in 350 µL of denaturing guanidine-thiocyanate–containing buffer RLT supplemented with β-mercaptoethanol (Carl Roth, Karlsruhe). 350 µL 70% EtOH was added and the lysate was mixed well by pipetting, then the whole lysate was transferred to a spin column with silica-based membrane attached to a 2 mL collection tube, and centrifuged at 10,000 g for 15 seconds (sec). After discarding the flow-through, 700 µL Buffer RW1 was added to the column and the tube was centrifuged at 10,000 g for 15 sec to eliminate unnecessary biomolecules such as carbohydrates, proteins, fatty acids. After discarding the flow-through, 500 µL Buffer RPE was added to the column and the tube was centrifuged at 10,000 g for 15 sec to wash the membrane. This step was repeated once more with centrifugation for 2 min. After discarding flow-through, the spin column attached to the collection tube was centrifuged at 10,000 g for 1 min to dry the membrane. The spin column was placed to a new 1.5 mL collection tube and 30 µL RNase-free water was added in the column then the tube was centrifuged at 10,000 g for 1 min to elute membrane-binding RNA. Concentration and 260 nm/280 nm absorbance of the obtained samples were analyzed by NanoPhotometer® NP80 (Implen GmbH, München). Collected RNA was kept in -80˚C until use.

2.10.2 RNA sequence

RNA sequence including library preparation in this project was performed with support provided by Dr. Sven Künzel at Max Planck Institute for Evolutionary Biology in Plön, Germany. Data processing and statistical analysis was performed by Dr. Yask Gupta, a bioinformatician at our department.

2.10.2-1 Library preparation

1 μg of isolated total RNA/sample was used for the sequence. The library was constructed according to manufacturer's instruction (TruSeq® Stranded mRNA Sample Preparation Kits, Illumina). Firstly, mRNA was enriched from total RNA on a 96-well MIDI plate (Biozym Biotech, Hessisch Oldendorf) using poly-T oligo attached magnetic beads so that poly-A containing RNA would be collected by binding to the beads. After placing the plate in a magnet and removing supernatant, elution buffer was added to the plate. For the elution of enriched mRNA, incubate the plate 80˚C for 2 min, then beads binding buffer was added to the plate so that mRNA would rebind to the beads. After placing the plate on a magnet stand, supernatant was remove and then RNA fragmentation was performed by adding Fragment, Prime, Finish Mix (supplied by Illumina) to the plate and incubate the plate at 94°C for 8 min. When the temperature reached 4°C, fragmented mRNAs were used as a template for the first strand of cDNA synthesis with random primers, dNTP mix, and SuperScriptII as well as Actinomycin D (to avoid DNA-dependent synthesis). First strand of cDNA was synthesized by the following program; pre-heat at 100°C, followed by 25°C for 10 min, 42°C for 15 min, 70°C for 15 min, and hold at 4°C. Immediately after this step, second strand of cDNA was synthesized with Second Strand Marking Master Mix (supplied by Illumina) containing dUTP instead of dTTP so that the strand synthesis would quench at this nucleotide. After adding Second Strand Marking Master Mix, the plate was incubated at 16°C for 1 hour. PCR product was purified with AMPure XP beads (Beckman Coulter, Krefeld) and 80% EtOH, then transfer the sample (cDNA) to a new plate. In order to avoid chimera formation, adenine was added to the 3' ends of the blunt fragments by adding A-Tailing Mix (supplied by Illumina) to the plate and then, the plate was incubated at 37°C for 30 min, followed by 70°C for 5 min and hold at 4°C. In order to identify each sample after the sequence step, unique

indexing adapters were ligated to the ends of prepared cDNA samples by adding Ligation Mix (supplied by Illumina) as well as RNA Adapter Indices (supplied by Illumina) to each well on the plate. The plate was incubated at 30°C for 10 min, then the reaction was stopped by adding Stop Ligation Buffer (supplied by Illumina).The sequence of adapter indice used in this project is the following (3 samples/donor from 3 donors were analyzed; nine samples in total, i.e., nice adapters were used);

Table2.1 Adapter sequence used in this project.

Adapter	Sequence		Adapter	Sequence
AR001	ATCACG(A)		AR008	ACTTGA(A)
AR003	TTAGGC(A)		AR013	AGTCAA(C)
AR004	TGACCA(A)		AR014	AGTTCC(G)
AR005	ACAGTG(A)		AR016	CCGTCC(C)
AR006	GCCAAT(A)			

After purifying twice with AMPure XP beads and 80% EtOH, samples were transferred to a new PCR plate. Finally, prepared DNA fragments possessing adapter index at both ends were enriched by PCR using PCR Master Mix as well as PCR Primer Cocktail (both supplied by Illumina) by the following program; 98°C for 30 sec, 15 cycles of 98°C for 10 sec, 60°C for 30 sec, 72°C for 30 sec, then 72°C for 5 min and hold at 4°C. After purifying PCR product with AMPure XP beads and 80% EtOH, samples were transferred to a new plate. The quality of the prepared library was individually analyzed with DNA 7500 Kit on Agilent 2100 bioanalyzer (Agilent Technologies, Waldbronn) to see whether the final product appears as a band with a peak at 260 bp. The sample content was quantified with nanodrop and adjusted to 40 ng in 10 μL per sample. Pooled samples were kept at -20˚C until sequencing.

2.10.2-2 Sequencing and Data analysis

RNA-Seq using NextSeq 500/550 v2 Kits (supplied by Illumina, San Diego, USA) was performed on NextSeq® 550 (Illumina, San Diego, USA) placed at Forschungszentrum Borstel, Borstel, Germany. The corresponding kits contained reagent, flow cell, and buffer required for a cycle run of sequencing. After loading into the NextSeq reagent cartridge, the prepared library is immobilized on a flow cell through the binding of its complimentary sequence region at both ends and either one of two types of oligonucleotides (P5/P7) coating the surface of a flow cell. By the action of polymerase included in the reagent, the library is amplified until millions of clusters are formed, when the reverse strands are cleaved out and only the forward strands are left. After cluster formation, sequence of the library is determined one by one by through the synthesis of each strand facilitated by polymerase and fluorescently labeled nucleotides. When each dNTP is incorporated, corresponding fluorescent dye is imaged to indicate which base is added to the template library. In this project, the sequence of samples was read 75 bp from both ends.

Fig 2.1 illustrates the work flow of RNA-seq data analysis. The original data generated by the sequencer was reported as per-cycle BCL base call files. Using bcl2fastq2 software, the files were converted to FastQ format (Illumina, San Diego, USA). Afterwards, the quality was checked using FASTQC (112), where parameters such as Per base sequence quality, Per sequence quality scores, Per base sequence content, Per sequence GC content, Per base N content, Sequence Length Distribution, Sequence Duplication Levels, and Adapter Content would be tested (Fig 2.2).

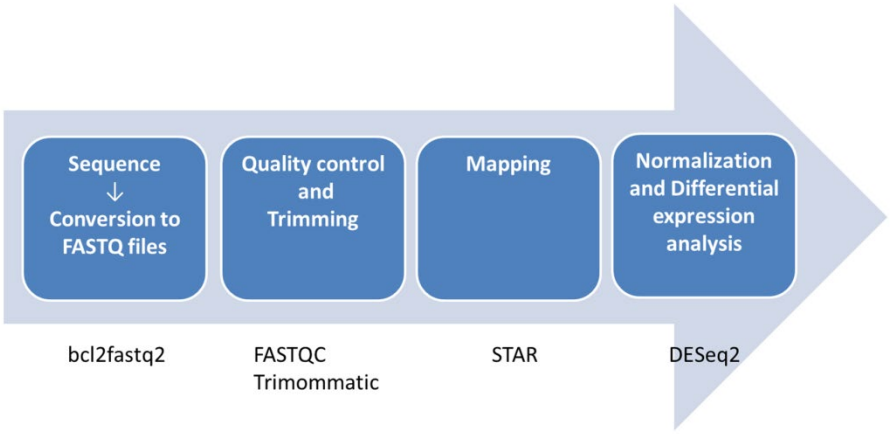

Fig2.1 Work flow of RNA-Seq data analysis. The steps and names of programs used for data analysis are shown.

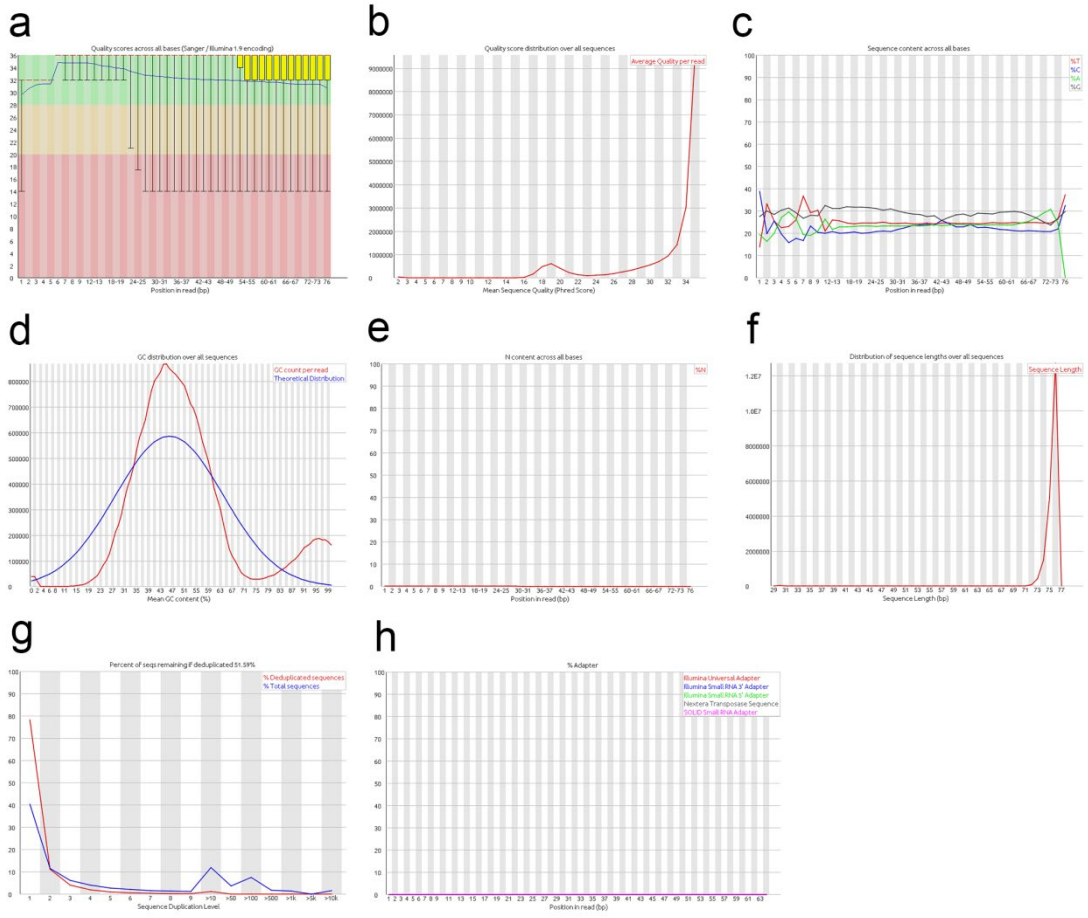

Fig2.2 Example of quality check of RNA-Seq data. (a) *Per base sequence quality*. The X axis indicates the position on the read, and the Y axis indicates the quality score. The program gives a “warning” either when the score of lower quartile is <10 or when the median score of <25 is observed at any position. A “failure” is given either when the score of lower quartile is <5 or when the median score of <20 is observed at any position. **(b)** *Per sequence quality scores*. The X axis indicate the quality score and the Y axis indicates the number of reads. A good sequence result would have a high number of reads with higher scores. A warning or a failure is given when the score at the highest read number is <27 or <20, respectively. **(c)** *Per base sequence content* indicates the frequency of each base (A, T, C, or G) in each read. A warning or a failure is given when the difference in the appearance of A/T and C/G is >10% or >20%, respectively. **(d)** *Per sequence GC content* indicates the distribution of GC content in each read, which is expected to follow the normal distribution (blue line). A warning or a failure is given when the difference from the expected distribution is >15% or >30%, respectively. **(e)** *Per base N content* indicates the frequency of N in each read. A warning or a failure is given when the frequency is >5% or >20%, respectively. **(f)** *Sequence Length Distribution* indicates whether the length of each read is equally distributed as programmed (75bp in this example). A warning is given when the sequence length is not the same number. A failure is given when the sequence length is 0. **(g)** *Sequence Duplication Levels*. The X axis indicates the duplication level and the Y axis indicates the frequency. Theoretically, there would be a no read with identical sequence. **(h)** *Adapter Content* gives the frequency of adapter sequence in each read.

The adapters and lower quality read (phred score < 20) were trimmed using software Trimommatic (113). Then remaining fastq sequence was aligned and mapped to the reference human genome (hg38) using Spliced Transcripts Alignment to a Reference (STAR) software (114). Htseq-count software (115) was used for quantification of gene expression across human transcriptome. Finally, gene expression was normalized using variance stabilizing transformation (VST) and differentially expressed genes were identified using DESeq2 program (116). Following comparison was made:

1) Unstimulated B cells vs stimulated B cells

2) Stimulated B cells vs Stimulated B cells with PP treatment

Afterwards, protein-coding genes overlapped in these two comparisons were further scrutinized by the subsequent real-time quantitative PCR.

2.10.3 Real-time quantitative PCR (qPCR)

For the confirmation of obtained RNA-Seq results, mRNA expression levels of candidate genes were analyzed by real-time quantitative PCR (qPCR). Human B cells were isolated and treated as described in RNA extraction section. Obtained RNAs were converted to complementary DNA (cDNA). Briefly, 100 ng total RNA from each sample was treated with 1 U DNase I (Sigma-Aldrich, Hamburg) and reverse-transcribed to cDNA in total volume of 20 µL reaction mix comprises 11.5 µL of DNase I digested RNA, 4 µL of 5x reaction buffer (250 mM Tris-HCl (pH 8.3), 250 mM KCl, 20 mM $MgCl_2$, 50 mM DTT, Thermo Scientific, cat#EP0452), 0.5 µL of recombinant RNase inhibitor (RNaseOUT™,40 U/µL, Invitrogen, Karlsruhe), 1 µL of random hexamer primer (100 µM, Thermo Scientific), 1 µL of dNTPs (10

mM, Thermo Scientific), and 0.5 µL of RevertAid H Minus Reverse Transcriptase (200 U/µL Thermo Scientific) on C1000™ Thermal Cycler (BIO RAD) with the following program; 10 min 25°C for 10 min, 42°C for 50 min, 70°C for 15 min, then hold at 4°C. Samples were kept in -20°C until use.

qPCR was performed on a 96 Fast PCR plate (Sarstedt, Nürmbrecht) using cDNAs as template, pre-designed gene specific primers (20x TaqMan® Gene Expression Assay, Thermo Scientific), and TaqMan® Gene Expression Master Mix (containing AmpliTaq Gold® DNA Polymerase, Ultra Pure, Uracil-DNA Glycosylase, deoxyribonucleotide triphosphates (dNTPs) with deoxyuridine triphosphate (dUTP), ROX™ Passive Reference, and buffer components, Applied Biosystems/ Thermo Fisher Scientific, Waltham, MA, USA). The list of primers used in this project is shown in Table 2.2. Single reaction was performed in 20 µL/well consisting of 1 µL cDNA, 1 µL primer, 10 µL Master Mix, and 8 µL UltraPure™ DNase/RNaseFree Distilled Water (gibco/Thermo Fisher Scientific, Waltham, MA, USA). Samples were analyzed in duplicate on Mastercycler® ep RealPlex2 (Eppendorf, Hamburg) with the following program; 95°C for 10 min, followed by 50 cycles of 95°C for 45 sec and 60°C for 60 sec. GAPDH expression was used as a reference and the expression level of target genes was calculated by ΔCt method (117).

Table2.2 List of gene names and assay IDs used in this project.

Genes	ID*		Genes	ID*
GAPDH	Hs02758991_g1			
ATP6V1C2	Hs00375969_m1		*CD37*	Hs01099648_m1
C9orf139	Hs01082575_s1		*COX20*	Hs02385899_g1
FAM166A	Hs01099748_m1		*GPS2*	Hs00409956_g1
SYNE2	Hs00794881_m1		*SNX22*	Hs01017487_g1

*TaqMan® Gene Expression Assay ID

2.11 Statistical analysis

Statistical analysis was performed using SigmaPlot v13.0 (Systat Software, Inc, San Jose, CA, USA). The names of applied methods are indicated in the figure legends and a p-value of < 0.05 was considered to be statistically significant.

3. Results

3.1 *In vitro* screening identified 48 out of 1,200 potential suppressors of aCD40Ab/IL-21 stimulated human B cell proliferation

IL-21 as well as CD40/CD40L interaction plays critical roles in B cell survival and proliferation (102, 118, 119), therefore these two molecules were chosen for B cell stimulation, and cell proliferation was assessed by colormetric BrdU proliferation assay. After a five-day culture, the proliferation signal obtained from B cells stimulated with recombinant human IL-21 (IL-21, 100 ng/mL) and anti-human CD40 antibody (aCD40Ab, 1 μg/mL) was significantly higher than that of unstimulated B cells, which was as low as background signal (signal from culture medium).

After establishing the B cell proliferation protocol, a primary screening was performed where the effect of each drug from the library on the proliferation of human B cells was evaluated. Due to the high number of the drugs in the library, each compound was tested at a fixed concentration of 1 μM, and the effect was assessed in two donors. As shown in Fig 3.1, using a cut-off of > 1.5, or < 0.5 change in ELISA signal, the *in vitr*o screening detected 42 potential enhancers as well as 48 potential suppressors of human B cells proliferation (For the details of each compound, see Appendix 7.3). The identified 42 potential B cell proliferation enhancers were investigated in another project, therefore the remaining 48 compounds will be further discussed in this thesis.

When the 48 potentially B cell proliferation-inhibiting drugs were classified by “therapeutic effect” according to the manufacturers’ taxonomy, 13 drugs (27.1%) were categorized as

anti-neoplasm, followed by 11 (22.9%) as anti-infection, 9 (18.8%) as anti-inflammatory including steroids, and 15 (31.2%) as others (Table 3.1).

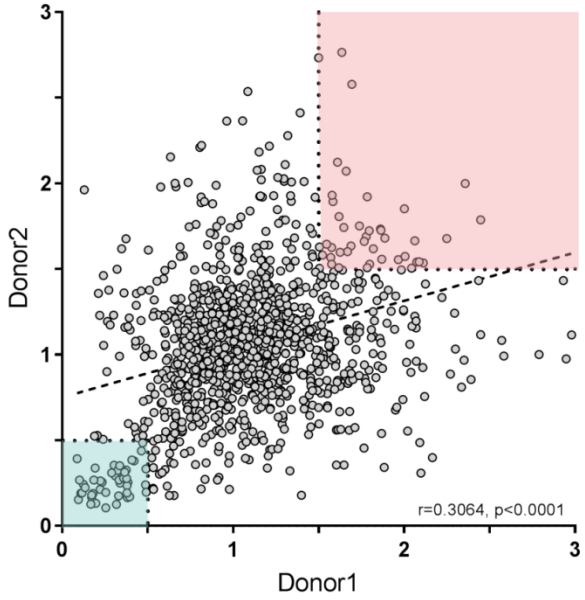

Fig3.1 Effect of 1μM compound on aCD40Ab/IL-21 stimulated B cell proliferation. Followed by PBMCs isolation from healthy donors, B cells were isolated by magnetic separation. Obtained B cells were stimulated with 100 ng/mL IL-21 and 1 μg/mL aCD40 Ab and cultured with or without 1μM of each compound from the library. On day 5, cell proliferation was assessed by Bromodeoxyuridine (BrdU) ELISA. For each experiment and donor, ELISA signal from drug-treated B cells were normalized to those obtained from untreated but aCD40Ab/IL-21 stimulated B cells and cell proliferation was presented as a relative value. Dots highlighted in blue or pink shaded area represent compounds which inhibited B cell proliferation by > 50% or promoted by > 150%, respectively. Each compound was tested in two donors.

Table3.1 Classification of the "hit" compounds.

Therapeutic effect	Number of compound (%)
Anti-neoplasm	13 (27.1)
Anti-infection	11 (22.9)
Anti-inflammatory	9 (18.8)
Others	15 (31.2)
Total	48

3.2 Six compounds were selected after the secondary screening by dose-dependency and cell viability assays

The selected 48 potential suppressors of B cell proliferation were further scrutinized by dose-dependency and toxicity assay. Based on the selection criteria (Table 3.2), the number of the candidates was narrowed down from 48 to six after this step. Except for docetaxel and gemcitabine which potently inhibited B cell proliferation at the lowest concentration tested (0.01 μM) with a high toxicity (criteria 3 in Table 3.2, Fig 3.2 (b) and (c)), the remaining four drugs, dipyridamole, proscillaridin A, cholchicine, and pyrvinium pamoate, showed dose-dependent effect on cell proliferation (Fig 3.2 (a),(d)-(f) upper panel). A detailed result of other 42 eliminated compounds is shown in Table 3.3.

Table3.2 Selection criteria after secondary screening.

Selection criteria
1. > 40% reduction in cell proliferation and > 60% cell viability at 1 μM (Dip)
2. > 30% reduction in cell proliferation at 0.1 μM, but not cytostatic agents (Col, PP, PA)
3. > 70% reduction in cell proliferation at 0.01 μM (Gem, Doc)

Dip:dipyridamole, Col:colchicine, PP:pyrvinium pamoate, PA:proscillaridin A, Gem:gemcitabine, Doc:docetaxel

Drug toxicity was assessed by Propidium Iodide (PI) staining. Overall, B cell viability with or without aCD40Ab/IL-21 stimulation at day 5 was 53.78 ± 13.82% and 9.97 ± 7.96%, respectively (mean viability calculated from 50 repeated assays using blood from 22 healthy donors). In general, low cell proliferation was accompanied by low viability (Fig 3.2). However, this was not the case with dypiridamole which inhibited cell proliferation with a dose-dependent manner without affecting cell viability (Fig 3.2(a)).

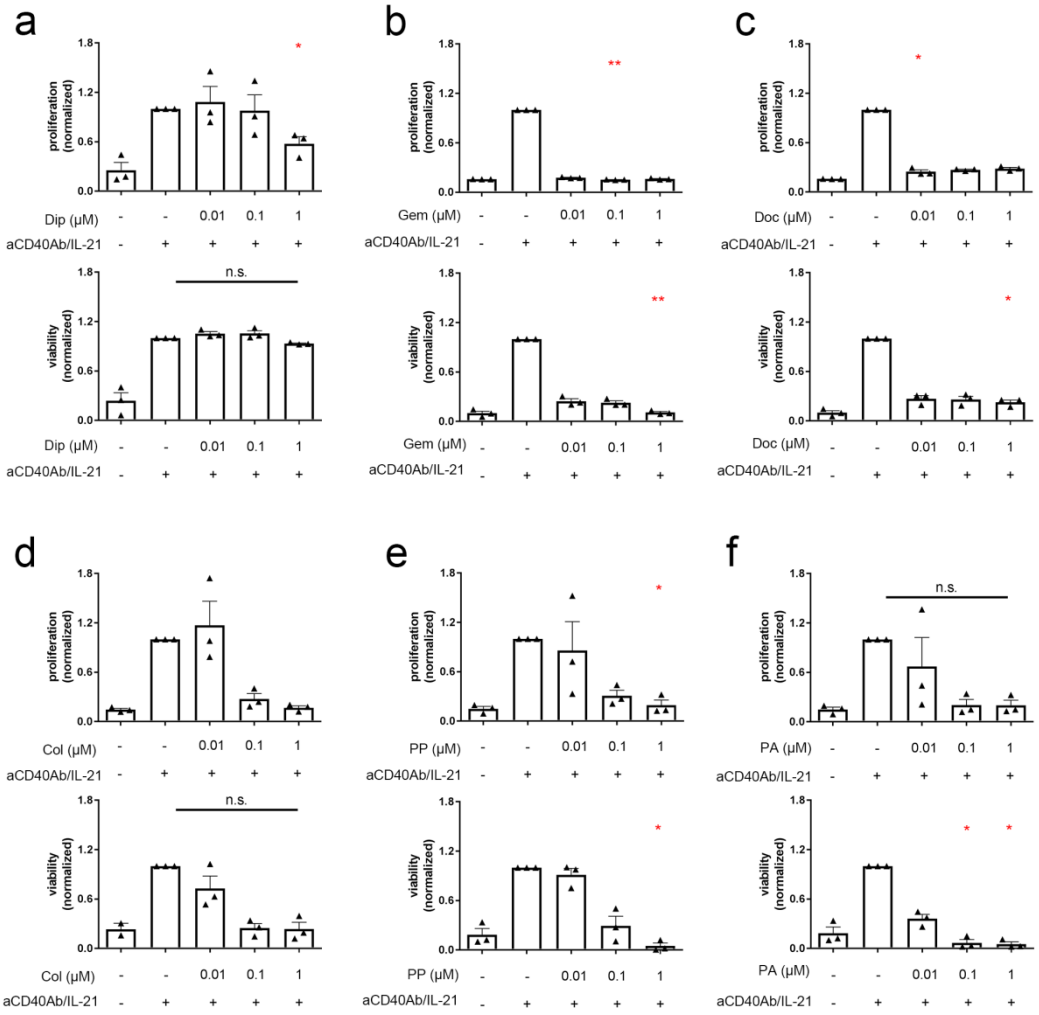

Fig3.2 Dose-dependent effect of candidate drugs on B cell proliferation and viability. Human B cell proliferation (**(a)-(f)**, upper panels) and viability (**(a)-(f)**, lower panels) under stimulation ± drug treatment at three different concentrations were investigated. Isolated B cells were either unstimulated or stimulated with aCD40Ab/IL-21. Stimulated cells were untreated or treated with drugs at indicated concentration. On day 5, BrdU ELISA and PI staining were performed for proliferation and viability test, respectively. Data obtained from drug-treated B cells were normalized to the one from aCD40Ab/IL-21 stimulated B cells. **(a)** Dip=dipyridamole. **(b)** Gem=gemcitabine. **(c)** Doc=docetaxel. **(d)** Col=colchicine. **(e)** PP=pyrvinium pamoate. **(f)** PA=proscillaridin A. *p<0.05, **p<0.01 (Kruskal-Wallis test, Dunn's multiple comparisons test). n=3. Data are presented as mean with error bars indicating SEM.

Table3.3 Detailed secondary screening results of other compounds.

		B-cell proliferation			B-cell viability		
	Drug	0.01μM	0.1μM	1μM	0.01μM	0.1μM	1μM
1	Disulfiram	1.1655±0.1899	1.1431±0.1610	0.2920±0.1045	1.0998±0.0979	1.1061±0.111	0.1752±0.1241
2	Camptothecine (S,+)	0.6271±0.1468	0.3347±0.0784	0.2424±0.0754	0.8414±0.0402	0.3732±0.1154	0.2950±0.1479
3	Betamethasone	1.2685±0.7357	0.8832±0.357	0.6759±0.1357	0.796±0.0642	0.6072±0.0550	0.4601±0.1446
4	Lidoflazine	0.8541±0.1968	0.8050±0.1488	0.5933±0.0884	0.9572±0.0630	0.9821±0.0804	0.9140±0.0301
5	Dequalinium dichloride	0.9791±0.1597	1.0171±0.1351	0.3558±0.2782	1.0244±0.0823	1.0303±0.0649	0.6160±0.1330
6	Amifostine	0.8754±0.1074	1.0038±0.1904	0.9711±0.1958	1.0511±0.1298	1.1460±0.0542	1.1165±0.0920
7	Digitoxigenin	0.7921±0.0653	0.8094±0.1128	0.166±0.023	1.0636±0.0785	0.8926±0.1408	0.2965±0.1447
8	Digoxin	1.0823±0.2525	0.3466±0.0446	0.2550±0.0738	0.9768±0.0453	0.3111±0.1454	0.1220±0.0407
9	Hydrocortisone base	0.9532±0.2541	0.7878±0.1927	0.2723±0.0879	0.9873±0.0521	0.9009±0.0503	0.2445±0.039
10	Thiostrepton	0.9937±0.2502	0.8474±0.2232	0.5176±0.1657	1.0202±0.0294	1.0663±0.017	0.6678±0.0792
11	Ciclopirox ethanolamine	1.2702±0.2354	1.2333±0.3587	0.1933±0.0562	1.0067±0.0263	0.9876±0.0988	0.3966±0.1169
12	Oxibendazol	1.2756±0.5520	1.0398±0.3013	0.9353±0.3407	0.9807±0.0802	1.0306±0.0636	0.9934±0.0249
13	Lanatoside C	1.2512±0.3443	0.6272±0.038	0.1597±0.0442	0.9131±0.0739	0.5017±0.1265	0.1560±0.0804
14	Avermectin B1a	0.7417±0.0652	1.0253±0.0761	1.0092±0.0964	1.1104±0.0932	1.1508±0.0823	1.1326±0.0896
15	Thimerosal	0.8519±0.1399	0.9144±0.1736	0.2308±0.0614	1.1053±0.1414	0.7436±0.2153	0.1828±0.0948
16	Methyl benzethonium chloride	0.7033±0.0683	0.8825±0.1692	0.5445±0.1772	1.0110±0.0417	1.0897±0.1940	0.5925±0.0564
17	Auranofin	1.1278±0.2251	0.9094±0.0850	0.1772±0.0161	1.0414±0.0227	0.2789±0.0144	0.1262±0.0891
18	Clinafloxacin	1.0176±0.2510	1.2040±0.1802	1.0933±0.2404	1.0571±0.0447	1.0536±0.0603	1.0727±0.0331
19	Digoxigenin	0.9574±0.3895	1.0402±0.2257	0.4054±0.1425	1.0658±0.0400	1.0873±0.0648	0.2566±0.0771
20	Clioquinol	1.2027±0.1367	1.1485±0.3024	0.9376±0.0432	1.0582±0.0371	1.0018±0.0844	0.9223±0.0639
21	Flubendazol	1.0080±0.2951	1.1045±0.2077	1.0578±0.1753	1.0533±0.0408	1.0627±0.0462	0.9707±0.1151
22	Thonzonium bromide	0.9513±0.2614	1.0168±0.1617	0.1767±0.0395	1.0021±0.0118	0.9309±0.0279	0.2023±0.0899
23	Methiazole	0.6867±0.2576	0.9798±0.2597	0.6313±0.1881	1.0858±0.0833	1.1699±0.1078	0.4652±0.1842
24	Verteporfin	1.4597±0.3378	1.3137±0.2377	0.8031±0.3831	1.1472±0.0537	1.1922±0.0713	0.9247±0.0485
25	Parbendazole	0.9538±0.3835	1.1342±0.5043	0.6534±0.1248	1.1002±0.0449	1.0921±0.0244	0.2859±0.1553
26	Topotecan	0.8117±0.2732	0.2098±0.0402	0.1840±0.0151	0.5617±0.08945	0.2427±0.1751	0.2175±0.1582
27	Nocodazole	1.8275±0.4530	1.7378±0.4503	0.4472±0.1159	1.1653±0.1239	0.9801±0.0247	0.1097±0.0150
28	Methylprednisolone, 6-alpha	1.5900±0.6389	1.4786±0.3011	0.8146±0.0886	0.8699±0.1186	0.4996±0.0869	0.2460±0.0745
29	Fludrocortisone acetate	1.5763±0.5986	1.2778±0.2828	1.1068±0.2051	1.0154±0.0798	0.6935±0.1503	0.5938±0.1434
30	Mitoxantrone dihydrochloride	0.6831±0.3862	0.2063±0.0339	0.2020±0.0225	0.3949±0.1458	0.1055±0.0352	0.1072±0.0938
31	Etoposide	1.1333±0.2178	1.2802±0.2210	0.2779±0.0472	0.9461±0.0298	0.6310±0.2087	0.1041±0.0742
32	Doxorubicin hydrochloride	0.7884±0.3101	0.2071±0.0299	0.1927±0.0213	0.4546±0.1760	0.0858±0.0671	0.0281±0.0317
33	Mometasone furoate	0.7174±0.2513	0.7988±0.3212	0.7953±0.2727	0.4787±0.1904	0.4794±0.2084	0.4286±0.1649
34	Cytarabine	0.9519±0.0640	0.2869±0.0531	0.1903±0.0222	0.7680±0.0177	0.1530±0.0606	0.0706±0.0755
35	Irinotecan hydrochloride trihydrate	0.9980±0.0447	1.0053±0.0825	0.2081±0.0239	0.9708±0.0274	0.6448±0.0622	0.1190±0.1060
36	Rimexolone	0.8834±0.1821	0.9765±0.0661	0.7817±0.1012	1.0421±0.0292	0.9211±0.0663	0.6413±0.0736
37	Prednicarbate	0.8652±0.0740	0.9123±0.1130	0.7300±0.1739	1.0401±0.0477	0.8323±0.0903	0.6097±0.0729
38	Vorinostat	1.0190±0.1275	1.0438±0.1583	0.1916±0.0327	1.0693±0.0529	1.0252±0.0915	0.1556±0.1470
39	Clocortolone pivalate	0.7520±0.1408	0.7975±0.0807	0.6687±0.0501	0.9221±0.2508	0.8393±0.1137	0.7170±0.0592
40	Fludarabine	0.8048±0.1479	0.8837±0.0556	0.5149±0.1903	1.0588±0.0839	1.0212±0.0498	0.4034±0.1888
41	Cladribine	0.8105±0.1577	0.2379±0.0509	0.1646±0.0252	0.9302±0.0073	0.2371±0.1450	0.1413±0.1540
42	Fluocinolone acetonide	0.5764±0.1880	0.5875±0.2087	0.5589±0.2069	0.5117±0.1536	0.4682±0.1081	0.4013±0.1327

Proliferation and viability were normalized to the corresponding values obtained from stimulated B cells cultured without compounds. Data was presented as mean±SD. Each compound was tested in 3 donors.

3.3 Candidate compounds suppressed immunoglobulin production and plasmablast generation from aCD40Ab/IL-21 stimulated B cells

Antibody production is the most crucial function of B cell-derived plasma cells and indispensable in humoral immune response. In order to investigate whether and how aCD40Ab/IL-21 stimulated B cell differentiation would be affected in the presence of candidate drugs, immunoglobulin production was assessed by ELISA in which IgM and IgG levels in the culture supernatant were measured. In accordance with the proliferation assay results, almost no immunoglobulin production was detected from unstimulated B cells at day five, and the compound treatment reduced both IgM and IgG production from aCD40Ab/IL-21 stimulated B cells with a dose-dependent manner (Fig 3.3).

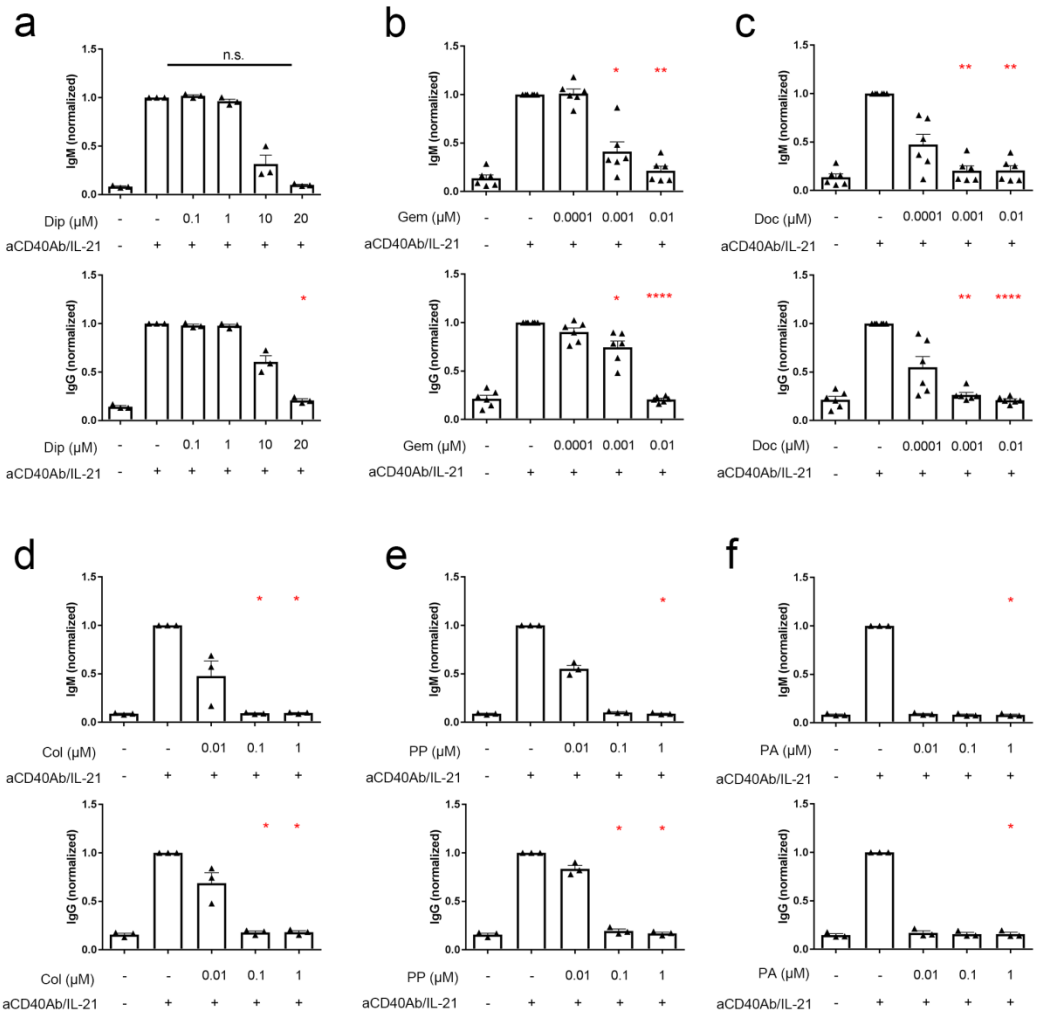

Fig3.3 Dose-dependent effect of candidate drugs on immunoglobulin production. IgM (**(a)-(f)**, upper panels) and IgG (**(a)-(f)**, lower panels) production from B cells were investigated. Human B cells preparation, stimulation, and drug treatment were similarly performed as described in Fig 3.1 and 3.2. On day five, the culture supernatant was collected and immunoglobulin concentration was measured by ELISA. Obtained data from drug-treated B cells were normalized to the value of aCD40Ab/IL-21 stimulated B cells without drug treatment. **(a)** Dip=dipyridamole. **(b)** Gem=gemcitabine. **(c)** Doc=docetaxel. **(d)** Col=colchicine. **(e)** PP=pyrvinium pamoate. **(f)** PA=proscillaridin A. *p<0.05, **p<0.01, ****p<0.001 (Kruskal-Wallis test, Dunn's multiple comparisons test). n=3-6. Data are presented as mean with error bars indicating SEM.

Surface marker expression is widely used for the classification of differentiating B cells (120). In response to antigen and/or cytokine stimulation, naïve and memory B cells can differentiate into plasmablasts, i.e. antibody-secreting cells characterized as

$CD19^{+}CD27^{++}CD38^{++}$ (102-104). As an alternative method to investigate the drug effect on B cell differentiation, *in vitro* plasamablast generation, which was presented as the frequency of $CD19^{+}CD27^{++}CD38^{++}$ population among B cells cultured for five days, was evaluated by flowcytometric analysis. On day 5, 14.5 ± 4.4% of aCD40Ab/IL-21 stimulated B cells were $CD19^{+}CD27^{++}CD38^{++}$ whereas no unstimulated cells showed such phenotype (Table 3.4, Fig 3.4). One thing of note was that a distinctive $CD19^{+}CD27^{+}CD38^{-}$ population was observed when stimulated B cells were treated with lower concentration of pyrvinium pamoate (Fig 3.4(e)). With regard to the effect of other drugs, a resembling finding that plasmablast formation was suppressed under the treatment with higher concentrations of the candidate drugs was observed.

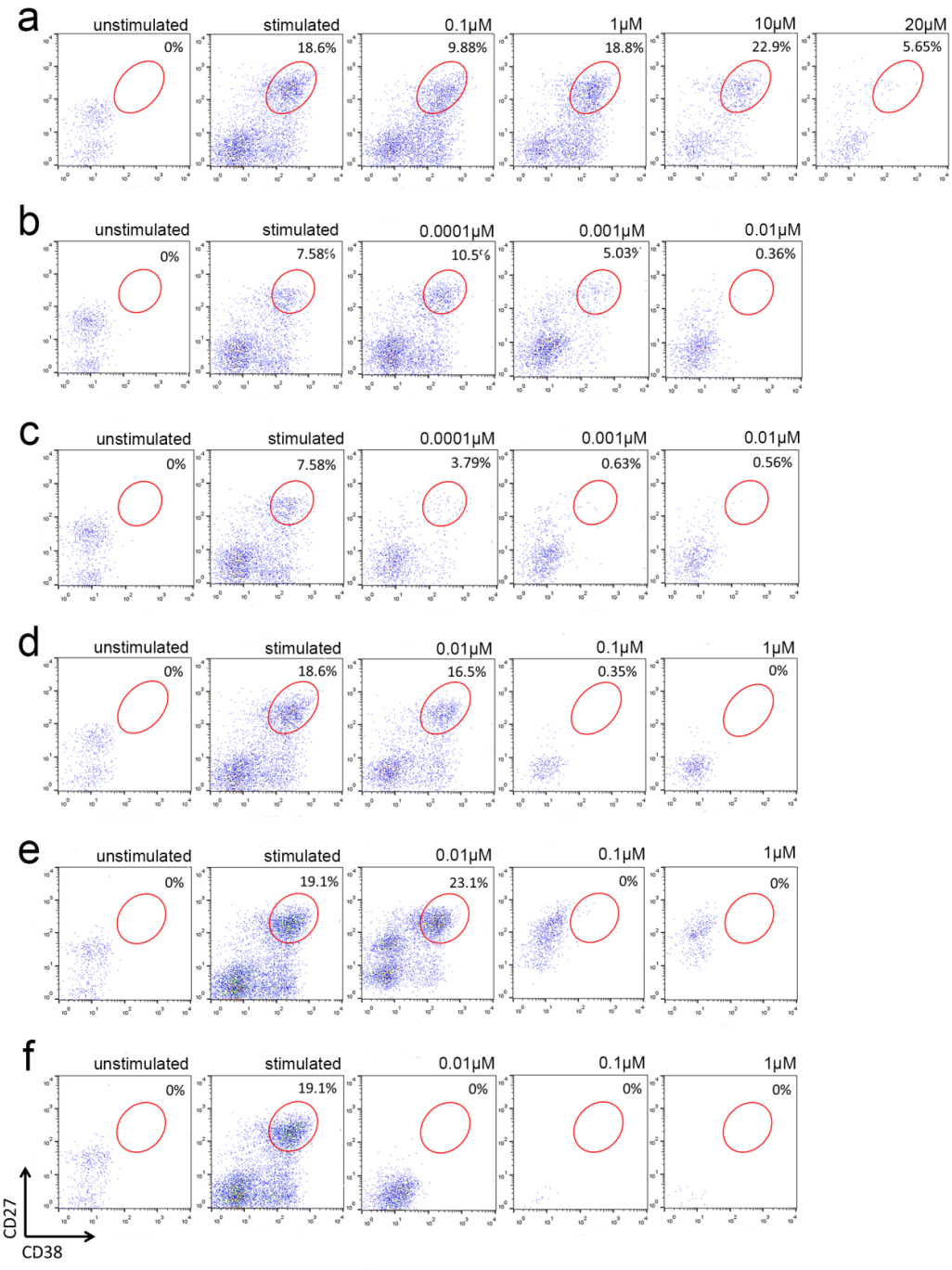

Fig3.4 Dose-dependent effect of candidate drugs on in vitro plasmablast generation. Human B cells preparation, stimulation, and drug treatment were similarly performed as described in Fig 3.1 and 3.2. On day five, the cultured cells were collected, washed, then surface-staining with fluorochrome-conjugated antibody to CD19, CD27, and CD38 was performed. The red circle indicates the proportion of plasmablasts ($CD19^{+}CD27^{++}CD38^{++}$ cells) among live cells. Each drug was tested in three different donors and a representative result from each tested drug is shown. **(a)** Dip=dipyridamole. **(b)** Gem=gemcitabine. **(c)** Doc=docetaxel. **(d)** Col=colchicine. **(e)** PP=pyrvinium pamoate. **(f)** PA=proscillaridin A.

Table3.4 Plasmablast formation *in vitro* (%).

Drug (μM)	**-**	**-**	**0.0001**	**0.001**	**0.01**	**0.1**	**1**	**10**	**20**
aCD40Ab/IL-21	**-**	**+**	**+**	**+**	**+**	**+**	**+**	**+**	**+**
Dip	0	16.3±1.65	n/a	n/a	n/a	10.20±2.81	15.23±3.22	14.51±6.27	3.05±1.95
Gem	0	9.39±3.44	12.59±4.24	2.62±1.75	0.43±0.32	n/a	n/a	n/a	n/a
Doc	0	9.39±3.44	7.31±5.0	0.5±0.31	0.3±0.26	n/a	n/a	n/a	n/a
Col	0	17.73±1.59	n/a	n/a	13.78±4.13	0.27±0.2	0	n/a	n/a
PP	0	17.9±1.7	n/a	n/a	22.67±2.67	1.17±0.45	0	n/a	n/a
PA	0	16.47±1.88	n/a	n/a	0	0	0	n/a	n/a

Dip:dipyridamole, Col:colchicine, PP:pyrvinium pamoate, PA:proscillaridin A, Gem:gemcitabine, Doc:docetaxel, n/a: not available, Each compound was tested in 3 donors. Data are presented as mean±SD. Dip=dipyridamole. Gem=gemcitabine. Doc=docetaxel. Col=colchicine. PP=pyrvinium pamoate. PA=proscillaridin A. n/a=not available.

3.4 Selected compounds did not affect reactive oxygen species (ROS) release from immunocomplex (IC)-activated polymorphonuclear leukocytes (PMNs) but two drugs also inhibited CD3/28 activated T cell proliferation

The aim of this study is to discover unknown B cell modulatory effects within existing, licensed drugs and to test their efficacy in autoimmune disorders. For this purpose, the selected drugs were tested *in vivo* using an EBA mouse model because the production of autoantibody directed at type VII collagen is a crucial pathogenic step in the disease induction. In addition to B cells, however, other immune cells play roles in the pathogenesis of EBA. It has been demonstrated that CD4+ T cell depletion resulted in a reduced disease severity as well as antigen-specific antibody production in immunization-induced EBA mouse model (45). On the other hand, in the effector phase of EBA, the degranulation from immunocomplex (IC)-activated neutrophils contribute to the blister formation (121). Therefore, the functional suppression of these cells would also lead to a disease prevention.

In order to exclude a possibility that the selected drugs might ameliorate the disease due to their effects on other immune cells than B cells, additional in vitro assays were performed: T cell proliferation assay and ROS release assay (122). As shown in Fig 3.5 (upper panels), all candidate drugs did not alter ROS release from IC-activated PMNs. However, T cell proliferation was inhibited more potently under the treatment with Proscillaridin A (Fig 3.5 (f), lower panel), and a similar effectiveness as seen in B cells proliferation was observed with gemcitabine where as low as 0.01 μM of this drug was able to suppress T cell proliferation. (Fig 3.5 (b), lower panel). With pyrvinium pamoate, T cell proliferation was inhibited at the highest concentration tested (1 μM) but not the one which was effective on B cells (0.1 μM) (Fig 3.5 (e), lower panel). At this point, Proscillaridin A and gemcitabine were excluded from the subsequent study. Obtained results should be interpreted with caution, however, because they did not confirm that the other drugs act exclusively on B cells. Nonetheless, it could be said that B cells are more likely to be the target of these drugs than PMNs or T cells.

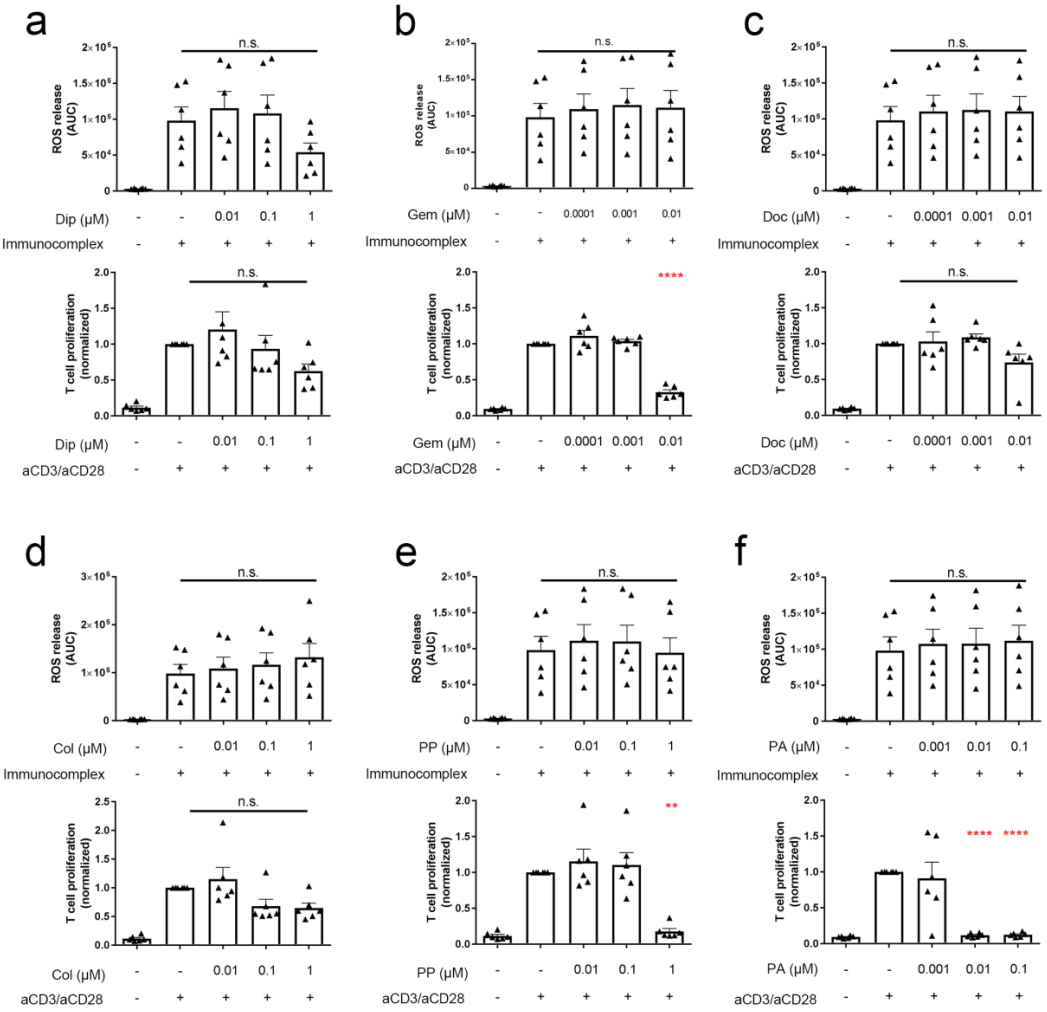

Fig3.5 Effect of candidate drugs on the function of other immune cells. Drug effect on ROS release from IC-stimulated human PMNs (**(a)-(f),** upper panels) as well as T cell proliferation (**(a)-(f),** lower panels) was investigated. **(a)-(f),** upper panels. Isolated human PMNs were labelled with luminol and unstimulated or stimulated with plate-fixed IC consisting of recombinant human collagen VII (hCol7) and recombinant anti-hCol7 IgG1 monoclonal antibody. Stimulated PMNs were further treated or untreated with candidate drugs at different concentrations. After one hour incubation, recording of luminescence from oxidized-luminol was started and presented as ROS release. Data were presented as AUC obtained from each assay. **(a)-(f)**, lower panels. Human T cells were enriched from PBMCs by magnetic separation. Obtained T cells were either unstimulated or stimulated with 0.5 µg/mL anti-human CD3 antibody (aCD3) and 1.0 µg/mL anti-human CD28 antibody (aCD28). Stimulated cells were treated or untreated with candidate drugs at different concentrations. On day 3, T cell proliferation at each culture condition was evaluated by BrdU ELISA. Obtained results were normalized to the value of stimulated T cells without drug treatment. **(a)** Dip=dipyridamole. **(b)** Gem=gemcitabine. **(c)** Doc=docetaxel. **(d)** Col=colchicine. **(e)** PP=pyrvinium pamoate. **(f)** PA=proscillaridin A. **p<0.01, ****p<0.001 (Kruskal-Wallis test, Dunn's multiple comparisons test). n=6. Data are presented as mean with error bars indicating SEM. PMNs=polymorphonuclear neutrophils. PBMC= Peripheral blood mononuclear cells, IC=immunocomplex. AUC=are under the curve.

3.5 Prophylactic effect of the candidate drugs on immunization-induced experimental EBA

3.5.1 Overview

The remaining four drugs, dipyridamole, docetaxel, colchicine, and pyrvinium pamoate, were tested *in vivo* using immunization induced experimental model of EBA, where the disease was induced in B6.s mice by immunizing them with recombinant vWFA2 domain of COL7 (vWFA2) (45). Firstly, the prophylactic effect of the candidate drugs on disease development was evaluated.

The experimental setup is shown in Fig, 3.6. The general effect of the drug was assessed using the following parameters: change in body weight, complete blood count (CBC), clinical disease score determined by the percentage of affected body surface area (%BSA). In order to investigate whether and how drug treatment would affect B cells and the subsequent adaptive immunity, the cell numbers of B cells (both overall B cells and antigen-specific B cells) and plasma cells (PCs, both overall PCs and antigen-specific PCs) as well as circulating immunoglobulin levels, total IgG, IgM, and antigen-specific IgG (vWFA2-IgG) and its subclasses, were evaluated (105).

In this mouse model, obvious clinical signs of the disease started to appear specifically in the ear as redness and/or thickness around four-week after immunization and continued to spread systemically to head, legs, and trunk during the experimental period. Upon immunization with vWFA2, vWFA2-IgG could be detected in the circulation as early as week 2 and kept on the rise. However, the time points when vWFA2-IgG reached its peak was different with each other according to the treatment. After the peak, the antibody titer gradually decreased even though vWFA2-IgG could be detected throughout the

experimental period. Detailed results of the prophylactic treatment with each drug will be discussed separately.

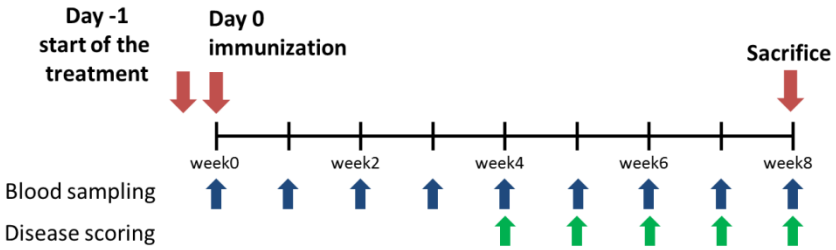

Fig3.6 Schematic diagram of the experimental setup (prophylactic approach). On day -1, treatment with either solvent or candidate drug was initiated and continued for 8 weeks. On day 0, B6.s mice were immunized with a mixture of 60 µg vWFA2 and Titermax® as an adjuvant in the footpad (120 µg/head, single immunization). During the eight-week experimental period, disease severity presented as affected body surface area was recoded every week from week 4 and blood sampling was done every week. vWFA2= recombinant von Willebrand factor A–like domain 2

3.5.2 Dipyridamole

Dipyridamole has been used as an anti-platelet agent due to its effect to increase cyclic Adenosine Monophosphate (cAMP) concentration in platelets (123). Based on a previously reported dose used in mice, the drug was tested at the dose of 60 mg/kg, 5-day on 2-day off cycle, and administered by intraperitoneal injection (108). During the eight-week treatment period, there was no difference in body weight and CBC between the drug-treated mice and those received the solvent (Appendix 7.4). However, two mice in the drug-treated group died; one at week 4 (day 28) just after receiving the i.p. injection and another one was found dead in the cage at week 6 (day 41). No gross intraperitoneal bleeding was observed and no further investigation was conducted, therefore, the cause of death remains unknown in both cases.

Clinically, drug-treated mice showed significantly lower disease score than the control group, where %BSA at week 8 was 5.53 ± 2.12% compared to 11.76 ± 2.64% in solvent-treated mice was (Fig 3.7 (a)). In the draining lymph nodes, there could be seen a tendency that dipyridamole received mice had fewer numbers of each cell fraction tested, total/Ag-specific B cells as well as total/Ag-specific plasma cells (Fig 3.7 (g)). However, this was not statistically significant. Overall, total IgM and IgG were lower in dipyridamole group especially at week 3 in IgM and weeks 3, 8 in IgG (Fig 3.7 (b)). With regard to the antigen-specific antibody production, there was one week delay in the time for vWFA2-IgG from drug-treated mice to reach its peak compared to the control; the time point of peak vWFA2-IgG in dipyridamole group was week 5 but it was week 4 in the control (Fig 3.7 (c)). There was no statistically significant difference in Ab titers. A similar delayed production of vWFA2-IgG1, 2a, and 2b was observed in dipyridamole treated group. Interestingly, compared to the other two subclasses, vWFA2-IgG1 production was more specifically suppressed under dipyridamole treatment (Fig 3.7 (d)-(f)).

In summary, dipyridamole treatment prevented disease development of the experimental EBA which was accompanied by a delayed antibody response against vWFA2. However, this was not supported by a significantly suppressed B cell or PCs response in the draining LNs (evaluated at week 8).

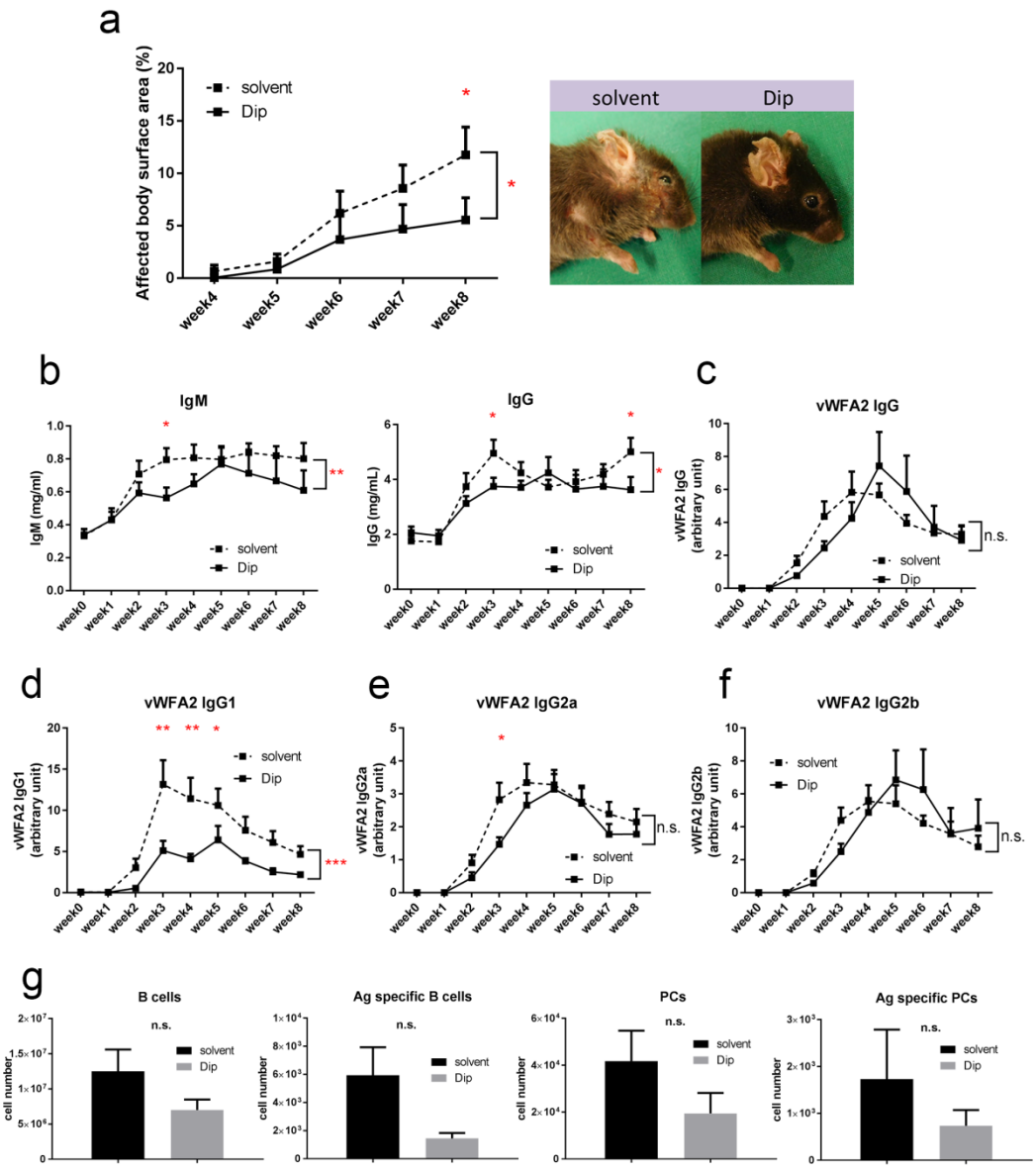
a
Affected body surface area (%)
solvent
Dip
week4
week5
week6
week7
week8
solvent
Dip
b
IgM
IgM (mg/ml)
IgG
IgG (mg/mL)
c
vWFA2 IgG
vWFA2 IgG (arbitrary unit)
n.s.
d
vWFA2 IgG1
vWFA2 IgG1 (arbitrary unit)
e
vWFA2 IgG2a
vWFA2 IgG2a (arbitrary unit)
f
vWFA2 IgG2b
vWFA2 IgG2b (arbitrary unit)
g
B cells
Ag specific B cells
PCs
Ag specific PCs
cell number

Fig3.7 Prophylactic effect of dipyridamole on experimental EBA. One day prior to the immunization with vWFA2, five-days on, two-day off i.p. treatment either with solvent or 60 mg/kg dipyridamole was started. **(a)** Clinical disease severity presented as affected body surface area (left panel) and representative clinical pictures from solvent-treated and dypiridamole-treated group at week 8 (right panel). *p<0.05 (Two Way Analysis of Variance, Sidak's multiple comparisons test). n=6-8**. (b)** Serum levels of total IgM and IgG measured by ELISA in indicated groups. Overall, there is an increase in IgG as well as IgM 1-2 weeks after immunization in both groups, and drug-treated group had lower levels of IgM and IgG. *p<0.05, **p<0.01 (Two Way Analysis of Variance, Sidak's multiple comparisons test). n=6-8. **(c)-(f)** Circulating levels of vWFA2-sprcific IgG (c), IgG1 (d), IgG2a (e), and IgG2b (f) levels measure by ELISA in indicated groups. Antigen-specific IgG and its subclasses could be detected approximately 2 weeks after immunization. A time delay for Antigen-specific IgG, IgG2a and IgG2b to reach its peak was observed in drug-treated group though it was not statistically significant (Two Way Analysis of Variance) however a lower level of vWFA2 IgG2a in dipyridamole-treated group was observed at week3 (Sidak's multiple comparisons test). vWFA2 IgG1 level was significantly lower in dipyridamole-treated group. *p<0.05, **p<0.01, ***p<0.001, n=6-8. **(g)** (from left to right) numbers of total B cells, vWFA2-specific B cells, total plasma cells, and vWFA2-specific plasma cells in pooled draining lymph nodes (unilateral popliteal and bilateral inguinal LNs) were determined by flowcytometric analysis at week 8. Despite a tendency of lower cell numbers in dipyridamole-treated group, there was no statistically significant difference. n=6-8. All data were presented as mean with error bars indicating SEM.

3.5.3 Docetaxel

Docetaxel inhibits cell division by binding to microtubules to promote microtubulin assembly and prevent depolymerization. Conventionally, this drug has been used for wide variety of tumors including breast, lung, ovarian, head and neck, gastric, and prostate cancers (124). In this thesis project, mice were treated with 10mg/kg of this drug once a week by i.p. route (109). Overall, no difference was observed in body weight and blood count in both drug-treated and solvent-treated group (Appendix 7.4). Two mice, one from each group, died during the experimental period; one from solvent-treated died at week 4 (day 27) just after blood sampling procedure, and the other one from docetaxel treatment group found dead in the cage at week 8 (day 53). The cause of death is not known for both.

Clinically, docetaxel-treated mice presented less severe symptoms and almost protected from disease development (Fig 3.8 (a)). When cell numbers in the draining LNs were analyzed with available samples, docetaxel-treated mice had fewer numbers of antigen-specific PCs, but this was not the case with other cell fraction tested (Fig 3.8 (g)). Similar to the previous results from dipyridamole treatment, circulating total IgM and IgG levels were lower in drug-treated group at multiple time points (Fig 3.8 (b)). In addition, docetaxel-treatment suppressed total vWFA2 IgG and IgG2a, but not vWFA2 IgG1 and IgG2b (Fig 3.8 (c)-(f)).

In conclusion, docetaxel treatment also demonstrated its preventative effect on disease development of experimental EBA which was accompanied by lower number of antigen-specific PCs. Ag-specific IgG and IgG2 productions were lower in drug-treated mice. However, total IgM and IgG levels were also suppressed, which could be an indication of non-specifically suppressed immune response instead of an antigen-specific reaction.

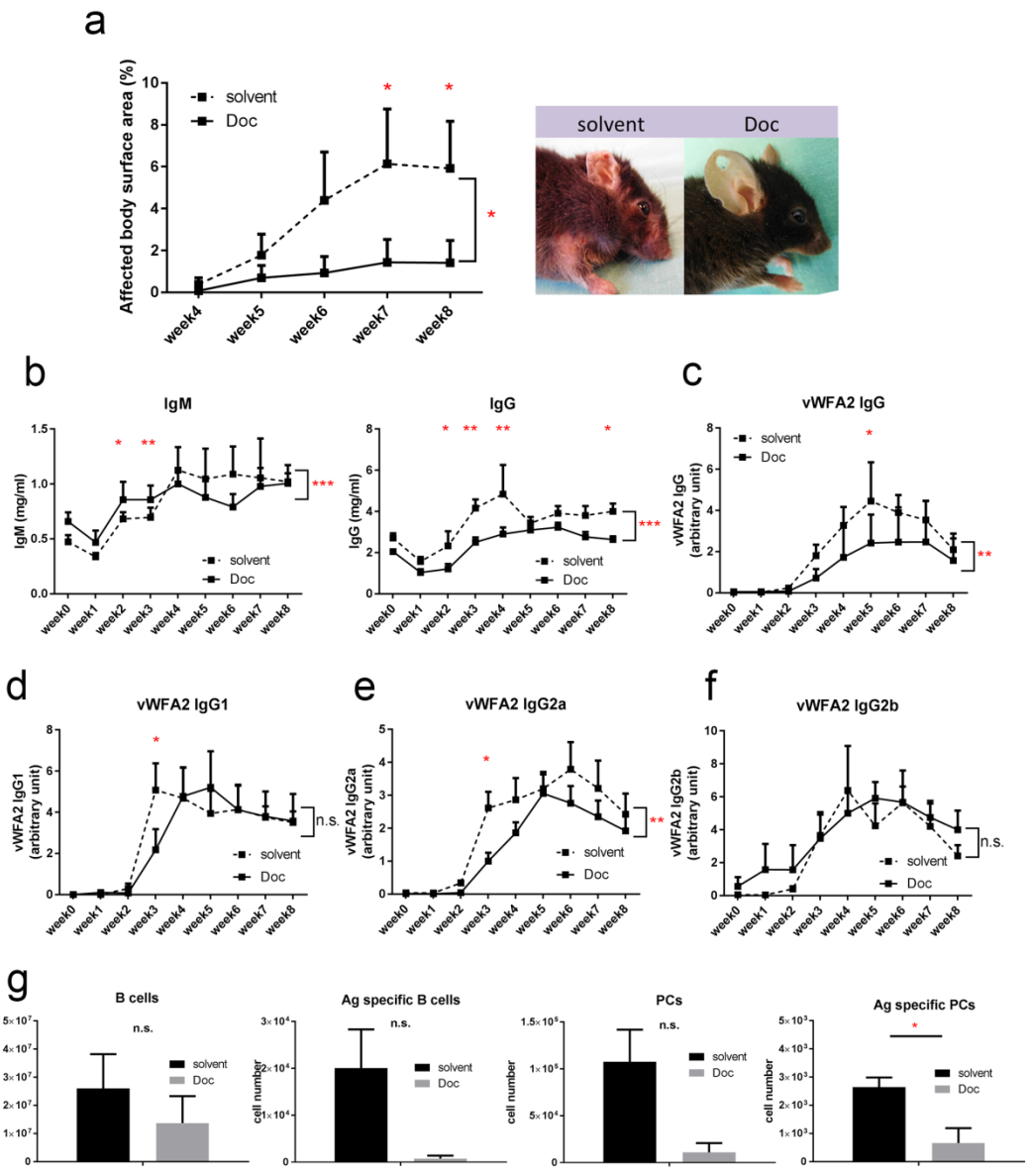
a
Affected body surface area (%)
solvent
Doc
week4
week5
week6
week7
week8
solvent
Doc
b
IgM
IgM (mg/ml)
IgG
IgG (mg/ml)
c
vWFA2 IgG
vWFA2 IgG (arbitrary unit)
d
vWFA2 IgG1
vWFA2 IgG1 (arbitrary unit)
e
vWFA2 IgG2a
vWFA2 IgG2a (arbitrary unit)
f
vWFA2 IgG2b
vWFA2 IgG2b (arbitrary unit)
n.s.
g
B cells
Ag specific B cells
PCs
Ag specific PCs
cell number

Fig3.8 Prophylactic effect of docetaxel on experimental EBA. One day prior to the immunization with vWFA2, once a week i.p. treatment either with solvent or 10 mg/kg docetaxel was started. **(a)** Clinical disease severity presented as affected body surface area (left panel) and representative clinical pictures from solvent-treated and docetaxel-treated group at week 8 (right panel). *p<0.05 (Two Way Analysis of Variance, Sidak's multiple comparisons test). n=5-8. **(b)** Serum levels of total IgM and IgG measured by ELISA in indicated groups. Docetaxel-treated group had lower levels of IgM and IgG at multiple time points. *p<0.05, **p<0.01, ***p<0.001 (Two Way Analysis of Variance, Sidak's multiple comparisons test). n=5-8. **(c)-(f)** Circulating levels of vWFA2-sprcific IgG (c), IgG1 (d), IgG2a (e), and IgG2b (f) levels measure by ELISA in indicated groups. Overall, significantly lower levels of Antigen-specific IgG and IgG2a were observed in docetaxel-treated group but not IgG1 and IgG2b subclasses.

(Two Way Analysis of Variance, Sidak's multiple comparisons test) *p<0.05, **p<0.01, n=5-8. **(g)** (from left to right) numbers of total B cells, vWFA2-specific B cells, total plasma cells, and vWFA2-specific plasma cells in pooled draining lymph nodes determined by flowcytometric analysis at week 8. Even though only available samples from each group were analyzed, significantly fewer number of vWFA2-specific plasma cells was observed in drug-treated mice. *p<0.05 (Mann-Whitney test). n=3. All data were presented as mean with error bars indicating SEM.

3.5.4 Colchicine

Colchicine binds to tubulin to prevent polymerization of microtubules and therefore inhibits mitosis. This tubulin disruption also inhibits neutrophil-endothelial cell adhesion by modulating the expression of adhesion molecules (125). In this project, mice were treated with 0.4 mg/kg i.p. colchicine with a 5-day on, 2-day off regimen (110). During the experimental period, two colchicine-received mice were found dead in the cage at week 4 (day 26) and at week 5 (day 36) with no gross abnormality. No difference in body weight and RBC count was observed. However, a CBC analysis showed that the colchicine treatment changed WBC as well as platelet count over the experimental period even though the difference in WBC and platelet number at each time point was not obvious (Appendix 7.4).

Even though there was a tendency that colchicine-treated mice showed lower disease score, it did not reach a statistically significant difference (p=0.067, Fig 3.9 (a)). Cell numbers in the draining LNs as well as total circulating IgM and IgG levels were not different between

drug-treated group and solvent-treated group (Fig 3.9 (b) and (g)). Interestingly, colchicine-treated mice had lower levels of antigen-specific IgG and its subclass IgGs (Fig 3.9 (c)-(f)).

To sum up this complicated data set, colchicine treatment conducted in this project did not provide a positive effect on disease development of experimental EBA. Even though there was a reduction in vWFA2-IgG and its subclass IgGs production without impairing total IgM and IgG, a possibility of generalized myelosuppression could not be excluded based on the observed WBC reduction in drug-treated mice. Therefore, a conclusive B cell modulatory effect of colchicine could not be confirmed in this study.

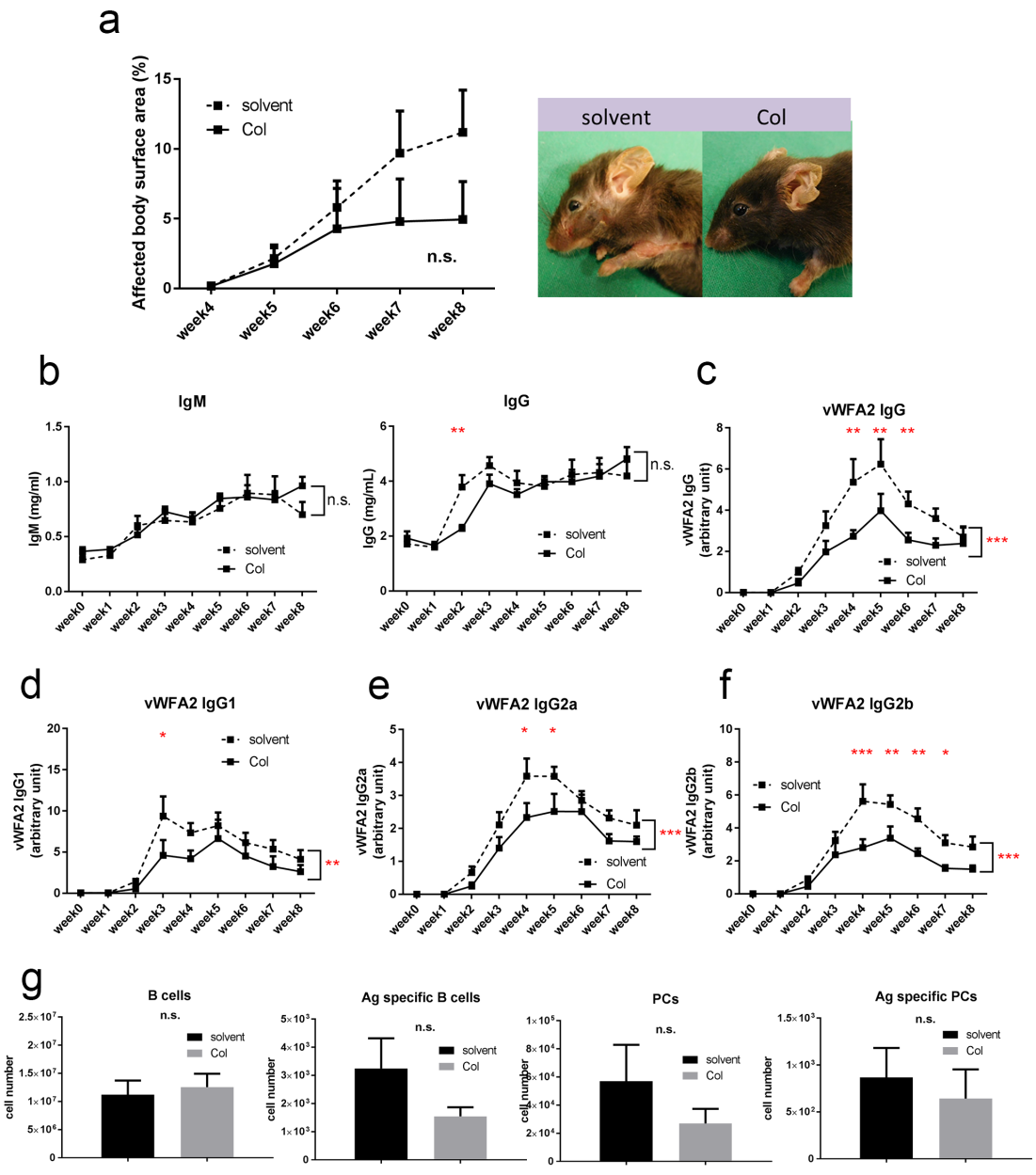
a
Affected body surface area (%)
solvent
Col
n.s.
week4
week5
week6
week7
week8
solvent
Col
b
IgM
IgM (mg/ml)
n.s.
IgG
IgG (mg/mL)
**
n.s.
c
vWFA2 IgG
vWFA2 IgG (arbitrary unit)
***
d
vWFA2 IgG1
vWFA2 IgG1 (arbitrary unit)
**
e
vWFA2 IgG2a
vWFA2 IgG2a (arbitrary unit)
***
f
vWFA2 IgG2b
vWFA2 IgG2b (arbitrary unit)
***
g
B cells
Ag specific B cells
PCs
Ag specific PCs
cell number
n.s.

Fig3.9 Prophylactic effect of colchicine on experimental EBA. One day prior to the immunization with vWFA2, five-days on, two-day off i.p. treatment either with solvent or 0.4 mg/kg colchicine was started. **(a)** Clinical disease severity presented as affected body surface area (left panel) and representative clinical pictures from solvent-treated and colchicine-treated group at week 8 (right panel). No significant difference in disease severity was observed. n=6-8. **(b)** Serum levels of total IgM and IgG measured by ELISA in indicated groups. No overall difference in both IgM and IgG level was observed (Two Way Analysis of Variance) even though total IgG level at week 2 was lower in colchicine-treated mice. *p<0.05. n=6-8. **(c)-(f)** Circulating levels of vWFA2-sprcific IgG (c), IgG1 (d), IgG2a (e), and IgG2b (f) levels measure by ELISA in indicated groups. Overall, colchicine treatment affected the antigen-specific IgG and its subclasses production (Two Way Analysis of Variance) which was accompanied by significantly lower antibody titer at multiple time points (Sidak's multiple comparisons test) *p<0.05, **p<0.01, ***p<0.01. n=6-8. **(g)** (from left to right) numbers of total B cells, vWFA2-specific B cells, total plasma cells, and vWFA2-specific plasma cells in pooled draining lymph nodes determined by flowcytometric analysis at week 8. No statistically significant difference was observed in all cell fractions tested. n=6-8. All data were presented as mean with error bars indicating SEM.

3.5.5 Pyrvinium pamoate

Pyrvinium pamoate (PP) is an anthelmintic drug used for pinworm infections (126). Recently, this dug has been attracting attentions due to its anti-cancer properties (111, 127). Based on previously reported use in mice (111), PP was tested *in vivo* by a dose escalating manner where animals received PP daily (5-day on, 2-day off cycle) by i.p. injection route. The dose escalation was conducted as follows; 0.1 mg/kg for the first week, 0.3 mg/kg for the second week, then the fixed dose of 0.6 mg/kg was continued until the end of experiment.

Overall, there was no deceased mouse in both drug-treated group and solvent-treated one and no change was observed with regard to body weight and CBC analysis (Appendix 7.4. Disease development in PP received mice was significantly milder than solvent treated group, where the %BSA at week 8 was 5.04 ± 1.87% and 11.76 ± 2.64%, respectively (Fig 3.10 (a)). In addition, lower cell numbers of B cell, vWFA2-specific B cells, and PCs in draining LNs were observed in drug-treated mice (Fig 3.10 (g)). An interesting finding was

that total IgM level in PP-treated mice was lower at multiple time points tested whereas the total IgG level was not affected by this drug (Fig 3.10 (b)). However, the timing for vWFA2-specific IgG to reach its peak titer was delayed in PP-treated mice, accompanied by lower titers at weeks 3 and 4 (Fig 3.10 (c)). Similarly, other IgG subclasses from drug-treated mice also reached its peak at delayed time points compared to solvent group (Fig 3.10 (d)-(f)), suggesting a slower development of adaptive immunity against the pathogenic protein.

In summary, treatment with PP was well-tolerated and demonstrated a prophylactic effect on disease development in experimental EBA. Considering the decreased cell numbers in LNs as well as antigen-specific antibody production, it could be speculated that the observed finding could result from the suppressed B cell function under the treatment of this drug.

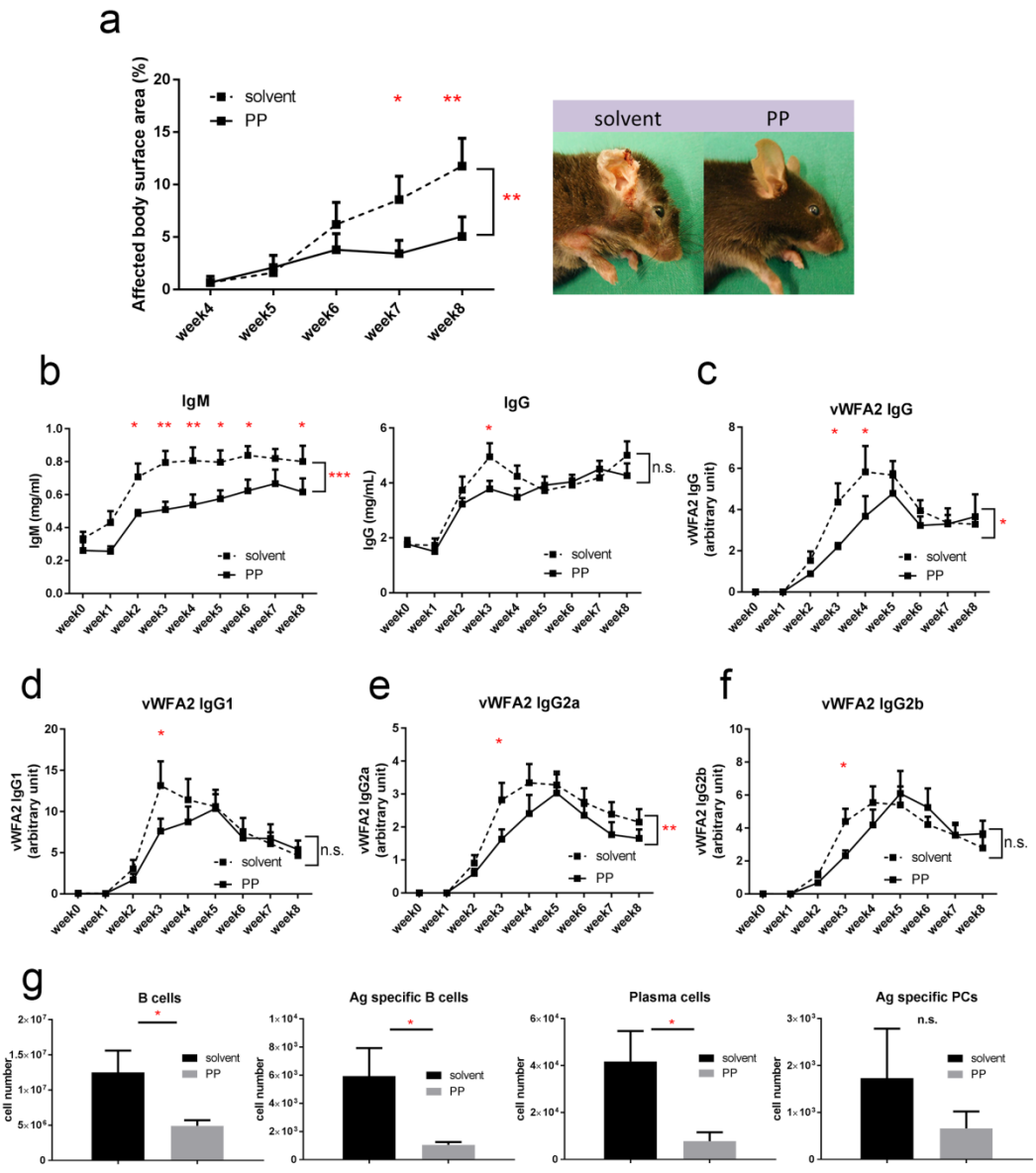
a
Affected body surface area (%)
solvent
PP
week4
week5
week6
week7
week8
solvent
PP
b
IgM
IgM (mg/ml)
IgG
IgG (mg/mL)
n.s.
c
vWFA2 IgG
vWFA2 IgG (arbitrary unit)
d
vWFA2 IgG1
vWFA2 IgG1 (arbitrary unit)
e
vWFA2 IgG2a
vWFA2 IgG2a (arbitrary unit)
f
vWFA2 IgG2b
vWFA2 IgG2b (arbitrary unit)
g
B cells
Ag specific B cells
Plasma cells
Ag specific PCs
cell number
n.s.

Fig3.10 Prophylactic effect of pyrvinium pamoate on experimental EBA. One day prior to the immunization with vWFA2, five-days on, two-day off i.p. treatment either with solvent or pyrvinium pamoate (PP) was started. The dose escalation method was employed in PP treatment, where the drug was given at 0.1 mg/kg for the first week, 0.3 mg/kg for the second week, followed by the fixed dose of 0.6 mg/kg until the end of the experiment. **(a)** Clinical disease severity presented as affected body surface area (left panel) and representative clinical pictures from solvent-treated and PP-treated group at week 8 (right panel). PP-treated group developed less severe disease compared to solvent-treated group. (Two Way Analysis of Variance, Sidak's multiple comparisons test) *p<0.05, **p<0.01. n=8. **(b)** Serum levels of total IgM and IgG measured by ELISA in indicated groups. Total IgM levels were significantly lower in PP-treated mice whereas no overall difference in IgG level was observed even though total IgG level at week 3 was lower in PP-treated mice. (Two Way Analysis of Variance, Sidak's multiple comparisons test). *p<0.05, **p<0.01, ***p<0.001. n=8. **(c)-(f)** Circulating levels of vWFA2-sprcific IgG (c), IgG1 (d), IgG2a (e), and IgG2b (f) levels measure by ELISA in indicated groups. PP-treated mice showed a delayed production of all Ag-specific antibodies tested, which was accompanied by significantly lower titers at week 3 in all antibodies tested, and vWFA2-IgG titer at week 4 (Sidak's multiple comparisons test). No statistically significant difference was detected in overall vWFA2-IgG1 and IgG2b production (Two Way Analysis of Variance). *p<0.05, **p<0.01. n=8. **(g)** (from left to right) numbers of total B cells, vWFA2-specific B cells, total plasma cells, and vWFA2-specific plasma cells in pooled draining lymph nodes determined by flowcytometric analysis at week 8. A significant reduction in numbers of B cells, vWFA2-specific B cells, total plasma cells in PP-treated group was observed. *p<0.05 (Mann-Whitney test). n=8. All data were presented as mean with error bars indicating SEM

3.6 Treatment with pyrvinium pamoate prevented disease progression in an established immunization-induced EBA

Followed by the confirmed preventative effect on disease development in EBA which could be linked with a suppressed B cell function, the possibility of PP as a therapeutic agent was further explored; B6.s mice with established EBA were treated with PP or solvent and how the treatment would affect the course of the disease was observed. As shown in Fig. 3.11, after immunization with vWFA2 and when the clinical disease score reached >2% affected body surface area, B6.s mice were allocated to either drug treatment or solvent treatment.

During the experimental period, two mice from PP-treated group died; One was found dead in the cage at week 3 of the treatment (day 45 after immunization), and the other one was also found dead at week 5 of the treatment (day 59 after immunization). The cause of death

was unknown for both cases. However, judging from circumstances, an environmental factor, i.e. fighting with another mouse in the same cage, could not be excluded for the first case.

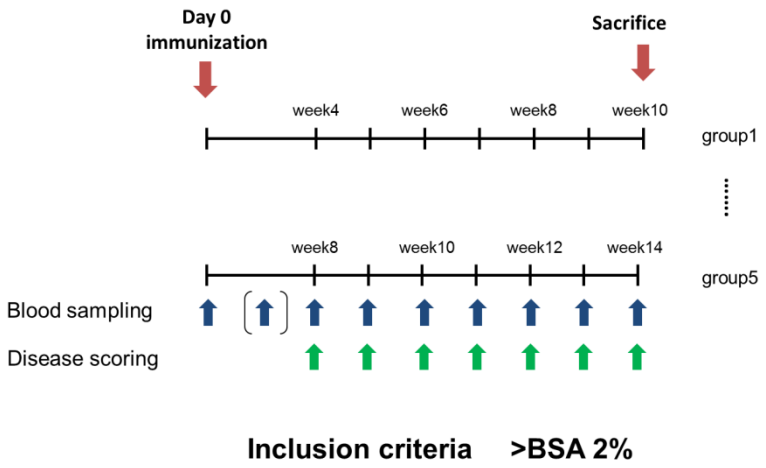

Fig3.11 Schematic diagram of the experimental setup (therapeutic approach). On day 0, B6.s mice were immunized with a mixture of 60 µg vWFA2 and Titermax® as an adjuvant in the footpad (120 µg/head, single immunization). Weekly recording of disease severity presented as affected body surface area (BSA) was started from week 4, and once affected BSA is >2%, mice were randomly allocated either to solvent-treated group or pyrvinium pamoate (PP)-treated group. The inclusion was continued until week 8 and mice with clinical score of <2% at week 8 were excluded from further study. Once recruited, mice received corresponding treatment for six weeks. In addition to the assessment of disease severity, blood sampling was also performed every week. vWFA2= recombinant von Willebrand factor A–like domain 2.

Clinically, even though the disease severity in solvent-treated mice was also relatively stable at later time points and spontaneous recovery occurred in both groups, a clear suppression in disease progression was observed in mice received PP treatment (Fig. 3.12 (a)). However, the mean relative disease score in PP group was always above 1.0, meaning that PP treatment did not reverse the course of the disease. Flowcytometric analysis of cell numbers in the draining LNs, which was conducted at the end of the experiment for each mouse, showed no difference in each cell fraction (Fig. 3.12 (g)), indicating a possibility of weakened immunological response at the end of the experiment.

With regard to the circulating immunoglobulin level, total IgG in the control group kept on the rise until the fifth week of the treatment whereas the change in IgG level in the PP-treated group was minimal. On the other hand, serum IgM level was similar in both groups where the titer showed an increase from week 3 to 5, then declined afterwards (Fig. 3.12 (b)). In both groups, vWFA2-specific IgG was at its peak when the treatment was initiated, after which kept decreasing over the experimental period. Of note, a more rapid decline was observed in drug-treated mice (Fig. 3.12 (c)). Additional antigen-specific IgG subclass ELISA showed a similar reduction pattern of IgG1 and IgG2b in both groups (Fig. 3.12 (d) and (f)). On the other hand, vWFA2 IgG2a in control group remained significantly higher than PP-treatment group (Fig. 3.12 (e)).

In summary, PP treatment was also effective in the established EBA where disease progression as well as antigen-specific immune response represented by vWFA2 IgG production was suppressed.

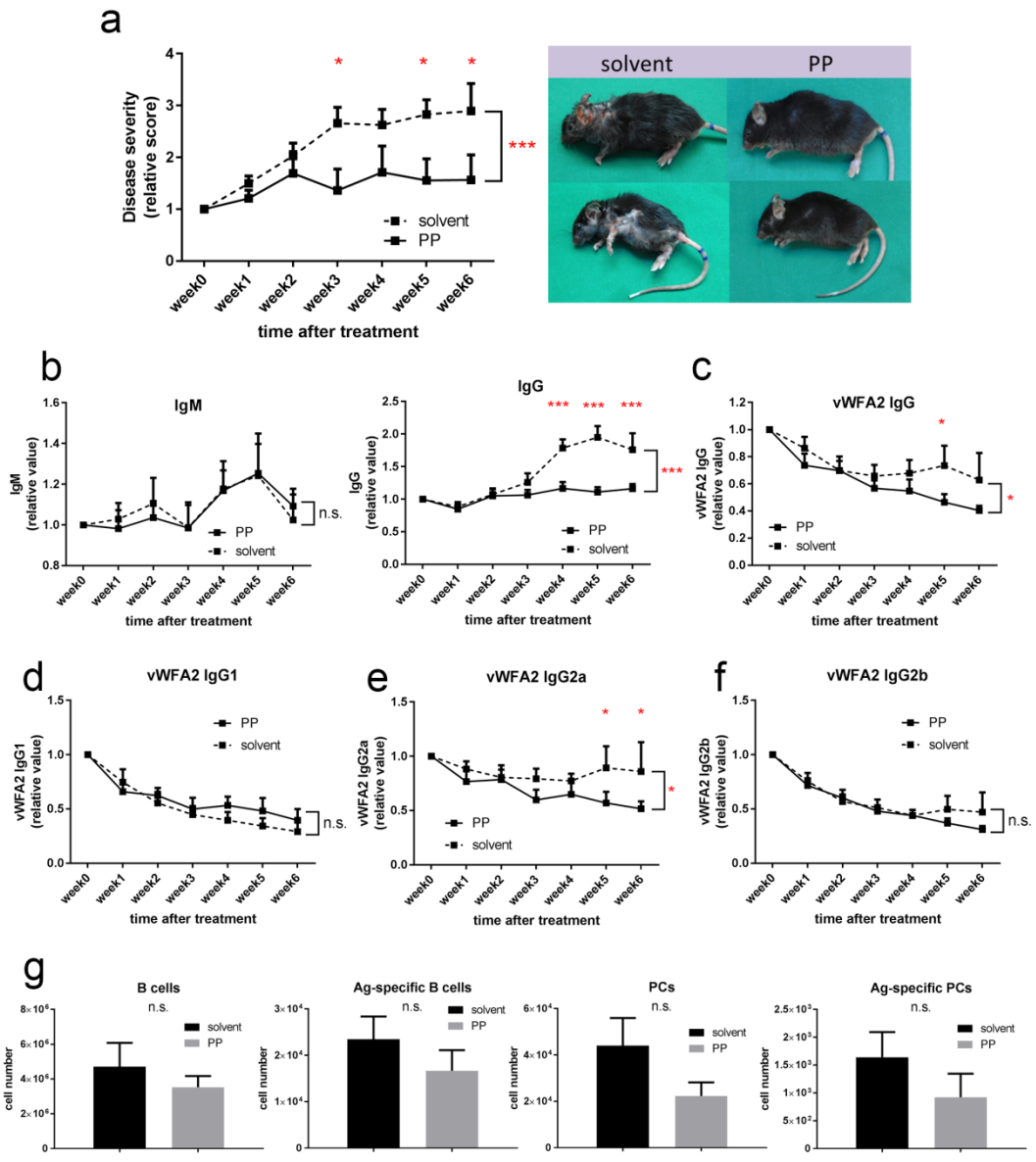
a
Disease severity (relative score)
solvent
PP
time after treatment
week0
week1
week2
week3
week4
week5
week6
b
IgM
IgM (relative value)
n.s.
IgG
IgG (relative value)
c
vWFA2 IgG
vWFA2 IgG (relative value)
d
vWFA2 IgG1
vWFA2 IgG1 (relative value)
e
vWFA2 IgG2a
vWFA2 IgG2a (relative value)
f
vWFA2 IgG2b
vWFA2 IgG2b (relative value)
g
B cells
Ag-specific B cells
PCs
Ag-specific PCs
cell number

Fig3.12 Therapeutic effect of pyrvinium pamoate on established EBA. EBA was induced in B6.s mice by single immunization with a mixture of 120 µg vWFA2 and Titermax® as adjuvant. When clinical disease score exceeded 2% after week 4, mice were recruited in the study and received either pyrvinium pamoate (PP) or solvent treatment for six weeks. PP was given at a dose-escalation manner described in Fig 3.9. **(a)** Clinical disease severity presented as relative affected body surface area (left panel) and representative clinical pictures from solvent-treated and PP-treated group at the end of the experiment. Disease progression was significantly inhibited under the treatment with PP. *p<0.05, ***p<0.001 (Two Way Analysis of Variance, Sidak's multiple comparisons test). n=8-10. **(b)** Serum levels of total IgM and IgG measured by ELISA in indicated groups. Results were normalized to the baseline value of each mouse which was obtained at the time of inclusion. No significant difference in IgM titers. Serum IgG levels in PP-treatment group was minimally changed in contrast to the prominent increase in solvent-treated group. ***p<0.001 (Two Way Analysis of Variance, Sidak's multiple comparisons test). n=8-10. **(c)-(f)** Circulating levels of vWFA2-sprcific IgG (c), IgG1 (d), IgG2a (e), and IgG2b (f) levels measure by ELISA in indicated groups. Normalized results are presented. PP-treatment did not affect the levels of vWFA2-IgG1 and IgG2b ((d) and (f)) whereas a significantly sharper decline in vWFA2-IgG and IgG2a levels under the treatment with PP was observed ((c) and (e), *p<0.05, Two Way Analysis of Variance, Sidak's multiple comparisons test). n=8-10. **(g)** (from left to right) numbers of total B cells, vWFA2-specific B cells, total plasma cells, and vWFA2-specific plasma cells in pooled draining lymph nodes determined by flowcytometric analysis at the end of experiment (week 10-16). No change in each cell fraction was detected. n=8-10. All data were presented as mean with error bars indicating SEM.

3.7 Altered CD37 expression was observed in pyrvinium pamoate-treated human B cells

Next generation sequencing (NGS) is a powerful technique to capture ongoing transcriptional activities in certain cells/tissues under particular circumstances (128, 129). In order to identify target genes affected by the treatment with PP, Illumina RNA-seq analysis was performed where gene expression in human B cells 1) without aCD40Ab/IL-21 stimulation nor PP treatment, 2) with stimulation but without PP treatment, or 3) with both stimulation and PP treatment (0.1 µM) was compared. Total RNA from human B cells was extracted after 24-hour incubation and gene expression of each sample was determined by reading 75 kb sequence from both ends (150 reads per sample) and by mapping them to the reference human genome. After eliminating low-quality data, 22.7-44.5 million reads per sample (80.84 - 88.44%) could be obtained and uniquely mapped (Table 3.5).

When aCD40Ab/IL-21 stimulated B cells and unstimulated B cells were compared, a total of 2,063 genes were differentially expressed. The number of genes was 19 when the comparison was done between stimulated cells with or without PP treatment. Among the 18 overlapping ones, eight genes, *ATP6V1C2*, *C9orf139*, *FAM166A*, *SYNE2*, *CD37*, *COX20*, *GPS2*, and *SNX22*, were annotated as protein-coding (130) and scrutinized further in this study. (Fig 3.13).

Table3.5 Number and percentage of uniquely mapped genes.

		Reads number	(%)
Donor1	Unstimulated	32218562	86.82
	Stimulated	33212083	86.5
	Stimulated+PP	29034767	86.43
Donor2	Unstimulated	34255507	88.44
	Stimulated	44518771	88.32
	Stimulated+PP	22674521	80.84
Donor3	Unstimulated	35253217	87.8
	Stimulated	33694089	88.1
	Stimulated+PP	32079762	82.77

Unstimulated=isolated human B cells without aCD40Ab/IL-21 and no PP treatment, Stimulated=isolated human B cells with aCD40Ab/IL-21 and no PP treatment, Stimulated+PP=isolated human B cells with aCD40Ab/IL-21 and PP treatment

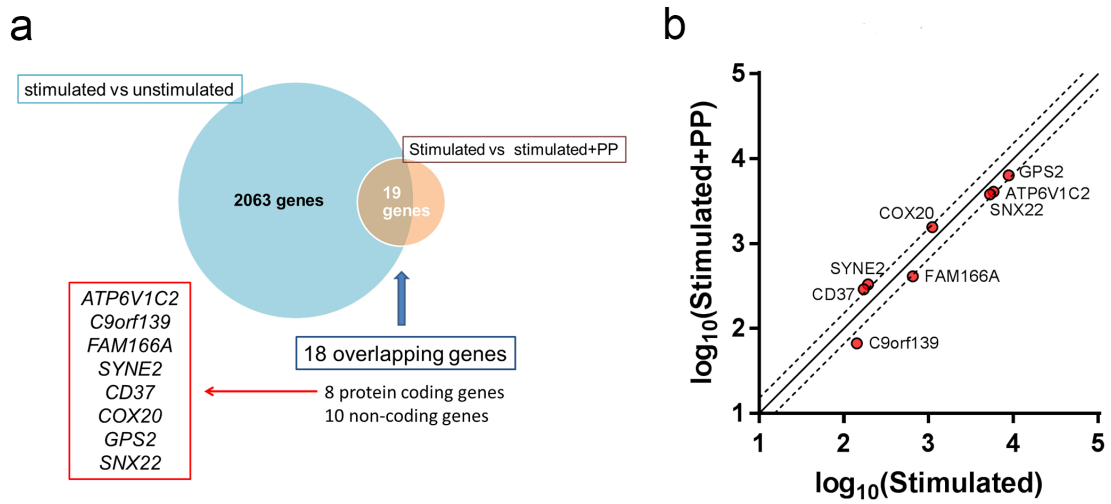

Fig3.13 RNA-sequence identified eight protein-coding genes differentially expressed in human B cells stimulated with aCD40Ab/IL-21 ± pyrvinium pamoate treatment. Human B cells preparation and stimulation were similarly performed as described in Fig 3.1 and 3.2. Stimulated cells were either untreated or treated with 0.1 μM pyrvinium pamoate (PP). After 24-hour incubation, cultured cells were collected and RNA extraction was performed as described in material and method.1 μg of RNA from each culture condition, 1) unstimulated B cells, 2) stimulated B cells, and 3) stimulated and PP-treated B cells, was used for RNA sequence. Samples from 3 donors were analyzed. **(a)** Venn diagram depicting an overlap of differentially expressed genes. A total of 2063 and 19 genes were differentially expressed when the expression profile was compared between unstimulated vs stimulated B cells, or stimulated vs stimulated with PP treatment B cells, respectively. Among the 18 overlapping genes, 8 protein-coding genes were further scrutinized. **(b)** A comparison of eight protein-coding gene expressions. Dotted lines indicate either 1.5 or 0.66 fold change calculated by [Gene expression of stimulated B cells with PP treatment]/[Gene expression of stimulated B cells].

In order to verify the RNA-seq result, the expression of these candidate genes was also evaluated by real-time quantitative PCR assays (qPCR). Obtained results showed a discrepancy in four out of eight genes with regard to the expression patterns in RNA-seq and qPCR (Fig 3.14 (a)). The remaining four genes showed a similar expression profile, however, the difference in expression level was no longer detected in *SYNE2*, *COX20* and *SNX22* in qPCR. On the other hand, the expression of *CD37* in PP-treated B cells was still significantly higher with a 1.65-fold change than those without drug treatment (Fig 3.14 (b) and Table 3.6).

These findings suggest that CD37, a member of tetraspanins which expression is relatively limited to on B cells (131, 132), is a potential target of PP in aCD40Ab/IL-21 stimulated human B cells.

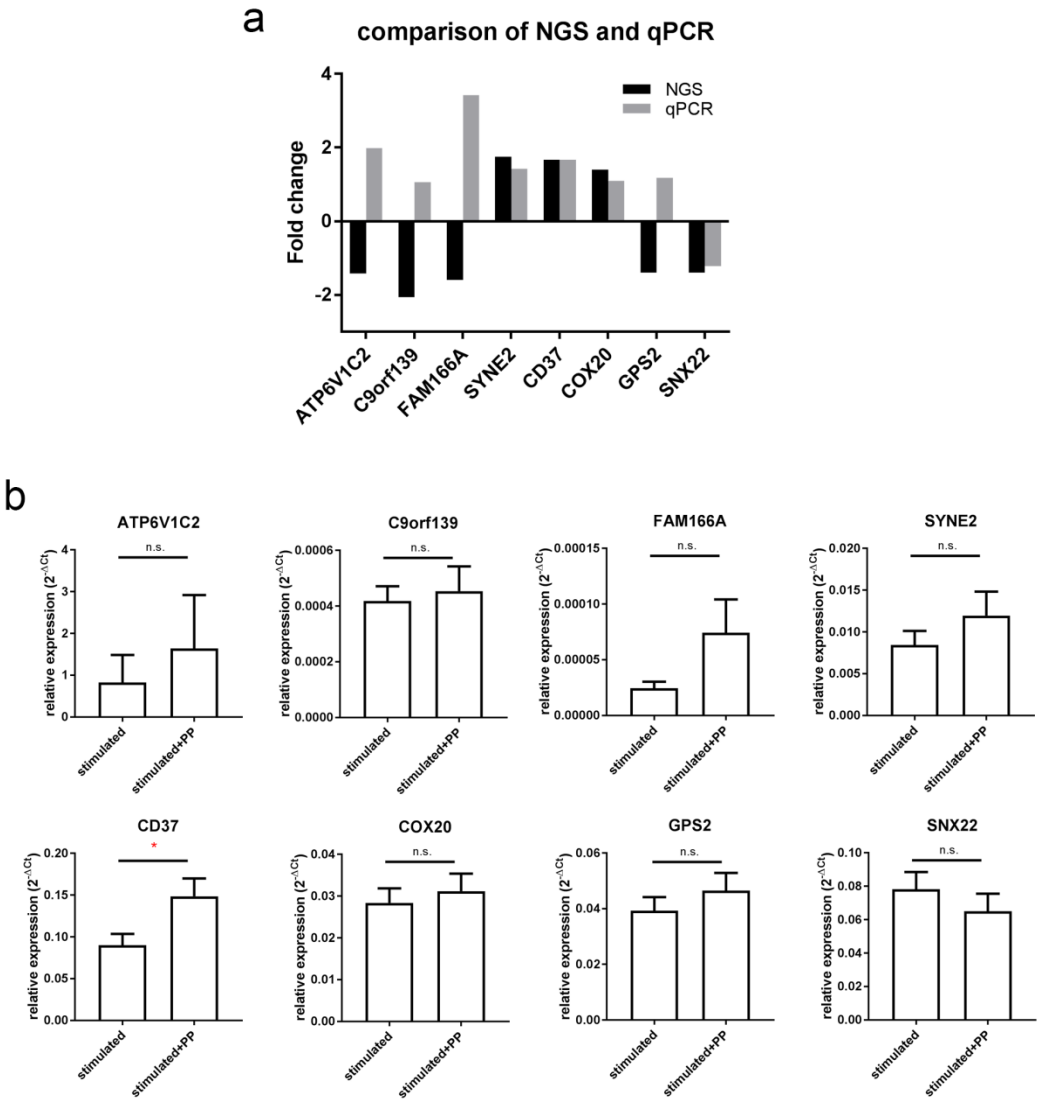

Fig3.14 Validation of RNA-sequence results by real-time quantitative PCR assays. mRNA levels of eight genes were analyzed by real-time quantitative PCR assays (q-PCR). For the comparison of mRNA levels, all results were normalized to the value obtained from GAPDH. **(a)** Compatibility of two different methods analyzing gene expression. A similar expression pattern was observed in *SYNE2*, *CD37*, *COX20*, and *SNX22* whereas expressions of *ATP6V1C2*, *C9orf139*, *FAM166A* and *GPS2* were not reproduced by qPCR. Fold change was calculated by [Gene expression of stimulated B cells with PP treatment]/[Gene expression of stimulated B cells]. **(b)** mRNA expressions of the eight protein-coding genes selected based on RNA-Seq analysis. *p<0.05 (Unpaired t-test). n=6. Data are presented as mean with error bars indicating SEM. NGS: Next generation sequencing (=RNA-sequence)

Table3.6 Summary of real-time quantitative PCR assays of eight protein-coding genes selected based on RNA-sequence.

Genes	Stimulated	Stimulated+PP	Fold change (Stimulated+PP/	*p*
SYNE2	0.008	0.012	1.41	0.2633
SNX22	0.078	0.065	0.83	0.3949
GPS2	0.039	0.047	1.18	0.3932
FAM166A	2.45E-05	7.43E-05	3.03	0.1508
COX20	0.028	0.031	1.1	0.6186
CD37	0.09	0.149	1.65	0.0429*
C9orf139	4.19E-04	4.54E-04	1.08	0.7411
ATP6V1C2	0.828	1.64	1.98	0.2403

mRNA levels were normalized to the value of GAPDH.

4. Discussion

4.1 Overview

In this study, I tested the hypothesis that specific, existing drugs might possess B cell modulatory effects and therefore could be used as therapeutic agents in ADs. The collected data exhibited that already-licensed drugs indeed showed inhibitory effects on human B cell proliferation/differentiation. Moreover, *in vivo* preventative effect of drugs on disease development in immunization-induced EBA was demonstrated, some of which was accompanied by findings suggestive of suppressed B cell immunity. Among the drugs tested, PP was also able to prevent disease progression in the established EBA and was the most promising compound in terms of suppressing B cell functions and the subsequent adaptive immunity. To my best knowledge, this is the first study to demonstrate a potential of PP as a treatment option in ADs.

4.2 Step by step in vitro screening effectively selected hit compounds

As the first screening, a total of 1,200 compounds were screened for their property to suppress human B cell proliferation, where a ≥ 50% reduction was achieved with 48 drugs at a fixed concentration of 1 μM. The rate of first hit was 0.04% and the identified compounds were classified as anti-neoplasm (13 drugs, 27.1%), anti-infection (11 drugs, 22.9%), anti-inflammatory (9 drugs, 18.8%), or others (15 drugs, 31.2%).

Followed by the proliferation assay, candidate drugs were tested their toxicity on B cells. After applying to the selection criteria shown in Table 3.2, the number of candidate drugs could be reduced from forty-eight to six. Of note, drugs with high toxicity on B cells were not eliminated in the current project because, even though a desirable drug would be a one demonstrates high efficacy on its target with minimal toxicity to off-target cells/tissues, a high toxicity on B cells does not necessarily mean that they are also toxic to other types of cells. In addition, low viability of cells in the toxicity assay could be misinterpreted because that result could be attributable not to the drug effect but to the suboptimal *in vitro* B cell stimulation.

The next *in vitro* validation step focused on testing the effects of drugs on B cell functions. Firstly, immunoglobulin production as well as plasmablast generation from aCD40Ab/IL-21 stimulated B cells was compared between with or without drug treatment. As shown in Fig 3.3, IgM or IgG production from drug-treated B cells was inversely correlated with drug concentration. i.e., when B cells were treated with higher concentrations of the drug, they produced lesser amount of immunoglobulins. Similarly, smaller or even no plasamablast population was yielded from B cells cultured under such conditions.

When interpreting these results, at least two inhibitory mechanisms for B cells to differentiate into plasma cells can be speculated. The first one is that an induction of cell death occurred in B cells at earlier stages of differentiation and the other one is that the drugs might have interfered with gene expression which facilitates B cells to become plasma cells. In the case of cell death, a sign of this process can be captured as a change on cell membrane where translocated phosphatidylserine (PS) would be detected with Annexin V on dying cells (133). For a further investigation regarding the drug effect on cell viability, a comparison of the intensity of this membranous change between B cells with/without drug

treatment could be performed. As for the latter possibility of altered gene expressions by drug treatment, studies of gene expression on drug-treated B cells might be informative. The process of B cell differentiation into plasma cells is regulated by transcription factors including *PAX5*, *EBF1*, *BLIMP-1*, *IRF-4*, *XBP-1*, and *BCL-6* (134), where, in brief, B cell lineage factors, *PAX5*, *EBF1*, repress the expression of plasma cell lineage factors, *BLIMP-1*, *IRF-4*, *XBP-1*, while B cell lineage factors will be suppressed when the plasma cell program is initiated. In the current study, it remains unknown which of these two inhibitory mechanisms of B cell development, or perhaps both, could be applied to the obtained results. For a clarification of detailed mechanisms of action, future studies can entail such assays to investigate kinetic change in the level of apoptosis and apoptosis related genes, or change in the expression of plasma cell development related genes.

In the phenotypic analysis investigating *in vitro* plasmablasts generation, a unique $CD19^{+}CD27^{+}CD38^{-}$ cell population was identified when aCD40Ab/IL-21 stimulated B cells were treated with PP, which was absent when cells were treated with other drugs (Fig 3.4 (e)). No further assessment of this population was conducted in the current study, therefore, there is no clue with regard to the significance of this cell population if there is any. However, one interesting finding of the observed $CD19^{+}CD27^{+}CD38^{-}$ cell population was the lack in CD38 expression.

In B cell studies, CD38 has been used as a surface marker arguing B cell differentiation; CD38 surface expression is discontinuous and limited to pre-B cells in bone marrow and B cells in germinal center, and plasamablasts/plasama cells (135, 136).

The source of B cells used in this assay was peripheral blood obtained from healthy donors. Therefore the enriched B cells were a mixture of naïve and memory B cells which had gone

through a development process in the bone marrow, and CD38 positive phenotype observed at day 5 after stimulation would reflect the process of B cell differentiation into plasmablasts.

With regard to the function of CD38, the signaling via this molecule has not been completely elucidated. However, the pathway activation in mature B cells appears to result in cell proliferation; when germinal center B cells interact with an agonistic antibody with CD38, these cells were anti-apoptotic and increased cell survival was observed (137). Moreover, CD38 expression has been recognized as a unfavorable prognostic marker in chronic lymphocytic leukemia (CLL), a hematological malignancy of mature B cells (138) in which CD38 also acts as a receptor mediating signals in favor of cell proliferation and survival (136, 138). About the mechanism how CD38 can influence on B cell immunological activities, even though no direct association was observed, one study suggested that CD38 could lower the threshold of BCR medicated B cell response (139). In another study, Deaglio *et al*. demonstrated the ability of CD38 to form a complex with CD19 molecule upon stimulation by monoclonal antibody or CD31 expressing cells (CD31 is a suggested natural ligand of CD38), which induced Ca^{++} influx and phosphorylation of ERK1/2 (140), and these events were observed in CD40L stimulated murine B cells (141-143).

Despite that the variations in the source of B cells (PB, cord blood, or secondary lymphoid tissue), the cell types to be tested (pan B cells, naïve, or memory cells), *in vitro* cell culture condition as well as B cell stimulation method generate a variety of findings in B cell proliferation/differentiation (102, 144-147), as a functional molecule, CD38 appears to be a controlling factor of B cell survival/proliferation. If CD38 expression on stimulated B cells was suppressed under the treatment with PP, the drug might negatively control cell survival and proliferation by preventing CD38 expression.

Even though there is too little information to define this population, a more informative finding could be obtained when kinetic study of change in surface molecule expression as well as immunoglobulin production is conducted separately between naïve and memory cells.

In order to eliminate possibilities for the candidate drugs to exhibit clinical benefit by acting on other immune cells involved in EBA pathogenesis, their effects on T cells and neutrophils were also tested. All of the tested drug did not affect ROS release form IC-activated neutrophils, however, two substances, gemcitabine and proscillaridin A, did suppress T cell proliferation. These results are in accordance with previous studies demonstrating toxicity of proscillaridin A on a variety of tumors including lymphoma cell lines (148-150). Likewise, gemcitabine, a deoxycytidine analogue widely used for the treatment of solid tumors and hematological malignancies (151-153), is effective on both B and T cell lineage lymphoproliferative disorders (154-156). Therefore, at this point, these two drugs were eliminated from further investigation.

As mentioned in the previous chapter (**Results 3.4 Selected compounds did not affect reactive oxygen species (ROS) release from immunocomplex (IC)-activated polymorphonuclear leukocytes (PMNs) but some also inhibited CD3/28 activated T cell proliferation**), the obtained results do not necessarily demonstrate exclusive effects of the drugs on B cells. However, the results of the absent effect on neutrophil function and/or T cell proliferation by some of the candidate drugs did demonstrate that the drug sensitivity is different from one cell type to another.

Finally, the drug library used in this study consists of clinically in-use compounds which had already gone through preclinical and clinical tests before approval. Therefore, in this study, it could have been possible to study the available published data investigating the mechanism

of action or target molecules of the library compounds and conduct a pre-selection before starting an actual screening assay. However, due to the high total number of the drugs covering a wide range of medical purposes, target-based screening was not a realistic option, thus, a phenotypic analysis focusing on the drug effect on B cell functions including proliferation and differentiation was employed. Moreover, considering the aim of this study of discovering unknown B cell modulatory properties within existing drugs, a phenotypic screening without knowing details of the compounds was more suitable approach, and it indeed enabled us to identify four candidates to be further investigated. It can be concluded that an effective *in vitro* screening was achieved in this study.

4.3 Pyrvinium Pamoate exhibited the most prominent inhibitory effect on B cell immunity and was an effective agent in suppressing immunization-induced EBA

In a drug development process, candidate compounds undergo preclinical *in vivo* test where the efficacy and safety will be evaluated using animals (157, 158). In this study, four drugs, dipyridamole, docetaxel, colchicine, and pyrvinium pamoate (PP), were firstly tested their prophylactic effect on disease development of immunization-induced EBA mouse model. As shown in the previous chapter (**3.5 Prophylactic effect of the candidate drugs on immunization-induced experimental EBA**), the treatment outcome was variable depending on the drug tested. Among them, pretreatment with PP prior to the immunization was not only successful in slowing down the disease development, it also resulted in a suppression of B cell development and the subsequent antigen-specific humoral immune response represented by reduction in cell numbers in LNs and circulating Ag-specific antibodies.

Autoantibody production in EBA is a triggering event ultimately leads to blister formation (discussed in **1.3.3 Epidermolysis bullosa acquisita (EBA)**). In addition, similar to other ADs (discussed in **1.4.3 B cell-targeted treatment in autoimmune diseases**), previous studies have suggested that B cell modulation is one strategy to treat EBA partly due to its preventative effect on the subsequent autoantibody production. For example, in 2007, Niedermeier *et.al*, reported 2 cases of mechanobullous EBA treated with a combination therapy of immunoabsorption (IA) and rituximab (159). Even though both patients had failed to respond to multiple immunosuppressive treatments including steroids, cyclophosphamide, azathioprine, methotrexate, and cyclosporine, a remarkable improvement in their skin lesions was observed after two cycles of IA followed by rituximab infusion. The clinical response was accompanied by the reduction in B cell count as well as circulating anti–collagen VII IgG titers. Similarly, rituximab was beneficial in other refractory EBA cases (160-162), one of which demonstrated that the successful clinical response was also accompanied by disappearance of the reaction between patient's serum and recombinant NC domain of type VII collagen by Western blotting (160), an indicative finding of decreased Ag-specific antibodies.

In this study, there was a delay in the production of vWFA2-specific Abs as well as Ag-specific IgG2a and IgG2b subclasses in PP-treated mice compared to the control group. With regard to the pathogenicity of autoantibodies in ADs, IgG2a/c and IgG2b subclasses are able to induce more potent pro-inflammatory response than IgG1 due to their affinity with FcγRIV and FcγRIII (163, 164). In the case of immunization induced EBA mouse model used in this study, previously demonstrated findings that 1) subclasses of Ag-specific IgG1, IgG2a and IgG2b but not IgG3 are induced in this mouse model (45), and 2) not FcγRI, FcγRIIb, or

FcγRIII but FcγRIV deficient or functionally impaired mice were protected from disease development when they passively received pathogenic antibody against type VII collagen (165), and 3) FcγRIV is a pro-inflammatory FcγR expressed on myeloid lineage cells and interact with IgG2a and IgG2b with intermediate affinity (166) lead to a speculation that the pathogenicity in EBA is likely to be dominantly modulated by Ag-specific IgG2a and IgG2b and FcγRIV. Therefore, the delayed development of clinical phenotype observed in PP-pretreated mice could be due to the decreased Ag-specific antibody, especially IgG2a and IgG2b subclasses, production.

Since PP was the most promising compound in terms of B cell suppression, this drug was further evaluated its therapeutic property against an established EBA. The result (**3.6 Treatment with pyrvinium pamoate prevented disease progression in an established immunization-induced EBA**) demonstrated a possible use of this drug as a therapeutic agent in ADs; a significantly slower disease progression was observed in drug-treated mice with established EBA. One thing to be mentioned, however, is that the clinical score in PP-treated mice was not reversed and the disease intensity in control group was also rather stable at later time points of the experimental period. One possible explanation for this finding would be the immunization protocol of this animal model, where mice were immunized with the pathogenic protein only once while patients with ADs are continuously being challenged by their endogenous autoantigens. The spontaneous reduction in titers of Ag-specific antibody and/or disease severity was also observed in previous studies using the same mouse model (45, 167). Therefore, it could be possible that the immunogenicity of the protein was not sustainable over that time of experimental period. In addition, no significant improvement in disease score among PP-treated mice might indicate that the main effect of

this drug lies in the inhibition of the de novo disease development and not in the healing of the established lesion.

The favorable clinical effect of PP treatment was supported by the reduction in Ag-specific antibodies. Even though a decline in titer of circulating vWFA2-specific IgG and its subclasses was observed in both drug-treated and solvent-treated groups, as mentioned in the previous chapter (**3.6 Treatment with pyrvinium pamoate prevented disease progression in an established immunization-induced EBA**), the rate of reduction was more facilitated in drug-treated group (Fig 3.12 (c) and (e)). Considering the inhibitory effect of PP on B cell proliferation both *in vitro* and *in vivo* this study has demonstrated, this difference in reduction rate may reflect a decreased antibody production in PP-treated mice due to the suppressed B cell proliferation and thus the subsequent differentiation into antibody-secreting plasma cells.

In this study, cell proliferation or expansion status in draining LNs was evaluated by means of flowcytometric analysis. Whereas prophylactic treatment with PP resulted in significantly lower numbers of cell fractions examined, the difference was no longer obvious when PP was used as a therapeutic agent despite a tendency that cell numbers in PP-treated animals were still lower (Fig 3.10 (g) and Fig 3.12 (g)). One explanation for this difference could be due to the timing of analysis. Even though GC reaction, which includes cellular proliferation, selection and affinity maturation can be seen 4 or 5 days after the first encounter with the antigen and continue for weeks to months (168), adjuvant and/or amount of the antigen can affect the degree of response (168, 169). In the current study, the samples for FACS were harvested at the end of experiment, meaning 10 to 14 week after the immunization when a spontaneous decline in disease severity and circulating Ag-specific Ab titer were observed.

Therefore, it is possible that the immunogenicity of the protein was not strong enough to yield a significant GC reaction in both PP-treated mice and the control.

In summary, in the experimental EBA, PP was the most promising candidate as a therapeutic agent that processes B cell modulatory properties. The drug was able to prevent both disease development and progression presumably due to its ability to suppress B cell development as well as *de novo* Ag-specific antibody production.

4.4 CD37 could be a potential target of PP in modulating B cell immunity

The current study has demonstrated a possibility of PP as a treatment option in ADs through its property to suppress B cell function. As mentioned in **3 Results** (**3.5.5 Pyrvinium pamoate**), PP, a traditional anti-parasitic drug, has attracted attentions due to its effect as an anti-cancer drug via modulations of mitochondrial respiration, STAT3 signaling, Wnt signaling as well as microenvironmental support required for tumor-growth (170-172). In the current study, which aim is particularly focused on the drug effect on B cell immunity, an NGS analysis studying gene expression in human B cells with or without PP treatment was performed. Apart from a low concordance between NGS and confirmatory q-PCR results in seven genes investigated (*ATP6V1C2*, *C9orf139*, *FAM166A*, *SYNE2*, *COX20*, *GPS2*, and *SNX22*), a higher expression of *CD37* was observed in aCD40Ab/IL-21 stimulated B cells with PP treatment than those without (Fig 3.14 (a)).

CD37 is a member of tetraspanin proteins expressed on the surface of pre-B to mature B cells, or malignant B cells but not on pro-B cells or terminally differentiated plasma cells (131, 132, 173). The function of tetraspanins has been recognized that they can indirectly

modulate cell functions by interacting with their neighboring plasma membrane proteins including adhesion molecules, immunoreceptors, intracellular signaling molecules (174).

Concerning CD37 expression level on B cell lineage, de Winde *et al*. reported a spontaneous lymphoproliferative disorder in $CD37^{-/-}$ mice compared to wildtype (WT), where more than 50% of CD37 deficient mice developed B-cell phenotype lymphoma in lymph nodes, spleens, and livers (175). Similarly, even in human, CD37 has been identified as a useful prognostic marker in diffuse large B-cell lymphoma (DLBCL) patients (176). When DLBCL patients were grouped based on immunohistochemically proven CD37 positivity in the biopsy sample taken at the time of diagnosis, those who were positive for CD37 had better overall survival as well as progressive-free survival compared to CD37 negative populations (HR (95% CI): 2.80 (1.95-3.38), P <0.0001).

Regarding the relevance of CD37 deficiency to lymphoproliferative disorders, excess level of IL-6, a crucial B cell growth and differentiation factor (177, 178), has been detected as a key cytokine in previous studies. In the case of spontaneous development of B cell lymphoma in CD37 deficient mice, tumorigenesis was IL-6 dependent (175); an elevated serum IL-6 level, upregulation of IL-6 signaling associated genes (*Jun, Akt1 and Stat3*), and increased phosphorylation of these molecules (pAKT, pSTAT3) were observed in lymphoma tissues from CD37 deficient animals. Also, the survival of tumor cells was reduced when they were treated with IL-6 blocking antibody.

Among those investigating the contribution of CD37 deficiency in development of humoral immunity, one study demonstrated that, at 14 days after intraperitoneal immunization with NP-KLH, even though the GC formation itself was not affected, IL-6 positive cells were detected within germinal center in the spleen of CD37 deficient mice whereas it was negative

in immunized WT mice (179), indicating an excess supply of IL-6 in GC of CD37 deficient animals.

Not only the increased supply of IL-6 in GC upon antigen challenge, an altered B cell response to IL-6 stimulation in CD37 deficiency by losing its association with suppressor of cytokine signaling 3 (SOCS3) was also indicated in the aforementioned study (175). They demonstrated the co-localization of CD37 and IL-6 receptor on B cells and, when human B cells were stimulated with IL-6, SOCS3 localized in cytoplasm was translocated to the membrane and could directly interact with CD37 to form a complex. Considering the negative feedback of IL-6 signaling mediated by SOCS3 via its interaction with gp130, the co-receptor for IL-6 family cytokines (180, 181), and IL-6 stimulation resulted in a lower level of pSTAT3 in B cells from CD37 expressing mice than from CD37 deficient animals (175), maintaining CD37 surface expression could indirectly diminish IL-6 signaling via letting SOCS3 exert its inhibitory function properly.

In the current study, aCD40Ab/IL-21 stimulated B cells with PP treatment were suppressed in proliferation and showed a higher expression of CD37 compared to those without the drug treatment. This finding is partially in accordance with the previous studies suggesting that a loss of CD37 expression is associated with B cell lymphoproliferative disorders. Based on the facilitating role of IL-6 on proliferation/differentiation of activated B cells and Ag-specific antibody formation (177), one speculative B cell modulatory mechanism of PP would include that this drug maintains CD37 expression on B cells to prevent IL-6-mediated B cell development.

5. Outlook

Using preexisting drugs, this study tested a potential of these compounds as B cell immunomodulatory agents. Among those tested, PP was able to prevent disease development as well as progression in animal model of EBA via suppressing production of pathogenic autoantibodies.

In vitro assessment showed that PP inhibited B cell proliferation and plasmablast formation. However, in-depth study regarding how this drug acts on B cell development has not been conducted yet. As discussed in the previous chapter (**4. Discussion**), possible future approach includes assays studying drug effect on apoptosis, interference with expression of genes involved in plasma cell development. It would be also intriguing to compare how differently PP acts on naïve cells and memory B cells.

The NGS analysis identified CD37 as a potential key molecule which expression would be affected by PP treatment. Previous studies have suggested a role of CD37 in B cell proliferation and its ability to modify intracellular IL-6 signaling. In order to confirm whether the inhibition of B cell development brought by PP treatment is associated with CD37, a parallel monitoring of CD37 expression on B cells and B cell proliferation/plasma cell development would be required. Also, in relation to the function of CD37 to modify IL-6 signaling, it would be interesting to investigate how B cells with or without PP treatment would response to IL-6 stimulation.

Even though many questions remain unanswered, this work reassured the benefit of drug repurposing in drug development and has provided a possibility of a novel utility of PP as a treatment option in ADs.

6. References

1. Paul SM, Mytelka DS, Dunwiddie CT, Persinger CC, Munos BH, Lindborg SR, et al. How to improve R&D productivity: the pharmaceutical industry's grand challenge. Nat Rev Drug Discov. 2010;9(3):203-14.

2. Feldman SR. The design of clinical trials in psoriasis: lessons for clinical practice. J Am Acad Dermatol. 2003;49(2 Suppl):S62-5.

3. Bhattacharyya S, Brown DE, Brewer JA, Vogt SK, Muglia LJ. Macrophage glucocorticoid receptors regulate Toll-like receptor 4-mediated inflammatory responses by selective inhibition of p38 MAP kinase. Blood. 2007;109(10):4313-9.

4. Prinz F, Schlange T, Asadullah K. Believe it or not: how much can we rely on published data on potential drug targets? Nat Rev Drug Discov. 2011;10(9):712.

5. Begley CG, Ellis LM. Drug development: Raise standards for preclinical cancer research. Nature. 2012;483(7391):531-3.

6. Wohlleben W, Mast Y, Stegmann E, Ziemert N. Antibiotic drug discovery. Microb Biotechnol. 2016;9(5):541-8.

7. Lee JA, Berg EL. Neoclassic drug discovery: the case for lead generation using phenotypic and functional approaches. J Biomol Screen. 2013;18(10):1143-55.

8. Swinney DC, Anthony J. How were new medicines discovered? Nat Rev Drug Discov. 2011;10(7):507-19.

9. Booth B. Cancer Drug Targets: The March of the Lemmings. Available from: http://www.forbes.com/sites/brucebooth/2012/06/07/cancer-drug-targets-the-march-of-the-lemmings/2/.

10. Hutchinson L, Kirk R. High drug attrition rates--where are we going wrong? Nat Rev Clin Oncol. 2011;8(4):189-90.

11. Shim JS, Liu JO. Recent advances in drug repositioning for the discovery of new anticancer drugs. Int J Biol Sci. 2014;10(7):654-63.

12. McCabe B, Liberante F, Mills KI. Repurposing medicinal compounds for blood cancer treatment. Ann Hematol. 2015;94(8):1267-76.

13. Dowling RJ, Goodwin PJ, Stambolic V. Understanding the benefit of metformin use in cancer treatment. BMC Med. 2011;9:33.

14. Soranna D, Scotti L, Zambon A, Bosetti C, Grassi G, Catapano A, et al. Cancer risk associated with use of metformin and sulfonylurea in type 2 diabetes: a meta-analysis. Oncologist. 2012;17(6):813-22.

15. Thakkar B, Aronis KN, Vamvini MT, Shields K, Mantzoros CS. Metformin and sulfonylureas in relation to cancer risk in type II diabetes patients: a meta-analysis using primary data of published studies. Metabolism. 2013;62(7):922-34.

16. Wu L, Zhu J, Prokop LJ, Murad MH. Pharmacologic Therapy of Diabetes and Overall Cancer Risk and Mortality: A Meta-Analysis of 265 Studies. Sci Rep. 2015;5:10147.

17. Decensi A, Puntoni M, Goodwin P, Cazzaniga M, Gennari A, Bonanni B, et al. Metformin and cancer risk in diabetic patients: a systematic review and meta-analysis. Cancer Prev Res (Phila). 2010;3(11):1451-61.

18. Gonzalez-Angulo AM, Meric-Bernstam F. Metformin: a therapeutic opportunity in breast cancer. Clin Cancer Res. 2010;16(6):1695-700.

19. Heckman-Stoddard BM, Gandini S, Puntoni M, Dunn BK, DeCensi A, Szabo E. Repurposing old drugs to chemoprevention: the case of metformin. Semin Oncol. 2016;43(1):123-33.

20. Queiroz EA, Puukila S, Eichler R, Sampaio SC, Forsyth HL, Lees SJ, et al. Metformin induces apoptosis and cell cycle arrest mediated by oxidative stress, AMPK and FOXO3a in MCF-7 breast cancer cells. PLoS One. 2014;9(5):e98207.

21. Bao B, Wang Z, Ali S, Ahmad A, Azmi AS, Sarkar SH, et al. Metformin inhibits cell proliferation, migration and invasion by attenuating CSC function mediated by deregulating miRNAs in pancreatic cancer cells. Cancer Prev Res (Phila). 2012;5(3):355-64.

22. Samarajeewa NU, Ham S, Yang F, Simpson ER, Brown KA. Promoter-specific effects of metformin on aromatase transcript expression. Steroids. 2011;76(8):768-71.

23. Prlic M, Bevan MJ. Immunology: A metabolic switch to memory. Nature. 2009;460(7251):41-2.

24. Joshua AM, Zannella VE, Downes MR, Bowes B, Hersey K, Koritzinsky M, et al. A pilot 'window of opportunity' neoadjuvant study of metformin in localised prostate cancer. Prostate Cancer Prostatic Dis. 2014;17(3):252-8.

25. Mitsuhashi A, Kiyokawa T, Sato Y, Shozu M. Effects of metformin on endometrial cancer cell growth in vivo: a preoperative prospective trial. Cancer. 2014;120(19):2986-95.

26. Riedel S. Edward Jenner and the history of smallpox and vaccination. Proc (Bayl Univ Med Cent). 2005;18(1):21-5.

27. Murphy K, Travers P, Walport M, Janeway C. Janeway's immunobiology. 8th ed. New York: Garland Science; 2012. xix, 868 p. p.

28. Jacobson DL, Gange SJ, Rose NR, Graham NM. Epidemiology and estimated population burden of selected autoimmune diseases in the United States. Clin Immunol Immunopathol. 1997;84(3):223-43.

29. Nemazee D. Receptor editing in lymphocyte development and central tolerance. Nat Rev Immunol. 2006;6(10):728-40.

30. Steinman RM, Nussenzweig MC. Avoiding horror autotoxicus: the importance of dendritic cells in peripheral T cell tolerance. Proc Natl Acad Sci U S A. 2002;99(1):351-8.

31. Arnold B. Levels of peripheral T cell tolerance. Transpl Immunol. 2002;10(2-3):109-14.

32. Goodnow CC, Crosbie J, Jorgensen H, Brink RA, Basten A. Induction of self-tolerance in mature peripheral B lymphocytes. Nature. 1989;342(6248):385-91.

33. Russell DM, Dembic Z, Morahan G, Miller JF, Burki K, Nemazee D. Peripheral deletion of self-reactive B cells. Nature. 1991;354(6351):308-11.

34. Cyster JG, Goodnow CC. Antigen-induced exclusion from follicles and anergy are separate and complementary processes that influence peripheral B cell fate. Immunity. 1995;3(6):691-701.

35. Hawiger D, Inaba K, Dorsett Y, Guo M, Mahnke K, Rivera M, et al. Dendritic cells induce peripheral T cell unresponsiveness under steady state conditions in vivo. J Exp Med. 2001;194(6):769-79.

36. Khattri R, Cox T, Yasayko SA, Ramsdell F. An essential role for Scurfin in CD4+CD25+ T regulatory cells. Nat Immunol. 2003;4(4):337-42.

37. Margery-Muir AA, Bundell C, Nelson D, Groth DM, Wetherall JD. Gender balance in patients with systemic lupus erythematosus. Autoimmun Rev. 2017;16(3):258-68.

38. McCarty DJ, Manzi S, Medsger TA, Jr., Ramsey-Goldman R, LaPorte RE, Kwoh CK. Incidence of systemic lupus erythematosus. Race and gender differences. Arthritis Rheum. 1995;38(9):1260-70.

39. McInnes IB, Schett G. The pathogenesis of rheumatoid arthritis. N Engl J Med. 2011;365(23):2205-19.

40. Silman AJ, Newman J, MacGregor AJ. Cigarette smoking increases the risk of rheumatoid arthritis. Results from a nationwide study of disease-discordant twins. Arthritis Rheum. 1996;39(5):732-5.

41. de Pablo P, Chapple IL, Buckley CD, Dietrich T. Periodontitis in systemic rheumatic diseases. Nat Rev Rheumatol. 2009;5(4):218-24.

42. Wegner N, Wait R, Sroka A, Eick S, Nguyen KA, Lundberg K, et al. Peptidylarginine deiminase from Porphyromonas gingivalis citrullinates human fibrinogen and alpha-enolase: implications for autoimmunity in rheumatoid arthritis. Arthritis Rheum. 2010;62(9):2662-72.

43. Hochberg MC. Rheumatology. 5th ed. Philadelphia, PA: Mosby/Elsevier; 2011.

44. Schmidt E, Zillikens D. Pemphigoid diseases. Lancet. 2013;381(9863):320-32.

45. Iwata H, Bieber K, Tiburzy B, Chrobok N, Kalies K, Shimizu A, et al. B cells, dendritic cells, and macrophages are required to induce an autoreactive CD4 helper T cell response in experimental epidermolysis bullosa acquisita. J Immunol. 2013;191(6):2978-88.

46. Ludwig RJ, Muller S, Marques A, Recke A, Schmidt E, Zillikens D, et al. Identification of quantitative trait loci in experimental epidermolysis bullosa acquisita. J Invest Dermatol. 2012;132(5):1409-15.

47. Lapiere JC, Woodley DT, Parente MG, Iwasaki T, Wynn KC, Christiano AM, et al. Epitope mapping of type VII collagen. Identification of discrete peptide sequences recognized by sera from patients with acquired epidermolysis bullosa. J Clin Invest. 1993;92(4):1831-9.

48. Sitaru C, Mihai S, Otto C, Chiriac MT, Hausser I, Dotterweich B, et al. Induction of dermal-epidermal separation in mice by passive transfer of antibodies specific to type VII collagen. J Clin Invest. 2005;115(4):870-8.

49. Woodley DT, Chang C, Saadat P, Ram R, Liu Z, Chen M. Evidence that anti-type VII collagen antibodies are pathogenic and responsible for the clinical, histological, and immunological features of epidermolysis bullosa acquisita. J Invest Dermatol. 2005;124(5):958-64.

50. Woodley DT, Ram R, Doostan A, Bandyopadhyay P, Huang Y, Remington J, et al. Induction of epidermolysis bullosa acquisita in mice by passive transfer of autoantibodies from patients. J Invest Dermatol. 2006;126(6):1323-30.

51. Abrams ML, Smidt A, Benjamin L, Chen M, Woodley D, Mancini AJ. Congenital epidermolysis bullosa acquisita: vertical transfer of maternal autoantibody from mother to infant. Arch Dermatol. 2011;147(3):337-41.

52. Kim JH, Kim YH, Kim SC. Epidermolysis bullosa acquisita: a retrospective clinical analysis of 30 cases. Acta Derm Venereol. 2011;91(3):307-12.

53. St Clair EW. Novel targeted therapies for autoimmunity. Curr Opin Immunol. 2009;21(6):648-57.

54. Wiseman AC. Immunosuppressive Medications. Clin J Am Soc Nephrol. 2016;11(2):332-43.

55. Clark AR, Belvisi MG. Maps and legends: the quest for dissociated ligands of the glucocorticoid receptor. Pharmacol Ther. 2012;134(1):54-67.

56. Rhen T, Cidlowski JA. Antiinflammatory action of glucocorticoids--new mechanisms for old drugs. N Engl J Med. 2005;353(16):1711-23.

57. Schwiebert LM, Beck LA, Stellato C, Bickel CA, Bochner BS, Schleimer RP. Glucocorticosteroid inhibition of cytokine production: relevance to antiallergic actions. J Allergy Clin Immunol. 1996;97(1 Pt 2):143-52.

58. Pitzalis C, Pipitone N, Bajocchi G, Hall M, Goulding N, Lee A, et al. Corticosteroids inhibit lymphocyte binding to endothelium and intercellular adhesion: an additional mechanism for their anti-inflammatory and immunosuppressive effect. J Immunol. 1997;158(10):5007-16.

59. Herold MJ, McPherson KG, Reichardt HM. Glucocorticoids in T cell apoptosis and function. Cell Mol Life Sci. 2006;63(1):60-72.

60. Liddicoat DR, Kyparissoudis K, Berzins SP, Cole TJ, Godfrey DI. The glucocorticoid receptor 1A3 promoter correlates with high sensitivity to glucocorticoid-induced apoptosis in human lymphocytes. Immunol Cell Biol. 2014;92(10):825-36.

61. Frankfurt O, Rosen ST. Mechanisms of glucocorticoid-induced apoptosis in hematologic malignancies: updates. Curr Opin Oncol. 2004;16(6):553-63.

62. Ploner C, Schmidt S, Presul E, Renner K, Schrocksnadel K, Rainer J, et al. Glucocorticoid-induced apoptosis and glucocorticoid resistance in acute lymphoblastic leukemia. J Steroid Biochem Mol Biol. 2005;93(2-5):153-60.

63. Breslin MB, Geng CD, Vedeckis WV. Multiple promoters exist in the human GR gene, one of which is activated by glucocorticoids. Mol Endocrinol. 2001;15(8):1381-95.

64. Pedersen KB, Vedeckis WV. Quantification and glucocorticoid regulation of glucocorticoid receptor transcripts in two human leukemic cell lines. Biochemistry. 2003;42(37):10978-90.

65. Pedersen KB, Geng CD, Vedeckis WV. Three mechanisms are involved in glucocorticoid receptor autoregulation in a human T-lymphoblast cell line. Biochemistry. 2004;43(34):10851-8.

66. Yudt MR, Cidlowski JA. Molecular identification and characterization of a and b forms of the glucocorticoid receptor. Mol Endocrinol. 2001;15(7):1093-103.

67. Gametchu B. Glucocorticoid receptor-like antigen in lymphoma cell membranes: correlation to cell lysis. Science. 1987;236(4800):456-61.

68. Chen F, Watson CS, Gametchu B. Multiple glucocorticoid receptor transcripts in membrane glucocorticoid receptor-enriched S-49 mouse lymphoma cells. J Cell Biochem. 1999;74(3):418-29.

69. Gametchu B, Watson CS. Correlation of membrane glucocorticoid receptor levels with glucocorticoid-induced apoptotic competence using mutant leukemic and lymphoma cells lines. J Cell Biochem. 2002;87(2):133-46.

70. Kumar A, Takada Y, Boriek AM, Aggarwal BB. Nuclear factor-kappaB: its role in health and disease. J Mol Med (Berl). 2004;82(7):434-48.

71. Zenz R, Eferl R, Scheinecker C, Redlich K, Smolen J, Schonthaler HB, et al. Activator protein 1 (Fos/Jun) functions in inflammatory bone and skin disease. Arthritis Res Ther. 2008;10(1):201.

72. Busillo JM, Cidlowski JA. The five Rs of glucocorticoid action during inflammation: ready, reinforce, repress, resolve, and restore. Trends Endocrinol Metab. 2013;24(3):109-19.

73. Ayroldi E, Cannarile L, Migliorati G, Nocentini G, Delfino DV, Riccardi C. Mechanisms of the anti-inflammatory effects of glucocorticoids: genomic and nongenomic interference with MAPK signaling pathways. Faseb J. 2012;26(12):4805-20.

74. Cruz-Topete D, Cidlowski JA. One hormone, two actions: anti- and pro-inflammatory effects of glucocorticoids. Neuroimmunomodulation. 2015;22(1-2):20-32.

75. Falagas ME, Manta KG, Betsi GI, Pappas G. Infection-related morbidity and mortality in patients with connective tissue diseases: a systematic review. Clin Rheumatol. 2007;26(5):663-70.

76. Saag KG, Koehnke R, Caldwell JR, Brasington R, Burmeister LF, Zimmerman B, et al. Low dose long-term corticosteroid therapy in rheumatoid arthritis: an analysis of serious adverse events. Am J Med. 1994;96(2):115-23.

77. Duru N, van der Goes MC, Jacobs JW, Andrews T, Boers M, Buttgereit F, et al. EULAR evidence-based and consensus-based recommendations on the management of medium to high-dose glucocorticoid therapy in rheumatic diseases. Ann Rheum Dis. 2013;72(12):1905-13.

78. Miloslavsky EM, Naden RP, Bijlsma JW, Brogan PA, Brown ES, Brunetta P, et al. Development of a Glucocorticoid Toxicity Index (GTI) using multicriteria decision analysis. Ann Rheum Dis. 2017;76(3):543-6.

79. van Staa TP, Leufkens HG, Cooper C. The epidemiology of corticosteroid-induced osteoporosis: a meta-analysis. Osteoporos Int. 2002;13(10):777-87.

80. Miner JN, Hong MH, Negro-Vilar A. New and improved glucocorticoid receptor ligands. Expert Opin Investig Drugs. 2005;14(12):1527-45.

81. Trence DL. Management of patients on chronic glucocorticoid therapy: an endocrine perspective. Prim Care. 2003;30(3):593-605.

82. Agca R, Heslinga SC, Rollefstad S, Heslinga M, McInnes IB, Peters MJ, et al. EULAR recommendations for cardiovascular disease risk management in patients with rheumatoid arthritis and other forms of inflammatory joint disorders: 2015/2016 update. Ann Rheum Dis. 2017;76(1):17-28.

83. Porter D, van Melckebeke J, Dale J, Messow CM, McConnachie A, Walker A, et al. Tumour necrosis factor inhibition versus rituximab for patients with rheumatoid arthritis who require biological treatment (ORBIT): an open-label, randomised controlled, non-inferiority, trial. Lancet. 2016;388(10041):239-47.

84. Moore PA, Belvedere O, Orr A, Pieri K, LaFleur DW, Feng P, et al. BLyS: member of the tumor necrosis factor family and B lymphocyte stimulator. Science. 1999;285(5425):260-3.

85. Petri M, Stohl W, Chatham W, McCune WJ, Chevrier M, Ryel J, et al. Association of plasma B lymphocyte stimulator levels and disease activity in systemic lupus erythematosus. Arthritis Rheum. 2008;58(8):2453-9.

86. Mackay F, Woodcock SA, Lawton P, Ambrose C, Baetscher M, Schneider P, et al. Mice transgenic for BAFF develop lymphocytic disorders along with autoimmune manifestations. J Exp Med. 1999;190(11):1697-710.

87. Gross JA, Johnston J, Mudri S, Enselman R, Dillon SR, Madden K, et al. TACI and BCMA are receptors for a TNF homologue implicated in B-cell autoimmune disease. Nature. 2000;404(6781):995-9.

88. Wallace DJ, Stohl W, Furie RA, Lisse JR, McKay JD, Merrill JT, et al. A phase II, randomized, double-blind, placebo-controlled, dose-ranging study of belimumab in patients with active systemic lupus erythematosus. Arthritis Rheum. 2009;61(9):1168-78.

89. Navarra SV, Guzman RM, Gallacher AE, Hall S, Levy RA, Jimenez RE, et al. Efficacy and safety of belimumab in patients with active systemic lupus erythematosus: a randomised, placebo-controlled, phase 3 trial. Lancet. 2011;377(9767):721-31.

90. Hauser SL, Waubant E, Arnold DL, Vollmer T, Antel J, Fox RJ, et al. B-cell depletion with rituximab in relapsing-remitting multiple sclerosis. N Engl J Med. 2008;358(7):676-88.

91. Bar-Or A, Calabresi PA, Arnold D, Markowitz C, Shafer S, Kasper LH, et al. Rituximab in relapsing-remitting multiple sclerosis: a 72-week, open-label, phase I trial. Ann Neurol. 2008;63(3):395-400.

92. Nelson RP, Jr., Pascuzzi RM, Kessler K, Walsh LE, Faught PP, Ramanuja S, et al. Rituximab for the treatment of thymoma-associated and de novo myasthenia gravis: 3 cases and review. J Clin Neuromuscul Dis. 2009;10(4):170-7.

93. Sieb JP. Myasthenia gravis: an update for the clinician. Clin Exp Immunol. 2014;175(3):408-18.

94. Hassan RI, Gaffo AL. Rituximab in ANCA-Associated Vasculitis. Curr Rheumatol Rep. 2017;19(2):6.

95. Huscher D, Mittendorf T, von Hinuber U, Kotter I, Hoese G, Pfafflin A, et al. Evolution of cost structures in rheumatoid arthritis over the past decade. Ann Rheum Dis. 2015;74(4):738-45.

96. Desai RJ, Rao JK, Hansen RA, Fang G, Maciejewski ML, Farley JF. Predictors of treatment initiation with tumor necrosis factor-alpha inhibitors in patients with rheumatoid arthritis. J Manag Care Spec Pharm. 2014;20(11):1110-20.

97. Evens AM, Jovanovic BD, Su YC, Raisch DW, Ganger D, Belknap SM, et al. Rituximab-associated hepatitis B virus (HBV) reactivation in lymphoproliferative diseases: meta-analysis and examination of FDA safety reports. Ann Oncol. 2011;22(5):1170-80.

98. Chang JJ, Lewin SR. Immunopathogenesis of hepatitis B virus infection. Immunol Cell Biol. 2007;85(1):16-23.

99. Xu X, Shang Q, Chen X, Nie W, Zou Z, Huang A, et al. Reversal of B-cell hyperactivation and functional impairment is associated with HBsAg seroconversion in chronic hepatitis B patients. Cell Mol Immunol. 2015;12(3):309-16.

100. Tavakolpour S, Alavian SM, Sali S. Hepatitis B Reactivation During Immunosuppressive Therapy or Cancer Chemotherapy, Management, and Prevention: A Comprehensive Review-Screened. Hepat Mon. 2016;16(4):e35810.

101. Recke A, Trog LM, Pas HH, Vorobyev A, Abadpour A, Jonkman MF, et al. Recombinant human IgA1 and IgA2 autoantibodies to type VII collagen induce subepidermal blistering ex vivo. Journal of immunology (Baltimore, Md : 1950). 2014;193(4):1600-8.

102. Ettinger R, Sims GP, Fairhurst AM, Robbins R, da Silva YS, Spolski R, et al. IL-21 induces differentiation of human naive and memory B cells into antibody-secreting plasma cells. J Immunol. 2005;175(12):7867-79.

103. Berglund LJ, Avery DT, Ma CS, Moens L, Deenick EK, Bustamante J, et al. IL-21 signalling via STAT3 primes human naive B cells to respond to IL-2 to enhance their differentiation into plasmablasts. Blood. 2013;122(24):3940-50.

104. Bryant VL, Ma CS, Avery DT, Li Y, Good KL, Corcoran LM, et al. Cytokine-mediated regulation of human B cell differentiation into Ig-secreting cells: predominant role of IL-21 produced by CXCR5+ T follicular helper cells. Journal of immunology (Baltimore, Md : 1950). 2007;179(12):8180-90.

105. Tiburzy B, Szyska M, Iwata H, Chrobok N, Kulkarni U, Hirose M, et al. Persistent autoantibody-production by intermediates between short-and long-lived plasma cells in inflamed lymph nodes of experimental epidermolysis bullosa acquisita. PloS one. 2013;8(12):e83631.

106. Bieber K, Koga H, Nishie W. In vitro and in vivo models to investigate the pathomechanisms and novel treatments for pemphigoid diseases. Exp Dermatol. 2017;26(12):1163-70.

107. Leineweber S, Schonig S, Seeger K. Insight into interactions of the von-Willebrand-factor-A-like domain 2 with the FNIII-like domain 9 of collagen VII by NMR and SPR. FEBS letters. 2011;585(12):1748-52.

108. Spano D, Marshall JC, Marino N, De Martino D, Romano A, Scoppettuolo MN, et al. Dipyridamole prevents triple-negative breast-cancer progression. Clinical & experimental metastasis. 2013;30(1):47-68.

109. Nomura T, Yamasaki M, Hirai K, Inoue T, Sato R, Matsuura K, et al. Targeting the Vav3 oncogene enhances docetaxel-induced apoptosis through the inhibition of androgen receptor

phosphorylation in LNCaP prostate cancer cells under chronic hypoxia. Molecular cancer. 2013;12:27.

110. Shirahama T, Cohen AS. Blockage of amyloid induction by colchicine in an animal model. The Journal of experimental medicine. 1974;140(4):1102-7.

111. Jones JO, Bolton EC, Huang Y, Feau C, Guy RK, Yamamoto KR, et al. Non-competitive androgen receptor inhibition in vitro and in vivo. Proceedings of the National Academy of Sciences of the United States of America. 2009;106(17):7233-8.

112. Andrews S. FastQC, quality control tool for high throughput sequence data. . 2010 [cited 2017 August 15]; Available from: http://www.bioinformatics.babraham.ac.uk/projects/fastqc/.

113. Bolger AM, Lohse M, Usadel B. Trimmomatic: a flexible trimmer for Illumina sequence data. Bioinformatics (Oxford, England). 2014;30(15):2114-20.

114. Dobin A, Davis CA, Schlesinger F, Drenkow J, Zaleski C, Jha S, et al. STAR: ultrafast universal RNA-seq aligner. Bioinformatics (Oxford, England). 2013;29(1):15-21.

115. Anders S, Pyl PT, Huber W. HTSeq--a Python framework to work with high-throughput sequencing data. Bioinformatics (Oxford, England). 2015;31(2):166-9.

116. Love MI, Huber W, Anders S. Moderated estimation of fold change and dispersion for RNA-seq data with DESeq2. Genome biology. 2014;15(12):550.

117. Silver N, Best S, Jiang J, Thein SL. Selection of housekeeping genes for gene expression studies in human reticulocytes using real-time PCR. BMC molecular biology. 2006;7:33.

118. Dadgostar H, Zarnegar B, Hoffmann A, Qin XF, Truong U, Rao G, et al. Cooperation of multiple signaling pathways in CD40-regulated gene expression in B lymphocytes. Proc Natl Acad Sci U S A. 2002;99(3):1497-502.

119. Chen S, Sims GP, Chen XX, Gu YY, Chen S, Lipsky PE. Modulatory effects of 1,25-dihydroxyvitamin D3 on human B cell differentiation. J Immunol. 2007;179(3):1634-47.

120. Maecker HT, McCoy JP, Nussenblatt R. Standardizing immunophenotyping for the Human Immunology Project. Nat Rev Immunol. 2012;12(3):191-200.

121. Chiriac MT, Roesler J, Sindrilaru A, Scharffetter-Kochanek K, Zillikens D, Sitaru C. NADPH oxidase is required for neutrophil-dependent autoantibody-induced tissue damage. J Pathol. 2007;212(1):56-65.

122. Recke A, Sitaru C, Vidarsson G, Evensen M, Chiriac MT, Ludwig RJ, et al. Pathogenicity of IgG subclass autoantibodies to type VII collagen: induction of dermal-epidermal separation. J Autoimmun. 2010;34(4):435-44.

123. Gresele P, Momi S, Falcinelli E. Anti-platelet therapy: phosphodiesterase inhibitors. Br J Clin Pharmacol. 2011;72(4):634-46.

124. Herbst RS, Khuri FR. Mode of action of docetaxel - a basis for combination with novel anticancer agents. (0305-7372 (Print)).

125. Cronstein BN, Molad Y, Reibman J, Balakhane E, Levin RI, Weissmann G. Colchicine alters the quantitative and qualitative display of selectins on endothelial cells and neutrophils. J Clin Invest. 1995;96(2):994-1002.

126. Beck JW, Saavedra D, Antell GJ, Tejeiro B. The treatment of pinworm infections in humans (enterobiasis) with pyrvinium chloride and pyrvinium pamoate. Am J Trop Med Hyg. 1959;8(3):349-52.

127. Xu W, Lacerda L, Debeb BG, Atkinson RL, Solley TN, Li L, et al. The antihelmintic drug pyrvinium pamoate targets aggressive breast cancer. PLoS One. 2013;8(8):e71508.

128. Wang Z, Gerstein M, Snyder M. RNA-Seq: a revolutionary tool for transcriptomics. Nat Rev Genet. 2009;10(1):57-63.

129. Huber-Keener KJ, Liu X, Wang Z, Wang Y, Freeman W, Wu S, et al. Differential gene expression in tamoxifen-resistant breast cancer cells revealed by a new analytical model of RNA-Seq data. PLoS One. 2012;7(7):e41333.

130. GeneCards. The Human Gene Database. [cited 2017 April 29]; Available from: http://www.genecards.org/.

131. Schwartz-Albiez R, Dorken B, Hofmann W, Moldenhauer G. The B cell-associated CD37 antigen (gp40-52). Structure and subcellular expression of an extensively glycosylated glycoprotein. J Immunol. 1988;140(3):905-14.

132. Maecker HT, Todd SC, Levy S. The tetraspanin superfamily: molecular facilitators. Faseb J. 1997;11(6):428-42.

133. Vermes I, Haanen C, Steffens-Nakken H, Reutelingsperger C. A novel assay for apoptosis. Flow cytometric detection of phosphatidylserine expression on early apoptotic cells using fluorescein labelled Annexin V. J Immunol Methods. 1995;184(1):39-51.

134. Eibel H, Kraus H, Sic H, Kienzler AK, Rizzi M. B cell biology: an overview. Curr Allergy Asthma Rep. 2014;14(5):434.

135. Tedder TF, Clement LT, Cooper MD. Discontinuous expression of a membrane antigen (HB-7) during B lymphocyte differentiation. Tissue Antigens. 1984;24(3):140-9.

136. Malavasi F, Deaglio S, Damle R, Cutrona G, Ferrarini M, Chiorazzi N. CD38 and chronic lymphocytic leukemia: a decade later. Blood. 2011;118(13):3470-8.

137. Zupo S, Rugari E, Dono M, Taborelli G, Malavasi F, Ferrarini M. CD38 signaling by agonistic monoclonal antibody prevents apoptosis of human germinal center B cells. Eur J Immunol. 1994;24(5):1218-22.

138. Deaglio S, Vaisitti T, Aydin S, Ferrero E, Malavasi F. In-tandem insight from basic science combined with clinical research: CD38 as both marker and key component of the pathogenetic network underlying chronic lymphocytic leukemia. Blood. 2006;108(4):1135-44.

139. Lund FE, Yu N, Kim KM, Reth M, Howard MC. Signaling through CD38 augments B cell antigen receptor (BCR) responses and is dependent on BCR expression. J Immunol. 1996;157(4):1455-67.

140. Deaglio S, Vaisitti T, Billington R, Bergui L, Omede P, Genazzani AA, et al. CD38/CD19: a lipid raft-dependent signaling complex in human B cells. Blood. 2007;109(12):5390-8.

141. Kashiwada M, Kaneko Y, Yagita H, Okumura K, Takemori T. Activation of mitogen-activated protein kinases via CD40 is distinct from that stimulated by surface IgM on B cells. Eur J Immunol. 1996;26(7):1451-8.

142. Li YY, Baccam M, Waters SB, Pessin JE, Bishop GA, Koretzky GA. CD40 ligation results in protein kinase C-independent activation of ERK and JNK in resting murine splenic B cells. J Immunol. 1996;157(4):1440-7.

143. Klaus GG, Choi MS, Holman M. Properties of mouse CD40. Ligation of CD40 activates B cells via a Ca(++)-dependent, FK506-sensitive pathway. Eur J Immunol. 1994;24(12):3229-32.

144. Neron S, Racine C, Roy A, Guerin M. Differential responses of human B-lymphocyte subpopulations to graded levels of CD40-CD154 interaction. Immunology. 2005;116(4):454-63.

145. Fecteau JF, Neron S. CD40 stimulation of human peripheral B lymphocytes: distinct response from naive and memory cells. J Immunol. 2003;171(9):4621-9.

146. Good KL, Bryant VL, Tangye SG. Kinetics of human B cell behavior and amplification of proliferative responses following stimulation with IL-21. J Immunol. 2006;177(8):5236-47.

147. Deenick EK, Avery DT, Chan A, Berglund LJ, Ives ML, Moens L, et al. Naive and memory human B cells have distinct requirements for STAT3 activation to differentiate into antibody-secreting plasma cells. J Exp Med. 2013;210(12):2739-53.

148. El-Seedi HR, Burman R, Mansour A, Turki Z, Boulos L, Gullbo J, et al. The traditional medical uses and cytotoxic activities of sixty-one Egyptian plants: discovery of an active cardiac glycoside from Urginea maritima. J Ethnopharmacol. 2013;145(3):746-57.

149. Winnicka K, Bielawski K, Bielawska A, Surazynski A. Antiproliferative activity of derivatives of ouabain, digoxin and proscillaridin A in human MCF-7 and MDA-MB-231 breast cancer cells. Biol Pharm Bull. 2008;31(6):1131-40.

150. Denicolai E, Baeza-Kallee N, Tchoghandjian A, Carre M, Colin C, Jiglaire CJ, et al. Proscillaridin A is cytotoxic for glioblastoma cell lines and controls tumor xenograft growth in vivo. Oncotarget. 2014;5(21):10934-48.

151. Ueno H, Kiyosawa K, Kaniwa N. Pharmacogenomics of gemcitabine: can genetic studies lead to tailor-made therapy? Br J Cancer. 2007;97(2):145-51.

152. Toschi L, Finocchiaro G, Bartolini S, Gioia V, Cappuzzo F. Role of gemcitabine in cancer therapy. Future Oncol. 2005;1(1):7-17.

153. Fossa A, Santoro A, Hiddemann W, Truemper L, Niederle N, Buksmaui S, et al. Gemcitabine as a single agent in the treatment of relapsed or refractory aggressive non-Hodgkin's lymphoma. J Clin Oncol. 1999;17(12):3786-92.

154. Zinzani PL, Baliva G, Magagnoli M, Bendandi M, Modugno G, Gherlinzoni F, et al. Gemcitabine treatment in pretreated cutaneous T-cell lymphoma: experience in 44 patients. J Clin Oncol. 2000;18(13):2603-6.

155. Sallah S, Wan JY, Nguyen NP. Treatment of refractory T-cell malignancies using gemcitabine. Br J Haematol. 2001;113(1):185-7.

156. Zinzani PL, Venturini F, Stefoni V, Fina M, Pellegrini C, Derenzini E, et al. Gemcitabine as single agent in pretreated T-cell lymphoma patients: evaluation of the long-term outcome. Ann Oncol. 2010;21(4):860-3.

157. Hooijmans CR, Ritskes-Hoitinga M. Progress in using systematic reviews of animal studies to improve translational research. PLoS Med. 2013;10(7):e1001482.

158. Hendriksen CF. Replacement, reduction and refinement alternatives to animal use in vaccine potency measurement. Expert Rev Vaccines. 2009;8(3):313-22.

159. Niedermeier A, Eming R, Pfutze M, Neumann CR, Happel C, Reich K, et al. Clinical response of severe mechanobullous epidermolysis bullosa acquisita to combined treatment with immunoadsorption and rituximab (anti-CD20 monoclonal antibodies). Arch Dermatol. 2007;143(2):192-8.

160. Schmidt E, Benoit S, Brocker EB, Zillikens D, Goebeler M. Successful adjuvant treatment of recalcitrant epidermolysis bullosa acquisita with anti-CD20 antibody rituximab. Arch Dermatol. 2006;142(2):147-50.

161. Crichlow SM, Mortimer NJ, Harman KE. A successful therapeutic trial of rituximab in the treatment of a patient with recalcitrant, high-titre epidermolysis bullosa acquisita. Br J Dermatol. 2007;156(1):194-6.

162. Saha M, Cutler T, Bhogal B, Black MM, Groves RW. Refractory epidermolysis bullosa acquisita: successful treatment with rituximab. Clin Exp Dermatol. 2009;34(8):e979-80.

163. Nimmerjahn F, Ravetch JV. Divergent immunoglobulin g subclass activity through selective Fc receptor binding. Science. 2005;310(5753):1510-2.

164. Karsten CM, Kohl J. A bone to pick with Fc gamma receptors. Ann Transl Med. 2015;3(15):218.

165. Kasperkiewicz M, Nimmerjahn F, Wende S, Hirose M, Iwata H, Jonkman MF, et al. Genetic identification and functional validation of FcgammaRIV as key molecule in autoantibody-induced tissue injury. J Pathol. 2012;228(1):8-19.

166. Nimmerjahn F, Bruhns P, Horiuchi K, Ravetch JV. FcgammaRIV: a novel FcR with distinct IgG subclass specificity. Immunity. 2005;23(1):41-51.

167. Koga H, Recke A, Vidarsson G, Pas HH, Jonkman MF, Hashimoto T, et al. PDE4 Inhibition as Potential Treatment of Epidermolysis Bullosa Acquisita. J Invest Dermatol. 2016;136(11):2211-20.

168. DeFranco AL. The germinal center antibody response in health and disease. F1000Res. 2016;5.

169. Gitlin AD, Shulman Z, Nussenzweig MC. Clonal selection in the germinal centre by regulated proliferation and hypermutation. Nature. 2014;509(7502):637-40.

170. Ishii I, Harada Y, Kasahara T. Reprofiling a classical anthelmintic, pyrvinium pamoate, as an anti-cancer drug targeting mitochondrial respiration. Front Oncol. 2012;2:137.

171. Thorne CA, Hanson AJ, Schneider J, Tahinci E, Orton D, Cselenyi CS, et al. Small-molecule inhibition of Wnt signaling through activation of casein kinase 1alpha. Nat Chem Biol. 2010;6(11):829-36.

172. Sugimoto K, Hayakawa F, Shimada S, Morishita T, Shimada K, Katakai T, et al. Discovery of a drug targeting microenvironmental support for lymphoma cells by screening using patient-derived xenograft cells. Sci Rep. 2015;5:13054.

173. Link MP, Bindl J, Meeker TC, Carswell C, Doss CA, Warnke RA, et al. A unique antigen on mature B cells defined by a monoclonal antibody. J Immunol. 1986;137(9):3013-8.

174. Beckwith KA, Byrd JC, Muthusamy N. Tetraspanins as therapeutic targets in hematological malignancy: a concise review. Front Physiol. 2015;6:91.

175. de Winde CM, Veenbergen S, Young KH, Xu-Monette ZY, Wang XX, Xia Y, et al. Tetraspanin CD37 protects against the development of B cell lymphoma. J Clin Invest. 2016;126(2):653-66.

176. Xu-Monette ZY, Li L, Byrd JC, Jabbar KJ, Manyam GC, Maria de Winde C, et al. Assessment of CD37 B-cell antigen and cell of origin significantly improves risk prediction in diffuse large B-cell lymphoma. Blood. 2016;128(26):3083-100.

177. Muraguchi A, Hirano T, Tang B, Matsuda T, Horii Y, Nakajima K, et al. The essential role of B cell stimulatory factor 2 (BSF-2/IL-6) for the terminal differentiation of B cells. J Exp Med. 1988;167(2):332-44.

178. Jego G, Bataille R, Pellat-Deceunynck C. Interleukin-6 is a growth factor for nonmalignant human plasmablasts. Blood. 2001;97(6):1817-22.

179. van Spriel AB, Sofi M, Gartlan KH, van der Schaaf A, Verschueren I, Torensma R, et al. The tetraspanin protein CD37 regulates IgA responses and anti-fungal immunity. PLoS Pathog. 2009;5(3):e1000338.

180. Croker BA, Krebs DL, Zhang JG, Wormald S, Willson TA, Stanley EG, et al. SOCS3 negatively regulates IL-6 signaling in vivo. Nat Immunol. 2003;4(6):540-5.

181. Babon JJ, Varghese LN, Nicola NA. Inhibition of IL-6 family cytokines by SOCS3. Semin Immunol. 2014;26(1):13-9.

7. Appendix

7.1 List of figures

7.2 List of tables

7.3 List of potential B-cell proliferation inhibitory/enhancing compounds

B-cell proliferation inhibitory compounds

	Drug	donor1	donor2	average
1	Disulfiram	0.38160	0.16472	0.27316
2	Dipyridamole	0.41976	0.37853	0.39915
3	Camptothecine (S,+)	0.09411	0.15279	0.12345
4	Betamethasone	0.12420	0.24167	0.18294
5	Colchicine	0.22200	0.21327	0.21764
6	Lidoflazine	0.31078	0.29115	0.30096
7	Dequalinium dichloride	0.10866	0.19019	0.14942
8	Amifostine	0.30296	0.35377	0.32837
9	Digitoxigenin	0.25493	0.10435	0.17964
10	Digoxin	0.25440	0.19497	0.22468
11	Hydrocortisone base	0.18010	0.18854	0.18432
12	Thiostrepton	0.23276	0.25496	0.24386
13	Ciclopirox ethanolamine	0.22308	0.26282	0.24295
14	Oxibendazol	0.40755	0.38360	0.39558
15	Lanatoside C	0.37390	0.32631	0.35010
16	Avermectin B1a	0.32961	0.17436	0.25199
17	Thimerosal	0.33848	0.24917	0.29382
18	Methyl benzethonium chloride	0.49077	0.19566	0.34322
19	Auranofin	0.19627	0.13093	0.16360
20	Clinafloxacin	0.35131	0.32284	0.33708
21	Digoxigenin	0.31715	0.12505	0.22110
22	Clioquinol	0.32771	0.17478	0.25125
23	Flubendazol	0.35943	0.27817	0.31880
24	Thonzonium bromide	0.16712	0.12625	0.14669

	Drug	donor1	donor2	average
25	Proscillaridin A	0.37872	0.23489	0.30680
26	Pyrvinium pamoate	0.19245	0.33780	0.26512
27	Methiazole	0.32500	0.32356	0.32428
28	Verteporfin	0.28883	0.30951	0.29917
29	Parbendazole	0.33559	0.35068	0.34313
30	Topotecan	0.11620	0.19251	0.15436
31	Nocodazole	0.38422	0.25281	0.31851
32	Methylprednisolone, 6-alpha	0.48917	0.33249	0.41083
33	Fludrocortisone acetate	0.39417	0.16936	0.28176
34	Mitoxantrone dihydrochloride	0.10053	0.26769	0.18411
35	Etoposide	0.08757	0.39200	0.23979
36	Doxorubicin hydrochloride	0.17163	0.16581	0.16872
37	Mometasone furoate	0.48703	0.23935	0.36319
38	Cytarabine	0.17184	0.17989	0.17586
39	Irinotecan hydrochloride trihydrate	0.33273	0.26757	0.30015
40	Rimexolone	0.46352	0.43741	0.45047
41	Prednicarbate	0.37669	0.27659	0.32664
42	Vorinostat	0.18531	0.26784	0.22657
43	Clocortolone pivalate	0.47013	0.48479	0.47746
44	Fludarabine	0.42842	0.48840	0.45841
45	Cladribine	0.21134	0.44088	0.32611
46	Fluocinolone acetonide	0.37955	0.19303	0.28629
47	Gemcitabine	0.13412	0.22308	0.17860
48	Docetaxel	0.36550	0.31328	0.33939

B-cell proliferation enhancing compounds

	Drug	donor1	donor2	average		Drug	donor1	donor2	average
1	Niclosamide	2.44720	1.78641	2.11681	22	Brompheniramine maleate	1.79472	1.72337	1.75904
2	Lidocaine hydrochloride	1.77765	1.68880	1.73322	23	Primaquine diphosphate	1.66027	2.07080	1.86554
3	Sulpiride	1.49936	2.73238	2.11587	24	Progesterone	1.61038	2.12296	1.86667
4	Tolazoline hydrochloride	1.69398	2.57766	2.13582	25	Closantel	1.78365	1.92131	1.85248
5	Trimethobenzamide hydrochloride	1.98386	1.49391	1.73889	26	Sulfamerazine	2.11114	1.53448	1.82281
6	Methyldopa (L,-)	2.04249	1.50449	1.77349	27	Venlafaxine	2.07359	1.54015	1.80687
7	Zoxazolamine	1.86893	1.55693	1.71293	28	Ethotoin	1.81996	1.61699	1.71848
8	Bisoprolol fumarate	1.76655	1.66079	1.71367	29	Tetrahydrozoline hydrochloride	2.00496	1.57263	1.78880
9	Clorgyline hydrochloride	1.88662	1.67952	1.78307	30	Famprofazone	2.08776	1.54082	1.81429
10	Maprotiline hydrochloride	1.86107	1.73364	1.79735	31	Folinic acid calcium salt	1.57017	1.56689	1.56853
11	Moclobemide	1.57598	1.62455	1.60027	32	Fenoprofen calcium salt dihydrate	1.50421	1.50303	1.50362
12	Clopamide	2.35730	1.99910	2.17820	33	Ribostamycin sulfate salt	1.62539	1.59749	1.61144
13	Amoxicillin	2.24818	1.67726	1.96272	34	Clofibric acid	1.78402	1.50647	1.64524
14	Pemirolast potassium	2.00141	1.85081	1.92611	35	Lithocholic acid	1.86405	1.72533	1.79469
15	Estradiol-17 beta	1.68906	1.63404	1.66155	36	Methotrimeprazine maleat salt	1.73829	1.75101	1.74465
16	Dicloxacillin sodium salt hydrate	1.61916	1.80603	1.71260	37	Lorglumide sodium salt	1.52174	1.58045	1.55110
17	Neostigmine bromide	1.64701	1.74150	1.69425	38	Memantine Hydrochloride	1.61785	1.50742	1.56263
18	Niridazole	1.79776	1.52751	1.66264	39	Proguanil hydrochloride	1.50420	1.62783	1.56602
19	Ceforanide	1.58353	1.89338	1.73845	40	Trapidil	1.54591	1.64398	1.59495
20	Vatalanib	1.96522	1.55429	1.75975	41	Nifurtimox	1.57808	1.92974	1.75391
21	Itopride	1.66799	1.60047	1.63423	42	Levocabastine hydrochloride	1.57501	1.52790	1.55146

ELISA signal from drug-treated B cells were normalized to those obtained from untreated but aCD40Ab/IL-21 stimulated B cells and cell proliferation was presented as a relative value. Compounds which inhibited or enhanced B cell proliferation by >50% or >150%were listed (see 2.4 in Material and Method).

7.4 Complete blood count and body weight in animal experiments

WBC (mean:×10^3/μL)

	week0	week1	week2	week3	week4	week5	week6	week7	week8
Dip	22.9508	10.6279	10.6279	11.73408	11.73831	12.58123	16.06467	12.3103	12.1873
PP	22.87457	10.13704	12.35102	10.49032	12.85489	12.94758	11.63181	11.10545	12.14627
solvent1	20.30078	9.333509	11.93411	11.05329	10.52745	14.15511	14.19429	13.69029	11.61354
Doc	15.11725	10.1985	14.75763	11.20812	10.49967	9.48662	9.700268	11.24219	9.640433
Doc solvent	16.82791	8.553955	9.293912	9.44084	10.90325	10.53092	13.47186	14.81684	11.33962
Col	19.62675	9.795999	9.92785	9.785994	8.731235	9.579748	10.02426	9.742708	10.05163
Col solvent	20.86121	8.992655	10.28952	10.86357	11.32464	12.85203	12.1114	12.66354	13.7221

Hemoglobin (mean:g/dL)

	week0	week1	week2	week3	week4	week5	week6	week7	week8
Dip	15.13125	13.69256	12.29719	14.52103	13.67181	12.73427	13.23174	11.99609	12.49184
PP	15.39312	13.70534	14.49164	13.8414	13.95487	13.15618	13.28565	13.30189	13.6601
solvent1	15.07473	13.32848	13.83074	14.49236	14.58848	14.18777	12.9356	12.81406	12.34119
Doc	13.69219	12.36747	12.27597	15.11387	13.6888	12.60066	13.46148	12.91418	13.78844
Doc solvent	15.23364	13.52849	13.66578	13.91632	13.7847	14.03086	13.55048	13.59098	12.52331
Col	14.84414	12.69032	12.42174	13.2156	12.9803	13.63235	12.36063	12.69196	13.4767
Col solvent	14.99801	12.95247	13.37825	14.31509	14.28167	13.9919	12.9867	12.46443	12.72611

Platelet (mean:×10^3/μL)

	week0	week1	week2	week3	week4	week5	week6	week7	week8
Dip	891.6288	852.133	1078.049	1007.689	947.9508	940.789	1074.514	1092.055	1063.342
PP	845.0828	914.0485	1188.43	724.6183	1031.117	1004.736	1011.39	874.5985	994.3013
solvent1	873.9306	871.808	1088.947	826.2098	872.0681	964.0271	986.9011	993.6941	1012.665
Doc	759.4703	1004.24	1116.855	1138.72	1285.476	1351.011	1338.636	1273.907	1520.306
Doc solvent	817.7394	909.7552	1138.416	943.465	837.9442	1026.055	1213.88	1178.426	1055.438
Col	868.8383	965.2226	1188.222	971.09	1089.937	1162.767	1005.433	1035.193	1256.78
Col solvent	896.8078	928.3078	1038.499	832.1375	846.5815	960.0841	966.5205	942.0396	995.9468

Body weight (mean:gram)

	week0	week1	week2	week3	week4	week5	week6	week7	week8
Dip	23.2	20.78	21.2	22.35	23.6	23.64	23.76	24.2	24.85
PP	21.46	20.64	21.15	21.09	21.93	22.05	22.68	23.7	23.41
solvent1	20.6	19.38	20.34	21.3	22.8	22.79	22.6	22.3	22.53
Doc	24.73	22.2	22.19	23.78	23.79	24.4	23.74	23.7	23.512
Doc solvent	24.2	22.53	23.6	24.52	24.52	25.3	25.08	25.4	25.6
Col	23.19	22.14	22.78	24.04	25.8	25.51	25.95	26.25	26.47
Col solvent	22.4	21.14	21.73	22.99	24.53	24.68	24.71	24.89	24.71

Dip=dipyridamole, PP=pyrvinium pamoate. Doc=docetaxel, Col=colchicine. Same solvent was used to dissolve Dip and PP (Solvent1).

7.5 List of laboratory equipment

Items	Company
Cell incubator, HERA cell 240i	Thermo Scientific, Germany
Centrifuge, 5804R	Eppendorf, Hamburg, Germany
Centrifuge, Biofuge Fresco	Haereus Instruments GmbH, Hanau, Germany
Centrifuge, Megafuge 2.0	Haereus Instruments GmbH, Hanau, Germany
FACS Calibur flow cytometer	Becton Dickinson, Heidelberg, Germany
LSRII flow cytometer	Becton Dickinson, Heidelberg, Germany
Wallac 1420 multilabel counter	PerkinElmer, Rodgau, Germany
NanoPhotometer® NP80	Implen GmbH, Munich, Germnay
Agilent 2100 bioanalyzer	Agilent Technologies, Waldbronn, Germany
C1000™ Thermal Cycler	BIO RAD, Munich, Germnay
Mastercycler® ep RealPlex2	Eppendorf, Hamburg, Germnay
NextSeq® 550	Illumina, San Diego, USA
Neubauer chamber	Marienfeld Superior, Lauda-Königshofen, Germany
MACS Separators	Miltenyi Biotec, Bergisch Gladbach, Germany

7.6 List of consumables

Items	Company
LD columns, LS columns	Miltenyi Biotec, Bergisch Gladbach, Germnay
S-MONOVETTE® (EDTA pre-coated 9mL tube)	Sarstedt, Nürmbrecht, Germnay
1.5mL/2.0mL tube	Sarstedt, Nürmbrecht, Germnay
15mL/ 50mL tube	Sarstedt, Nürmbrecht, Germnay
5mL FACS tubes	Sarstedt, Nürmbrecht, Germnay
TC Plate 96 Well,Suspension,F	Sarstedt, Nürmbrecht, Germnay
96 well, F, WHITE, HIGH BINDING MICROPLATE,	Greiner Bio-One, Frickenhausen, Germany
96-well NUNC immunolplate	Thermo Scientific, Waltham, MA, USA
CELLSTAR® Cell Culture Multiwell Plates, 24-well	greiner bio-one, Frickenhausen, Germany
96-well MIDI plate	Biozym Biotech, Hessisch Oldendorf, Germany
96 Fast PCR plate	Sarstedt, Nürmbrecht, Germany
LD columns, LS columns	Miltenyi Biotec, Bergisch Gladbach, Germnay

70µm cell strainers	BD Falcon, Heidelberg, Germany

7.7 List of chemicals, reagents, and kits

Items	Company
Ficoll-Paque PLUS	GE Healthcare, Uppsala. Sweden
PolymorohprepTM	Axis-Shield/ Alere Technologies AS, Oslo, Norway
NaCl	Carl Roth, Karlsruhe, Germany
Na2HPO4	Carl Roth, Karlsruhe, Germany
NaH2PO4	Carl Roth, Karlsruhe, Germany
Na2CO3	Merck, Darmstadt, Germany
NaHCO3	Merck, Darmstadt, Germany
EDTA	Carl Roth, Karlsruhe, Germany
Polyethylene glycol 400	Sigma-Aldrich, Hamburg, Germany
propylene glycol	Sigma-Aldrich, Hamburg, Germany
Tween80®	Sigma-Aldrich, Hamburg, Germany
Tween20®	Sigma-Aldrich, Hamburg, Germany
luminol	Sigma-Aldrich, Hamburg, Germany
2N NaOH solution	Carl Roth, Karlsruhe, Germany
DMSO	Sigma-Aldrich, Hamburg, Germany
non-essential amino acids solution (NEAA)	gibco/Thermo Fisher Scientific, Waltham, MA, USA
penicillin and streptomycin	PAN Biotech, Aidenbach, Germnay
glucose	Sigma-Aldrich, Hamburg, Germany
HEPES	PAN Biotech, Aidenbach, Germnay
fetal calf serum (FCS)	Biochron GmbH, Berlin, Germany
bovine serum albumin (BSA)	Carl Roth, Karlsruhe, Germany
ketamine	Sigma-Aldrich, Hamburg, Germany
xylazine	Sigma-Aldrich, Hamburg, Germany
Prestwick chemical Library®	Prestwick Chemical, Illkirch-Graffenstaden, France
dipyridamole	Sigma-Aldrich, Hamburg, Germany
colchicine	Sigma-Aldrich, Hamburg, Germany
pyrvinium pamoate	Sigma-Aldrich, Hamburg, Germany

docetaxel	Selleck Chemicals, Houston, TX, USA.
recombinant human collagen VII	in house production
anti-human Col7 IgG1 antibody	in house production
Recombinant human IL-21	Cell Sciences, Newburyport, MA, USA
anti-human CD40 antibody	clone # 82111, R&D systems, Minneapolis, MN, USA
anti-human CD3 antibody	clone UCHT1, BioLegend, Fell, Germany
anti-human CD28 antibody	clone CD28.2, BioLegend, Fell, Germany
FITC-conjugated mouse anti-human CD19	clone HIB19, BD Biosciences, Heidelberg, Germany
PE-conjugated mouse anti-human CD27 antibody	clone M-T271, BD Biosciences, Heidelberg, Germany
APC-conjugated mouse anti-human CD38 antibody	clone HIT2, BD Biosciences, Heidelberg, Germany
rat anti-mouse CD16/CD32	Clone 2.4G2, BD Biosciences, Heidelberg, Germany
PE-conjugated rat anti-mouse CD138	Clone 281-2, BioLegend, Fell, Germany
Alexa405-coupled anti-mouse B220 antibody	Alexa405 (Life Technologies, Darmstadt), anti-mouse B220 (clone GK1.5, eBioscience), In house production
Alexa Flour 488-coupled recombinant murine vWFA2	Alexa Flour 488(Life Technologies, Darmstadt), murine vWFA2 (in house production)
propidium iodine	BioLegend, Fell, Germany
Affinity purified Goat anti-Human IgM Coating Antibody	Bethyl Laboratories, Montgomery, TX, USA
HRP Conjugated Goat anti-Human IgM Detection Antibody	Bethyl Laboratories, Montgomery, TX, USA
Affinity purified Goat anti-Human IgG-Fc Coating Antibody	Bethyl Laboratories, Montgomery, TX, USA
HRP Conjugated Goat anti-Human IgG-Fc Detection Antibody	Bethyl Laboratories, Montgomery, TX, USA
Affinity purified Goat anti-Mouse IgG-Fc Coating Antibody	Bethyl Laboratories, Montgomery, TX, USA
HRP Conjugated Goat anti-Mouse IgG-Fc Detection Antibody	Bethyl Laboratories, Montgomery, TX, USA
Affinity purified Goat anti-Mouse IgM Coating Antibody	Bethyl Laboratories, Montgomery, TX, USA
HRP Conjugated Goat anti-Mouse IgM	Bethyl Laboratories, Montgomery, TX, USA

Detection Antibody	
peroxydase conjugated affinity pure donkey anti-mouse IgG(H+L)	Jackson Immuno Research, West Grove, PA, USA
HRP Conjugated Goat anti-Mouse IgG1 Detection Antibody	Bethyl Laboratories, Montgomery, TX, USA
HRP Conjugated Goat anti-Mouse IgG2a Detection Antibody	Bethyl Laboratories, Montgomery, TX, USA
HRP Conjugated Goat anti-Mouse IgG2b Detection Antibody	Bethyl Laboratories, Montgomery, TX, USA
1 step Turbo TMB-ELISA	Thermo Scientific, Germany
recombinant vWFA2 protein of mCOL7	in house production
Titermax®	CytRx Corporation, Los Angeles, CA, USA)
DNase I	Sigma-Aldrich, Hamburg, Germany
RNaseOUT™, recombinant RNase inhibitor	Invitrogen, Karlsruhe,Germany
random hexamer primer	Thermo Scientific, Germany
RevertAid H Minus Reverse Transcriptase	Thermo Scientific, Germany
dNTPs	Thermo Scientific, Germany
20x TaqMan® Gene Expression Assay	Thermo Scientific, Germany
TaqMan® Gene Expression Master Mix	Thermo Scientific, Germany
Pan T Cell Isolation Kit, human	Miltenyi Biotec, Bergisch Gladbach, Germany
B Cell Isolation Kit II, human	Miltenyi Biotec, Bergisch Gladbach, Germany
Cell Proliferation ELISA, BrdU (colorimetric)	Roche applied science, Penzberg, Germany
Cytofix/Cytoperm™ Fixation/Permeabilization Solution Kit	BD Biosciences, Heidelberg, Germany
RNeasy® Mini Kit	QIAGEN, Hilden, Germany
TruSeq® Stranded mRNA Sample Preparation Kits	Illumina, San Diego, CA, USA
NextSeq 500/550 v2 Kits	Illumina, San Diego, CA, USA

7.8 List of buffers/recipes

Items	Company
Dulbecco's Phosphate-Buffered Saline	gibco/Thermo Fisher Scientific, Waltham, MA, USA
RPMI 1640 with 0.3 g/L L-glutamine	Lonza, Basel, Switzerland
RPMI 1640 with HEPES and L-Glutamine	Lonza, Basel, Switzerland
RPMI 1640 without phenol	GENAXXON bioscience, Ulm, Germnay
0.9% NaCl	Fresenius KABI, Bad Homburg v. d. Höhe, Germnay
distilled water,Ampuwa®	Fresenius KABI, Bad Homburg v. d. Höhe, Germnay
UltraPure™ DNase/RNaseFree Distilled Water	gibco/Thermo Fisher Scientific, Waltham, MA, USA
Phosphate-Buffered Saline (PBS), pH 7,2	9 g NaCl, 1,74 g Na2HPO4 *2H2O, 0,18 g NaH2PO4 *H2O in 1 L Aqua dest
MACS buffer	PBS with 0.5% BSA and 2 mM EDTA
FACS buffer	PBS with 0.5% BSA
Cell culture medium	RPMI 1640 with 0.3 g/L L-glutamine, 10% heat-inactivated FCS,1% NEAA,100 U/mL penicillin and 100 µg/mL streptomycin
Chemiluminescence (CL) medium	RPMI 1640 without phenol, 1% heat-inactivated FCS, 2 g/mL glucose,5.95 g/L HEPES
0.05 M carbonate-bicarbonate buffer, pH 9.6	1.59 g Na2CO3 ,2.93 g NaHCO3, dissolve in 1 L deionized water
PBS-T	PBS with 0.05% Tween 20®
blocking buffer	1% BSA in PBS-T
erythrocyte lysis buffer	distilled water and 0.9% NaCl at 4:1 (v/v)

Publication list

Poster presentation

- 10th International Congress on Autoimmunity

  April 2016. Leipzig, Germany

- Annual European Congress of Rheumatology : EULAR 2016

  June 2016, London, UK

  (Guided poster tour)

- Pathogenesis of Pemphigus and Pemphigoid Meeting (PPP 2016)

  September 2016, Munich, Germany